BULLETIN 33

Geologic Section of the Black Range at Kingston, New Mexico

BY FREDERICK J. KUELLMER

Structure and stratigraphy of the Black Range, detailed petrology of igneous rocks, and general guides to ore exploration

1954

STATE BUREAU OF MINES AND MINERAL RESOURCES
NEW MEXICO INSTITUTE OF MINING & TECHNOLOGY
CAMPUS STATION SOCORRO, NEW MEXICO

Contents

Illustrations

TABLES

Page

FIGURES

PLATES

Abstract

Granite, graywacke, and metadiabase, presumably Precambrian in age, are found only in small isolated areas within the mapped region.

An aggregate thickness of 2,400± feet of sediments, representing a part of each Paleozoic period, overlies the Precambrian rocks. Within the mapped area they are not exposed in a simple continuous sequence. The ages and chief lithologic characters of the Paleozoic rocks are: (1) Cambrian (?) Bliss sandstone—hematitic, glauconitic, or quartzose; (2) Ordovician El Paso limestone—bluish-gray slabby to massive, with abundant yellow-brown silty partings; (3) Ordovician Montoya limestone—basal sandstone, massive to thin, black or gray, limestone or dolomite, with abundant chert; (4) Silurian Fusselman dolomite—massive gray or brownish-gray; (5) Devonian Percha shale—black fissile shale, green limy shale; (6) Mississippian Lake valley limestone—gray to black massive limestones with chert and thin-bedded shaly limestone; (7) Pennsylvanian Magdalena limestone—massive limestone, shale; and (8) Permian Abo formation—massive red shale, red sandstone. Rock units 1 through 4 (above) contain little shale, whereas 5 through 8 have no dolomite. Igneous sills are much more abundant at the shale horizons in the upper Paleozoic rocks than elsewhere in the section, presumably because of the lower mechanical resistance of the shales.

Tertiary igneous rocks may be divided into three groups, from oldest to youngest: (1) andesitic and latitic rocks, which include the intrusive quartz monzonite porphyry; (2) rhyolitic extrusives and intrusives; and (3) andesitic volcanic rocks. The total estimated thickness of the Tertiary volcanics is approximately 3,000 feet. Terrestrial conglomerates, sandstones, and shales occurring in a nearby area between the rocks of items 2 and 3 (above) contain a fossil flora dated between the limits early Miocene and early Pliocene. The andesitic and latitic rocks (item 1, above) are intensely altered on a regional scale, whereas the younger igneous rocks are not.

Feldspars in the shallow depth quartz monzonite porphyry dikes and sills exhibit optical anomalies suggesting that both high- and low-temperature forms are present.

The tuffaceous rhyolite, with both pyroclastic and flow features, probably flowed for the most part either as a loose, granular, essentially solid mass lubricated by liquid, or by means of actual liquid flow. Oxidized biotite of the tuffaceous rhyolite may indicate a temperature during extrusion greater than 400°-500°C, whereas the green hornblende may represent one or more of the following: (a) conversion from the brown to the green varieties during cooling, (b) an extrusion temperature below 850° C, or (c) a low oxygen concentration during the extrusion. Large concentrations of xenoliths in the tuffaceous rhyolite may either represent a vent agglomerate or indicate proximity to a fissure zone. Such xenolith zones are geologically contemporaneous and consanguineous with the enclosing tuffaceous rhyolite.

Abundant intrusive rhyolitic bodies, consanguineous with the extrusive tuffaceous rhyolite on the basis of compositional and textural

similarity, suggest proximity to a major eruptive center. Both intrusive and extrusive rhyolitic rocks may have been emplaced as crystalline, and glassy, granular masses. The following features, commonly regarded as being restricted to plutonic rocks, occur in this volcanic igneous environment: (1) quartz-sanidine pegmatite bodies in rhyolite porphyry; (2) even-grained xenomorphic-granular lenses in rhyolite porphyry; (3) primary granophyric phenocrysts, which appear to have formed by eutectic crystallization and by sanidine crystallization on corroded quartz phenocrysts, in glassy rhyolitic dikes containing 10 percent phenocrysts; (4) perthitic phenocrysts in a rhyolitic sill; (5) geochemical culminations in silicon and potassium produced by a lack of equilibrium during the formation of crystalline reaction rims about accidental xenoliths enclosed in rhyolite vitrophyre.

The above phenomena do not substantiate the hypothesis that volcanic processes cannot produce plutonic features.

Late andesite flows and agglomerates display a repeated cyclical sequence ranging from massive flow rock through scoriaceous rock in turn overlain by a pumiceous agglomerate, and are partly interbedded with the early gravel deposits.

Quaternary events include deposition of later gravels, formation of several stream terraces, and erosional dissection of the Black Range.

Moderate folding of the sediments resulted probably from their adjustment to the undulatory surface produced by a highly-faulted basement complex, with possible assistance from igneous intrusive forces. Thus, high-angle normal faulting, predominantly of a north-south trend, appears to be the major structural determinant. Faults are more abundant in the pre-Devonian rocks, because the Percha shale was capable of plastic deformation and thereby compensated for, and insulated the upper Paleozoic rocks from, minor ruptures in the earth's crust. The major periods of faulting were concluded before the eruption of the rhyolitic rocks.

The best explanation of the extremely irregular distribution of the quartz monzonite porphyry is that it was emplaced along high-angle faults or fractured zones, and spread laterally into shale horizons of low mechanical resistance.

Lead, zinc, silver, manganese, copper, and gold ores with an estimated total value of more than 7 million dollars have been produced from the Kingston mining district, the Gray Eagle, and Grandview mines. Discontinuous pockets of high-grade ore have been found in fissures and fault zones, or as replacement bodies in the Fusselman, Montoya, and El Paso limestones and dolomites, which would, barring erosion, underlie the Percha shale. The ore deposits were formed after the quartz monzonite porphyry was emplaced and before all younger rocks were formed. Future exploration for ore deposits not now exposed at the surface might well be directed toward areas of arched Paleozoic rocks or those areas where Paleozoic rocks are covered by sills of the quartz monzonite porphyry.

Introduction

The area studied is a narrow strip across the Black Range along State Highway 180, in Sierra and Grant Counties, New Mexico. The townsite of Kingston, which lies approximately 50 miles east of Silver City, is at the eastern boundary of the mapped area (see index map, pl 1, in Pocket).

Most of the previous geologic work has been confined to investigations of the mining districts, especially those in the vicinity of Kingston. Lindgren, Graton, and Gordon (1910) recognized and differentiated some of the stratigraphy, outlined the major structural features of New Mexico, and investigated most of the mining districts. Darton's (1928-a, 1928-b) excellent reconnaissance work included part of this area. Harley's (1934) reconnaissance and detailed mining report on Sierra County includes the eastern third of the mapped area (see pl 1). No other work has been done except for numerous United States Bureau of Mines investigations, some of which contain maps of mine localities.

Physiographically the region is in the Mexican Highland portion of the Basin and Range province (Fenneman, 1931), which consists largely of dissected block mountains separated by alluvial basins. Prominent and complex north-south faulting is well known, and Tertiary igneous activity, both intrusive and extrusive, is widespread. In the area under study, which is not far removed from the southern boundary of the greater Colorado Plateau, the following statement of Fenneman's (1931, p 381) is applicable: "... the entire area when seen from a high point is one of irregular ridges and uplands without apparent plan or order. It does not in the least conform to the simple conception of basin ranges, but with its complicated history of intrusion, faulting, lava flows, and various erosion cycles it resembles still less the horizontal plateau on the north."

This project is part of a regional study of the volcanic and sedimentary rocks, and their relation to the ore deposits, which is being undertaken by the New Mexico Bureau of Mines and Mineral Resources. In New Mexico volcanic rocks predominate north and west of "a line drawn from El Paso to the northeast corner" (Lindgren, Graton, and Gordon, 1910, p 42). In many localities where the volcanic rocks have been removed by erosion valuable ore deposits are found. Extrusive rocks cover the usual ore-bearing sediments in large parts of the state. Can some way be found to detect the presence of significant ore deposits now concealed by volcanic rocks? This study, the first of many related to the major project, is restricted to 60-odd square miles out of a total area of thousands of square miles; it provides, therefore, an inadequate sample to answer this and other questions satisfactorily.

Geologic mapping was done primarily on aerial photographs (scale, 1:31,680) with assistance from the various maps listed on Plate 1. In addition, petrographic, chemical, and some X-ray determinations were carried out in the laboratory.

The author believes that the significance of volcanic rocks with respect to the current discussion concerning the origin of plutonic

rocks (i.e., the granite problem) has not been properly evaluated, except in rare cases. Geologists apply very readily simple binary or ternary silicate phase-diagrams to explain composition and sequence of numerous plutonic rocks. This approach is validated by the high degree of correlation between these two. However, in many cases ambiguity results, and the final interpretation is unsatisfactory. Volcanic rocks, especially the acidic varieties, should be the object of increased study, because, in a sense, they may be considered as inter-mediate between the laboratory and the natural pluton. In addition, volcanic glass, primarily perlite, has become of economic importance.

For these reasons, the rhyolitic igneous rocks, especially the volcanic glasses in the Black Range of New Mexico, have been studied in considerable detail. However, the problem of the origin, crystallization, and chemical variation of the volcanic glasses is still in its incipient stages. Nevertheless this presentation may be of value as a first approximation and as an aid in formulating new approaches to the problem.

Acknowledgments

The field and map expenses for this study were paid by the Field Assistance Fellowship Fund of the New Mexico Bureau of Mines and Mineral Resources, without which this project would have been impossible. Dr. Eugene Callaghan, Director, and the other staff members have rendered generous assistance in every possible way.

Grateful acknowledgment is hereby made to Dr. Robert Balk for his helpful suggestions and advice both in the field and in the laboratory. The author is indebted to Dr. J. Marvin Weller and Dr. C. L. Balk, who examined the fossils collected by the author. For the X-ray determinations the author was assisted by Dr. Fritz Laves. Generous assistance was rendered by the entire staff of the Department of Geology at the University of Chicago. A grant from the latter department paid for four of the chemical analyses and some of the thinsections. During the last six months of laboratory work the author was assisted financially by the Salisbury Fellowship Fund of the University of Chicago. Mr. Oiva Joensuu kindly made the spectrometric determinations. Dr. Ernest Ehlers was very helpful in some of the X-ray studies. Thanks are due also to Dr. Robert Hernon and Mr. Andrew Shride of the U. S. Geological Survey. Mrs. Hilda Kalish prepared Plate 1, Mr Wright Putney the stratigraphic diagrams, and. Mr. Oscar Rubio the micro-graphic sketches.

Figure 1. GENERALIZED ROCK SECTION OF THE BLACK RANGE AT KINGSTON, NEW MEXICO.

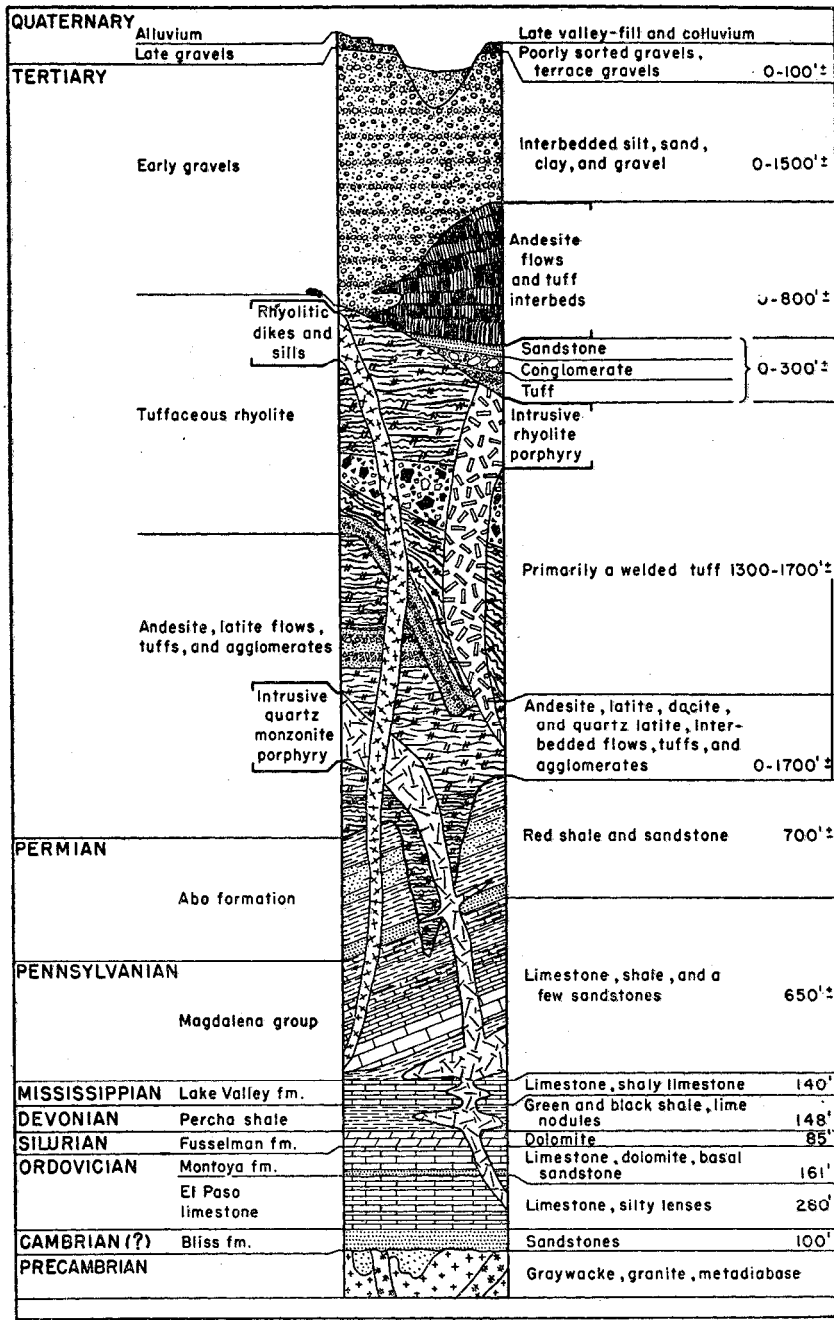
QUATERNARY
Alluvium
Late gravels
TERTIARY
Early gravels
Rhyolitic dikes and sills
Tuffaceous rhyolite
Andesite, latite flows, tuffs, and agglomerates
Intrusive quartz monzonite porphyry
PERMIAN
Abo formation
PENNSYLVANIAN
Magdalena group
MISSISSIPPIAN
Lake Valley fm.
DEVONIAN
Percha shale
SILURIAN
Fusselman fm.
ORDOVICIAN
Montoya fm.
El Paso limestone
CAMBRIAN (?)
Bliss fm.
PRECAMBRIAN
Late valley-fill and colluvium
Poorly sorted gravels, terrace gravels 0-100'±
Interbedded silt, sand, clay, and gravel 0-1500'±
Andesite flows and tuff interbeds 0-800'±
Sandstone
Conglomerate
Tuff
0-300'±
Intrusive rhyolite porphyry
Primarily a welded tuff 1300-1700'±
Andesite, latite, dacite, and quartz latite, interbedded flows, tuffs, and agglomerates 0-1700'±
Red shale and sandstone 700'±
Limestone, shale, and a few sandstones 650'±
Limestone, shaly limestone 140'
Green and black shale, lime nodules 148'
Dolomite 85'
Limestone, dolomite, basal sandstone 161'
Limestone, silty lenses 280'
Sandstones 100'
Graywacke, granite, metadiabase

Figure 1

Precambrian Sequence

INTRODUCTION

The oldest rocks in the Black Range are believed to be of Precambrian age because they have been intensely deformed in comparison with the overlying Paleozoic sediments and are unconformably overlain by a sandstone tentatively correlated with the Bliss sandstone of Cambrian or Early Ordovician (King, P.B., 1940) age. The secondary planar structures of the Precambrian graywacke, metadiabase, and granite dip in general 60 degrees or more northward, although the strike varies considerably. Locally these rocks, especially the graywacke, have a lineation which deviates very little from a mode[1] of N. 63° E., 51° NE., bearing and plunge, respectively. Detailed mapping (see pl 1) has shown that the exposures of the Precambrian are small and discontinuous in the Kingston region, in contrast with an early reconnaissance map (Darton, 1928-b), which depicted a continuous narrow belt of Precambrian rocks elongated in a north-south direction, just west of the town of Kingston.

GRAYWACKE

The Precambrian sediments are best exposed along South Percha Creek for a distance slightly less than a mile, just downstream from the Gray Eagle mine. Another small exposure is found west of the crest of the range, approximately half a mile east of the Grandview mine. Because the graywacke crops out in a small area and is intensely folded and deformed, any estimate of its stratigraphic thickness would be of little significance.

Megascopically the graywacke is fine- to coarse-grained, massive- to thin-bedded, gray to dark-green or black, weathering green to brown, and penetrated by a few thin quartz stringers which approach ptygmatic veins in appearance. Locally the graywacke shows graded bed-ding and commonly contains flattened and elongated pebbles in lenses and thin beds. The elongation of pebbles is due largely to post-depositional deformation, inasmuch as many of the pebbles show small-scale shearing and faulting. Some pebbles and granules are found even in the finest-grained beds. One small ripple-marked surface (4 by 6 feet) was seen, a rare feature in graywackes. The ripple-mark axes deviate about 60 degrees from the adjacent lineations. It is believed that the angular discordance between the ripple marks and the unimodal lineation is a sufficient criterion for identifying these markings (Ingerson, 1940).

A small mass of Precambrian rocks southwest of Emory Pass (pl 1) shows no positive evidence of sedimentary origin. These rocks are gray, fine-grained, with abundant small specks of chloritized hornblende (?), and are interbedded with thick to thin, black, fine-grained beds.

1. The lineations were plotted on a Schmidt net, contoured, and the center of the area of greatest point-density was selected as the modal value. The distribution of the points is unimodal.

The microscopic texture of the Precambrian sediments along South Percha Creek is that of typical graywacke with angular grains of quartz, feldspar, and rock fragments distributed irregularly throughout the matrix. Sizes of grains range from 2 inches down to submicroscopic size. The rock fragments consist of quartzite, shale, graywacke, and possibly some considerably altered igneous rocks. Most grains have irregular, sutured contacts and are penetrated, on their boundaries, to a small extent by fibrous sericite and chlorite, suggesting slight replacement of the larger grains. The matrix is a fine-grained intergrowth of sericite, chlorite, and quartz. Magnetite and a few euhedral grains of sphene were also found.

The sericite and chlorite show a slight alignment at a high angle to the bedding. Sparse grains of pyrite as well as veinlets of epidote and quartz form part of the rock. In one thinsection the matrix was found to be partly replaced by biotite grains several times larger than the usual sericite and chlorite grains in the matrix. The concentration and grain size of the biotite flakes is greatest around and within some of the large clastic grains.

GRANITE

Granite crops out in three small isolated areas north and north-west of Kingston. The age relation between the granite and the graywacke is not revealed in this area; however, both have been transected by metadiabase dikes.

Megascopically the granite is massive, brown to pink, medium-grained, and weathers to a reddish brown or yellowish brown. It contains irregular dark-green to black masses of very fine-grained mafic minerals.

The microscopic texture is holocrystalline, seriate xenomorphicgranular, and granophyric. Granophyric intergrowths exhibit patterns which are radial, cuneiform, subparallel elongated blebs, or irregular. Bent and microfaulted feldspar (see fig 2) and finely granulated quartz between grain boundaries and in microfaults suggest internal deformation of this rock.

TABLE 1. ESTIMATED MODES OF THE PRECAMBRIAN PLUTONIC ROCKS

GRANITE		METADIABASE	
Perthite	49%	Hornblende	51%
Quartz	38	Chlorite	33
Plagioclase (An_{31})	8	Biotite	2
Biotite	5	Magnetite and Ilmenite	7
Magnetite and Ilmenite	x	Plagioclase (An_{11})	7
Zircon,	x	Epidote	x
Fluorite	x		
Chlorite	x		
Total	100%	Total	100%

x Indicates present.

The estimated mode of the granite is listed in Table 1. The quartz occurs as anhedra showing undulatory extinction, in very fine grains between larger minerals, and as part of the granophyric intergrowths.

Plagioclase has a maximum extinction of 16 degrees normal to (010), and an optic angle ($2V\alpha$) of 81 degrees. According to Kennedy's (1947) charts, this corresponds to a composition of An_{31}. The plagioclase is anhedral, appears somewhat corroded, and is more clouded than the quartz or perthite. In general it is surrounded by a thin discontinuous clustering of fine quartz anhedra, which may extend into the plagioclase grain, or by the radiating type of granophyric intergrowth. For the most part the potash feldspar in the perthite is clear, untwinned,, and has optical properties corresponding very closely to those of orthoclase or microcline. Locally it has a barely perceptible fine grid-twinning. Both the quartz and feldspar have abundant minute inclusions, which in some parts of the quartz are arranged in arcuate lines, suggesting distribution along irregular conchoidal surfaces.

Biotite, pleochroic from dark green to colorless, occurs as small shreds in irregular aggregates and as thin shreds between the quartz, plagioclase, and granophyric grains. Accessory minerals include magnetite and zircon.

Two varieties of minute veinlets, which intersect approximately at right angles, occur in the granite. The thicker veins are xenomorphicgranular quartz. Walls of the thinner veins are lined with an opaque material, which probably is magnetite, and the central part is fine-grained xenomorphic-granular quartz. Several cavities within this vein quartz are lined with a few small fluorite crystals. Megascopic veins of this nature were not observed.

METADIABASE

Metadiabase dikes were found to transect both the graywacke and granite in their respective outcrops. Nevertheless the secondary linear and planar features of the metadiabase are approximately parallel to those of the graywacke. The dike contacts truncate the graded bedding of the graywacke; the orientation of the dikes in the granite is random; and small inclusions of the Precambrian country rock are found in the metadiabase dikes.

Megascopically the metadiabases are dark green to black, medium-to fine-grained rocks that contain abundant laths (5 mm and less) of a chloritic material, although in many places it is completely fine-grained. The rocks also contain ptygmaticlike quartz veinlets.

Microscopically the diabase has a holocrystalline, seriate porphyritic fibrous texture and a very fine-grained groundmass. Internal deformation is manifested by the bent and shredded hornblende fibers (see fig 3). The estimated mode of a metadiabase is given in Table 1.

Hornblende occurs as fibrous, prismatic grains, commonly bent or broken; many grains contain abundant ilmenite and albite inclusions, some of which are elongated parallel to the hornblende cleavage. The pleochroic orientation is: gamma, green; beta, pale greenish blue; and alpha, pale blue.

Figure 2 (left). BENT PLAGIOCLASE WITH SOME FINELY GRANULATED QUARTZ ALONG FRACTURES. PRECAMBRIAN GRANITE. CROSSED NICOLS.

Figure 3 (right). SHREDDED HORNBLENDE FIBERS IN METADIABASE. CROSSED NICOLS.

DIAMETER OF FIELD IS 5 MM.

Chlorite occurs in fibrous and irregular masses and has apparently been formed by alteration of hornblende. Pleochroism ranges from green to colorless; the interference color is a first-order brownish gray, and the indices of refraction are lower than those of the hornblende. In many grains the alteration of hornblende to chlorite has apparently been preserved in intermediate stages. The net result is that some grains may have a chlorite index (relative to hornblende), a hornblende cleavage, and birefringence higher than chlorite. Universal-stage determinations have also given anomalous results. For this reason the estimated mode must be considered only as an approximation.

Biotite is pleochroic from brown to colorless and occurs as small subhedral grains which are enclosed by hornblende. Magnetite and ilmenite, coated by leucoxene, occur as single anhedral grains (0.4 mm and less) or grain clusters. Plagioclase (An_{11}) occurs in the groundmass as small anhedral grains enclosed by euhedrally terminated hornblende. Some hornblende grains also project slightly into thin dilation veins of plagioclase.

The deduced order of mineral development on the basis of the mineral phenomena described above might be:

1. Biotite replaced by hornblende.
2. Formation of albitic plagioclase in cavities, and possibly as a replacement of other plagioclase and some of the hornblende. The hornblende growth may have been of longer duration than the albitization.
3. Replacement of hornblende by chlorite.

The effect of the deformational stresses involved in the folding of the Precambrian rocks was probably small, because primary sedimentary features have survived in the graywacke. In addition, the chlorite-sericite-biotite-quartz mineral assemblage of the graywacke suggests no more than a low-grade metamorphism.

Paleozoic Stratigraphy

INTRODUCTION

Each Paleozoic system is represented in the structurally complex Kingston area, although individual systemic units are thin in comparison to those of adjoining regions. The total thickness of the Paleozoic rocks is about 2,400 feet (see fig 1). At no single locality in the area can the entire Paleozoic sequence be studied in a simple "layer cake" fashion, as has been suggested by Harley (1934, p 99).

The Paleozoic rocks were studied megascopically, only, though some microscopic mineral determinations were made. Wherever possible, the affinity of the sediment to the orthoquartzite, graywacke, or arkose families has been indicated (Pettijohn, 1949; Krynine, 1948).

CAMBRIAN (?) SYSTEM

The Bliss sandstone was originally named and described by Richardson (see Wilmarth, 1938, p 212) in the Franklin Mountains,, west Texas. It is separated from the underlying Precambrian rocks by an angular unconformity and in the Kingston region is approximately conformable under the overlying Ordovician El Paso limestone. Richardson (1909, p 3) found that the Bliss sandstone locally was separated from the overlying El Paso limestone by an unconformity, but that in most places the sequence was conformable. On the basis of its linguloid brachiopods, Richardson considered it to be Upper Cambrian in age. However,, P. B. King (1940, pp 152-156) has collected a Lower Ordovician (Beekmantown) gastropod fauna from the Bliss sandstone in the Van Horn region, Texas. So much doubt was raised concerning the age of the Bliss sandstone that in this report the Bliss has been classified as Cambrian (?), although no fossils were found in the Kingston area. Kelley (1951) has presented an excellent discussion of the age and correlation of the Bliss sandstone. After the first draft of this manuscript was completed, R. H. Flower (1953) demonstrated that the lower part of the Bliss sandstone contains an Upper Cambrian (middle Franconian) fauna, while the uppermost 35 feet contain trilobites of Lower Ordovician age. Dr. Flower (personal communication) subsequently has collected additional fossils indicating the presence of beds of both Upper Cambrian and Lower Ordovician ages on each side of the Black Range. It seems likely, therefore, that the Bliss sandstone of' the Kingston region also includes beds of these two age groups.

In the mapped area (see pl 1), the Bliss sandstone crops out in South Percha Creek Valley east of the Gray Eagle mine, in Silver Creek west of Kingston, and in Sawpit Canyon 1½ miles north of Kingston. Its outcrop area is small, but the rock unit is easily recognizable.

Lithologically the Bliss consists of glauconitic and hematitic sandzstone, siltstone, and shale, and to a lesser extent it includes thin lime-stones, pebble conglomerates, and orthoquartzite (silica-cemented quartzose sandstone; see Pettijohn, 1949, pp 237-241) beds. Pebble-

to granule-conglomerate beds are found locally at or near the base. Where the conglomerate is absent, the lowest beds are either oolitic hematitic sandstone or glauconitic shales and sandstones. The sandstones are rather coarse-grained and contain sparse rounded quartz pebbles. Above this were found gray, white, or brown, medium- to coarse ,grained orthoquartzite beds. White, gray, brown, or violet, hematitic and glauconitic, medium- to coarse-grained, locally cross-bedded sandstones overlie these beds. Near the top, the formation consists of gray to black limestones, green glauconitic shales and sandstones, and thin brown, red, or purple hematitic, or quartzose sandstones. The limestones become more abundant toward the top of the formation, and the lithology begins to resemble that of the overlying El Paso limestone.

The upper limit of the Bliss sandstone was chosen arbitrarily as the top of the highest sandstone unit underlying the typical El Paso limestone. , The thickness of the Bliss formation in the measured sections varies from 85 to 102 feet. It is interesting to note that the Bliss sandstone belongs to the orthoquartzite-limestone suite of rocks (Pettijohn, 1949, p 191) and is not a basal arkose. Furthermore, hematitic sandstones occur within that part of the Bliss which is probably of Lower Ordovician age.

ORDOVICIAN SYSTEM

EL PASO LIMESTONE

The El Paso limestone of Lower Ordovician age overlies the Bliss sandstone. In the Black Range this formation is the lower part of the Paleozoic limestone sequence which was named the Mimbres limestone by Gordon and Graton (see Kirk, 1934, p 445). The Mimbres limestone also includes the overlying Montoya and Fusselman formations. Gordon (Lindgren, Graton, and Gordon, 1910, pp 226-227) used Mimbres lime stone as a general term pending more detailed studies, although the Ordovician and Silurian age of the sequence was known. The El Paso limestone was originally described by Richardson (see Wilmarth, 1938, p 680) and was named for its exposures in the Franklin Mountains, Texas. In the area covered by this report, no fossils were found except in Ladrone Gulch, where a few slabs showing cross-sections of a gastropodlike fauna were collected, These bear a resemblance to the *Ophileta* fauna (indicating Lower Ordovician age) identified by E. O. Ulrich (Richardson, 1909, p 4) in the type area. Wheeler (1942) maintains that in the Franklin Mountains the upper part of the El Paso contains a Middle Ordovician fauna. Kelley and Silver (1952) have elevated the El Paso to group status in the Caballo Mountains and have divided it into two formations. In the Kingston area the correlation is based on the lithology and stratigraphic position.

The thickness of the El Paso limestone in the Kingston area is between 280 and 300 feet. Over 90 percent of the formation consists of a gray fine-grained limestone in slabby to massive beds. The lime-stone weathers gray or bluish gray and contains abundant yellow-brown siltstone lenses (2 mm and less thick). On a weathered surface normal

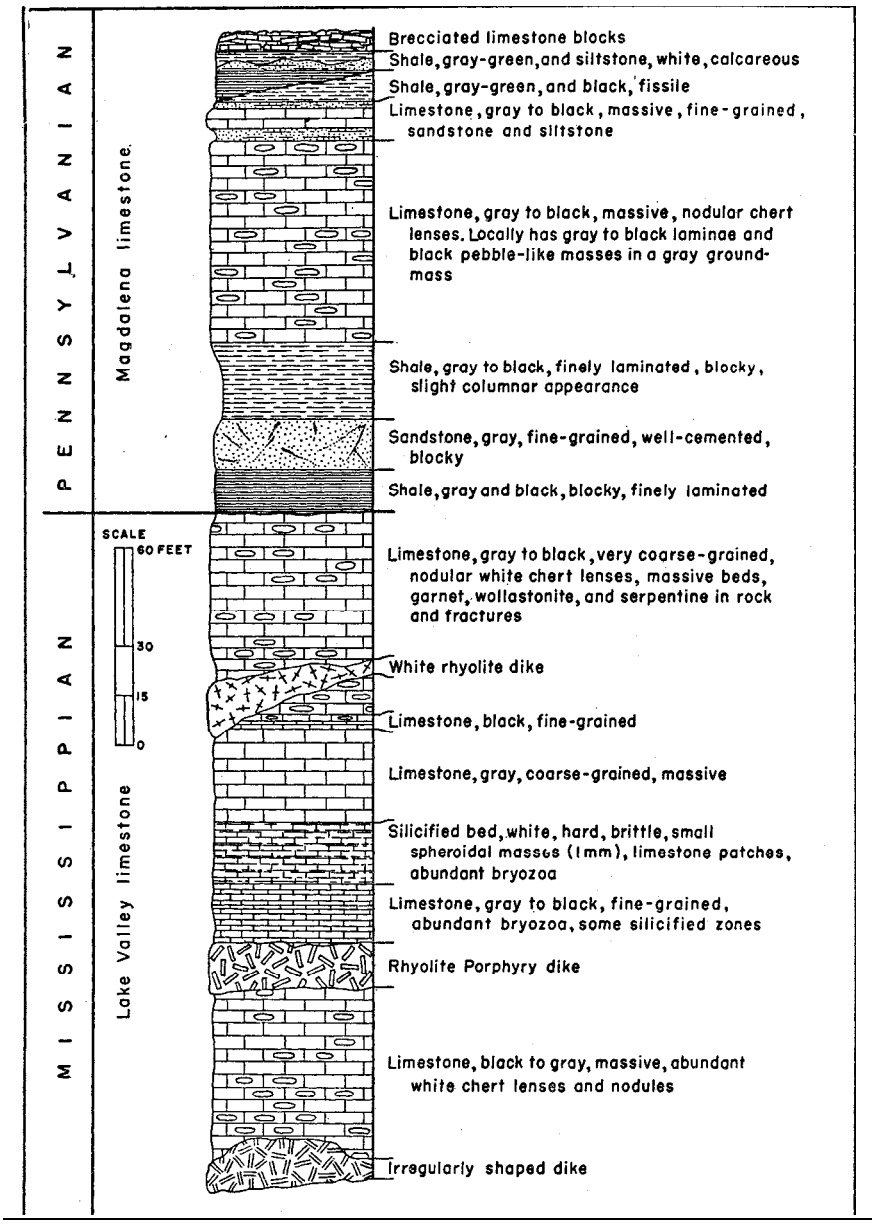

Figure 4. SECTION I. ROAD CUT, ONE-EIGHTH MILE EAST OF IRON CREEK CAMPGROUND, ON STATE HIGHWAY 180.

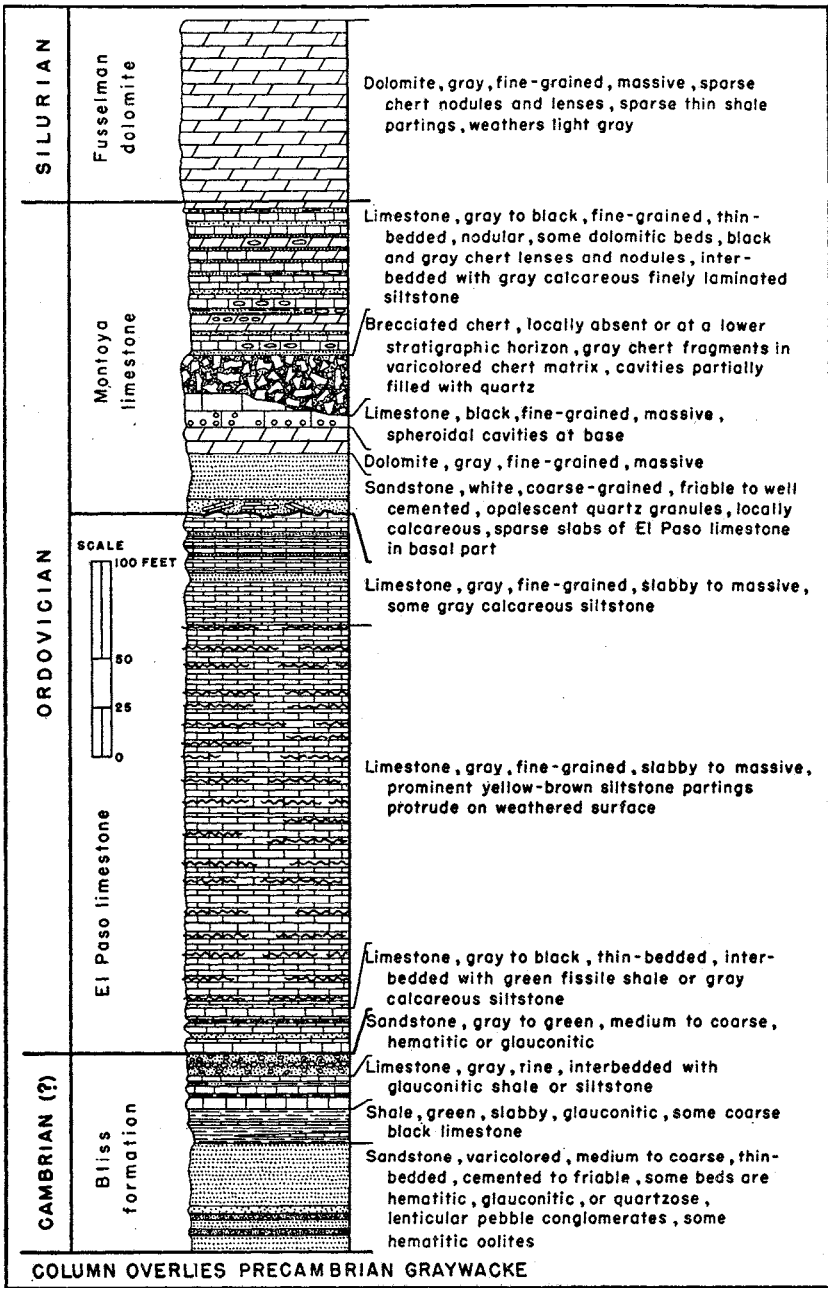

Figure 5. SECTION IT. COMPOSITE OF 4 SECTIONS IN LADRONE GULCH AND SOUTH PERCHA CREEK, SECS. 13, 24, AND 25, T. 16 S., 9 W. (UNSURVEYED).

to the bedding, these siltstone lenses protrude a fraction of an inch, and on surfaces parallel to the bedding, the lenses have a very irregular anastomosing distribution. Sparse, thin, black or brown chert lenses occur in the upper part of the El Paso limestone. Many bedding planes show on weathering a reticulating network of yellow-brown siliceous worm-shaped masses. Some of the beds are dolomitic. The ratio of limestone to dolomite beds is approximately 20 to 1. Sparse gray friable calcareous siltstone and shale beds are interbedded with the typical El Paso limestone beds. In the lower portion several thin fissile green shale beds are present. The El Paso limestone crops out in the vicinity of the Gray Eagle mine, along parts of Sawpit Canyon north of the town of Kingston, and in several other localities. Detailed descriptions are found in Section II.

The two features which lead to prompt recognition of the El Paso can be emphasized by the following statement of Darton (1928-a, p 10): "The surface of many layers is covered by thin reticulating brown deposits of silica, and most of the rock weathers to a pale-gray tint—two features which are distinctive...." Later in the same article, Darton (p 184) suggests that these reticulating brown deposits may be due to seaweeds. On the basis of the field work, it seems more reasonable to suggest that there are three varieties of siliceous deposits, namely:

1. Thin quartzose siltstone lenses, which may have originated by a winnowing out of the finer-grained lime-mud fraction from a thin bottom layer during periods of increased turbulence at, or shortly after, the time of deposition. Cyclical repetition of such turbulence would produce the tremendous number of siliceous partings.
2. The worm-shaped masses, in part, may have been an indigestible quartz and clay residue left behind in worm tubes.
3. The chert lenses may be primary deposits of siliceous sponges, secondary deposits, or combinations of both. Items 1 and 2 (above) may also owe some of their prominence to secondary silicification.

MONTOYA LIMESTONE

The Montoya limestone overlies the El Paso formation, from which it is seprated by a slight erosional disconformity. As no fossils except sparse crinoid columnals were found, correlation is based on lithology. The Montoya was named by Richardson (see Wilmarth, 1938, p 1411) from its exposures in the Franklin Mountains, Texas. Its age was determined as latest Ordovician (Richmond) by Ulrich (Richardson, 1909) and Ulrich and Kirk (Darton, 1928-a, p 13). Kelley and Silver (1952) have recently elevated the Montoya to group status and divided it into four formations.

The base is well marked by a unit which ranges from a loose friable calcareous sandstone to a well-cemented orthoquartzite. This unit contains well-rounded coarse quartz grains which commonly show some opalescence. In Ladrone Gulch, and in several other localities, the basal part of this sandstone contains flattened slabs of boulder and cobble size from the underlying El Paso limestone. The maximum measured thickness of this sandstone is 31 feet, although lesser thick-

nesses are more common and in one locality the sandstone is entirely absent. Above the sandstone is a gray to black fine-grained massive dolomitic limestone or dolomite whose thickness ranges from 2 to 24 feet. It contains sparse crinoid columnals, sparse small black chert lenses, and a few thin beds of a calcareous siltstone.

Overlying the dolomite is a massively bedded, gray to black fine-grained limestone. The maximum thickness for this unit is 47 feet. Locally it contains sparse, small, ellipsoidal gray chert nodules. Near the base, it has been considerably fractured and brecciated. The brecciated portions have been recemented by a lighter-gray dolomitic limestone and, to a very small extent, by white vein calcite. In the lower part of this unit are numerous large spheroidal or ellipsoidal cavities and masses (4-12 inches in diameter) elongated and layered parallel to the bedding (pl 2). In general the interior of the cavities contains remnants of a white material. The spheroidal or ellipsoidal masses, which presumably are the equivalent of the material that once filled the cavities described above, reveal a concentric structure as follows:

1. An outer shell of finely laminated black or gray, and white limestone. The laminae are concentric.
2. An intermediate shell of white friable sugary calcite.
3. A central core of coarsely crystalline white calcite.

The origin of these spheroidal masses remains a problem. Possible hypotheses of the origin might be outlined as follows:

I. Primary origin
   Formed at time of deposition by conditions similar to those causing formation of mud balls.
II. Secondary origin
   A. Originally the nodules represented a material of greater solubility than the surrounding limestone, e.g., a different limestone or phosphatic material, etc. This material was dissolved out and subsequently the cavities were filled with their present material.
   B. The original nodule material has undergone a replacement which occurred in three phases corresponding to each con-centric shell.

A striking feature of this approximate stratigraphic horizon is a massive chert bed or zone 25-35 feet thick. It consists of angular chert pebbles and cobbles in a black, gray, or reddish-brown silicified matrix. In some localities it is missing. Near the Gray Eagle mine, in the vicinity of the juncture of South Percha Creek and Drummond Gulch, a massive chert zone is at a much lower horizon. Here it is found inter-mingled with, and forming a large part of, the basal orthoquartzite bed. The fact that massive chert zones occur at differing stratigraphic horizons suggests that they are of secondary origin. Furthermore, in the vicinity of the Gray Eagle mine ore deposits are found in the El Paso

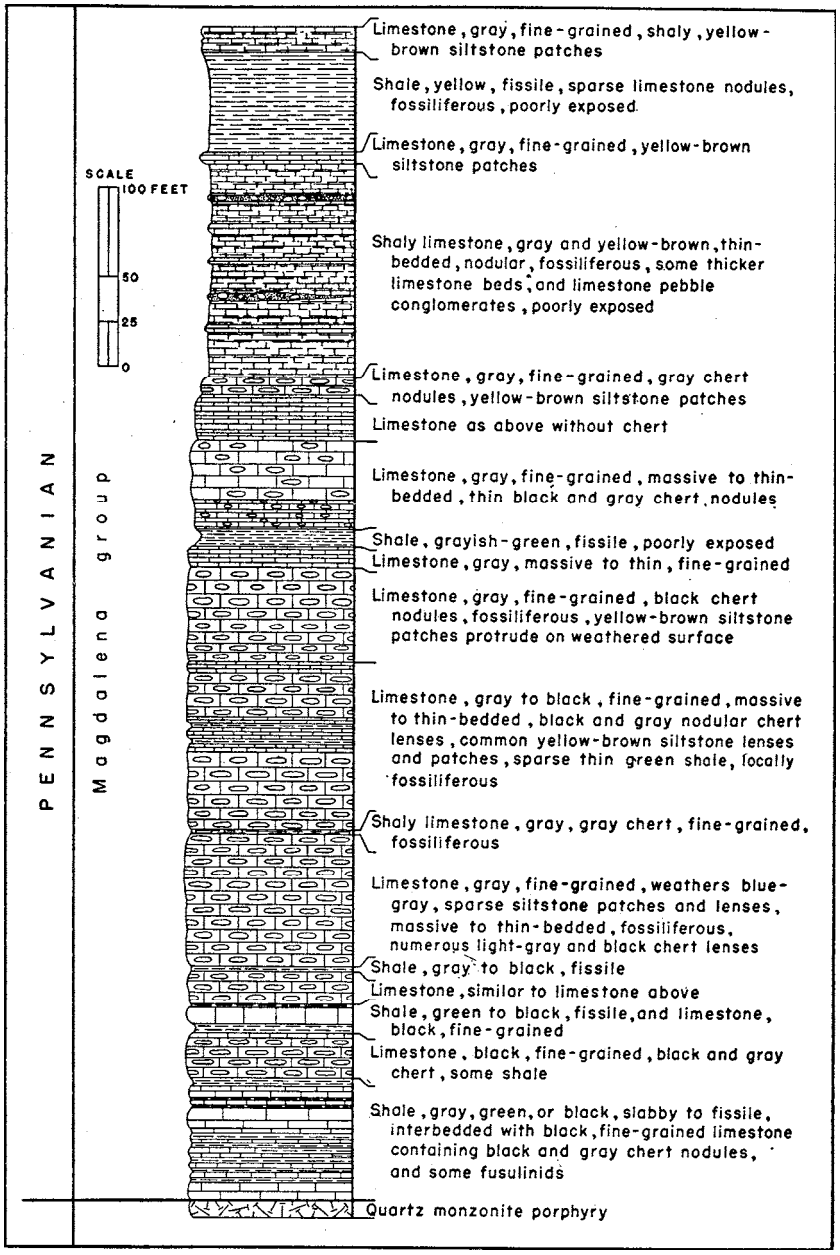

Figure 6. SECTION III. COMPOSITE OF TWO SECTIONS: ROAD CUT (SEC. 19), AND IN DRY GULCH (SEC. 18) , T. 16 S., R. 8 W.

limestone, not too far from the chert zone described above. Toward Kingston (Section II), where ore deposits are found at or near the top of the Montoya (or in the overlying Fusselman dolomite), the chert zone is higher. This massive chert zone may represent a phase of the mineralization.

The top unit of the Montoya formation is a black to gray fine-grained limestone or dolomite which weathers gray and is very thin-bedded (5 inches and less for most beds, very rarely up to 2 feet in thickness). Nodular limestone in this top unit is interbedded with one or two of the following materials, varying from one outcrop to another and within the same outcrop: nodular thin gray and/or black chert lenses; gray friable calcareous siltstone; or lenses, larger irregular masses, and/or very thin beds of black nodular chert. The thickness of this thin-bedded limestone ranges from 70 to 90 feet.

The Montoya limestone crops out near the Grandview, Gray Eagle, Lady Franklin, Iron King, and United States mines. Its maximum measured thickness is 161 feet (see Section II). As the Montoya closely resembles the Fusselman dolomite and underlies it conformably, it can be separated only approximately. The approximate ratio of limestone to dolomite beds in the Montoya limestone is 2:1.

SILURIAN SYSTEM

The Fusselman dolomite, like the formations previously described, was named by Richardson (see Wilmarth, 1938, p 788) from its exposures in Fusselman Canyon, Franklin Mountains, Texas. In the Kingston area, as in other localities, it is apparently conformable over the Montoya limestone. Very sparse crinoid columnals were the only fossils found. However, several other workers (Darton, 1917-a, p 43; 1917-b, p 5; Dunham, 1935, pp 43-44; Paige, 1916, p 5; and Richardson, 1909, p 4) in nearby localities, while mentioning the rarity of the faunal remains, have succeeded in collecting enough material to establish the Niagaran age (Middle Silurian) of this formation.

The estimated ratio of dolomite to limestone beds is 6:1 in the Fusselman. The average thickness of the Fusselman dolomite in all measured sections (Section II) is 85 feet. Owing to the lithologic similarity and to the small outcrop area of the Fusselman, it is represented on the map (pl 1) as combined with the Montoya. In the stratigraphic measurements, the contact of the Montoya and Fusselman formations was chosen arbitrarily as the top of the thin-bedded nodular limestone or dolomite and the base of the overlying massively bedded gray to black dolomite. This conforms closely to previous descriptions of the formations by Darton (1928, pp 11-14), Dunham (1935, pp 43-44), and Lloyd (1949, pp 52-54).

Most of the formation consists of a gray, brownish-gray, or black, fine-grained, massive dolomite, which weathers a light gray. In the middle part it contains several thin black fine-grained limestone beds. Very sparse gray chert nodules and lenses are found in the Fusselman. In one locality the dolomite is thin-bedded in the upper part of the formation. Most of the known ore deposits in the Kingston area occur as veins and replacements in the Fusselman.

DEVONIAN SYSTEM

The Percha shale was first described by Gordon (1907) and named for its exposures along Percha Creek in the vicinity of Kingston and Hillsboro, New Mexico. The Percha seems to be conformable over the Fusselman. The relations could not be determined with certainty because:

1. The Percha shale is the least competent of all Paleozoic formations in this area, and consequently has been deformed the most as a result of faulting, slight folding, and igneous intrusion.
2. The Percha shale offers the least weathering resistance, so that outcrops consisting of more than loose slope wash are rare.
3. The underlying Fusselman, for the most part, is very massive, showing almost no structure.
4. Finally, in many places (west and northwest of Kingston, see pl 1) the top of the Fusselman has been extensively mineralized and altered, so that most structures are not apparent.

The Percha shale is about 147 feet thick and may be divided into two members. The lower unit has been named the Ready Pay member (Stevenson, 1945, p 241) and consists of a black fissile unfossiliferous shale. The upper unit, the Box member, is a green to grayish-green calcareous shale which contains black fine-grained limestone nodules and lenses, and a few thin limestone beds. The Box member is highly fossiliferous and most of the fauna is found in the limy portions.

The fauna of the Box member of the Percha shale consists chiefly of brachiopoda, bryozoa, and crinoid stems and columnals. Stainbrook (1947) and Fritz (1944), respectively, have described the brachiopoda and bryozoa of the Percha shale. A few brachiopods, collected and tentatively identified by the author, appear to be identical with those described by Stainbrook. Until recently this formation was regarded as Upper Devonian in age (Stevenson, 1945; Cooper, et al., 1942; and Darton, 1928). However, Stainbrook (1947), after studying the Percha fauna and the fauna of other Devonian formations in New Mexico, concluded that the entire Percha shale is younger than the other Devonian formations in New Mexico and is probably of Mississippian age. Dr. J. Marvin Weller has examined briefly the fauna collected by the author and has suggested that the brachiopods appear to be a transitional fauna which might represent either uppermost Devonian or lowermost Mississippian. Although the Percha is relatively thin and lithologically uniform, the possibility that it may contain faunas of two ages, as suggested by Stoyanow (1948), cannot be excluded.

No fossils have been found in the lower or Ready Pay member of the Percha. In west Texas and southeastern New Mexico, the Wood-ford black shale is similar lithologically to the Ready Pay member and occupies approximately the same stratigraphic position (Lloyd, 1949, pp 48-49). The Woodford black shale is Upper Devonian, according to Ellison (1946), on the basis of conodonts and fossil wood.

The Percha shale crops out in the vicinity of most of the mines.

Excellent exposures may be seen along State Highway 180, several miles west of Kingston. The overlying unit is the Mississippian Lake Valley limestone which is separated by a disconformity from the Percha shale.

MISSISSIPPIAN SYSTEM

The Lake Valley limestone was first named by Cope (see Wilmarth, 1938, p 1138). It is separated from the Percha shale by a disconformity. In the Kingston area, the thickness of the Lake Valley formation is approximately 140 feet.

The base is a gray coarsely crystalline limestone, largely composed of crinoid-columnal fragments, in lenticular beds 18 inches and less thick. This lenticular unit has a maximum thickness of 8 feet. It is possible that this basal unit may be all that is present of the Andrecito member (Laudon and Bowsher, 1949).

Overlying the basal limestone is a black fine-grained limestone, massively bedded, the upper part of which contains abundant black and gray nodular chert lenses. Many of the chert lenses have the black and gray color arranged in alternating lieseganglike bands. This unit, which is approximately 23 feet thick, with respect to lithology and stratigraphic position is probably the equivalent of the Alamogordo member described by Laudon and Bowsher. These two lower units form a massive and prominent scarp in most of their outcrops.

The middle unit, approximately 36 feet thick, consists of a black slabby shaly fine-grained limestone which weathers a bluish green or yellowish green. It is highly fossiliferous and all the fossils were collected from this horizon. Thin limestone beds are interbedded with the shaly limestone. The uppermost unit is a gray coarse-grained crystalline limestone which contains abundant gray-white nodular chert lenses, I foot and less in thickness. The beds of this 75-foot unit range from massive to thin. The Nunn and Tierra Blanca members, as defined by Laudon and Bowsher, probably correspond to the middle and upper-most units, respectively.

West of the crest of the Black Range, near the Iron Creek camp-ground (Section I), a measured section of the Lake Valley limestone is considerably thicker. However, three igneous dikes cut across the sediments and might represent zones of displacement, so that the apparent increase in thickness may be due to faulting. In this vicinity (Section I) the stratigraphic section contains the crest of a gentle anti-cline plunging northward. Near the crest of the anticline the limestone is very coarse-grained in part and slightly mineralized, although still showing most of the primary features of the Lake Valley limestone. Many of the chert nodules and lenses are enclosed by a thin rim of fibrous wollastonite. Garnet and a mineral whose optical properties

Figure 7. SECTION IV. COMPOSITE OF SECTIONS: ALONG LADRONE GULCH (SEC. 13) , ROAD CUT AND HILL SLOPE (NE¼ SEC. 24) . T. 16 S., R. 9 W. (UNSURVEYED) .

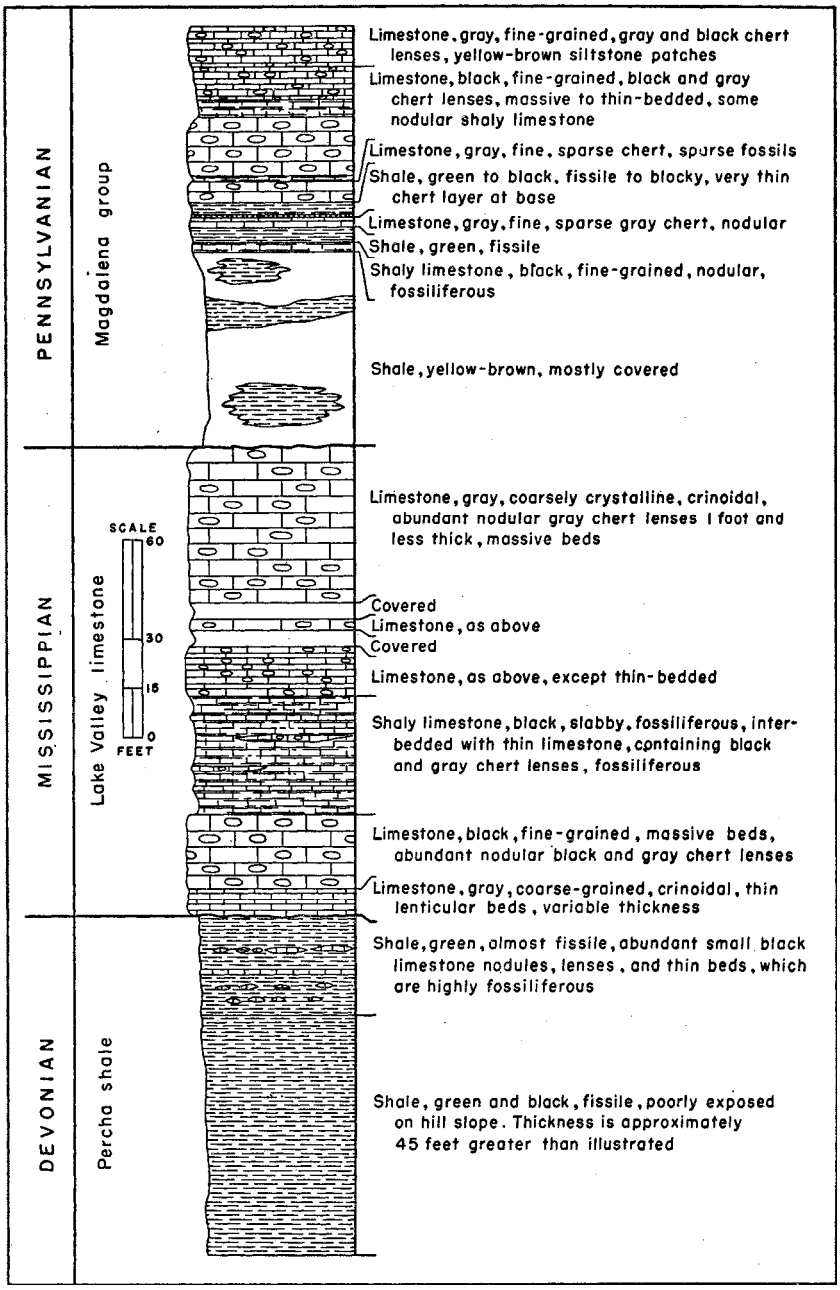
PENNSYLVANIAN
Magdalena group
Limestone, gray, fine-grained, gray and black chert lenses, yellow-brown siltstone patches
Limestone, black, fine-grained, black and gray chert lenses, massive to thin-bedded, some nodular shaly limestone
Limestone, gray, fine, sparse chert, sparse fossils
Shale, green to black, fissile to blocky, very thin chert layer at base
Limestone, gray, fine, sparse gray chert, nodular
Shale, green, fissile
Shaly limestone, black, fine-grained, nodular, fossiliferous
Shale, yellow-brown, mostly covered
MISSISSIPPIAN
Lake Valley limestone
SCALE
60
30
15
0
FEET
Limestone, gray, coarsely crystalline, crinoidal, abundant nodular gray chert lenses 1 foot and less thick, massive beds
Covered
Limestone, as above
Covered
Limestone, as above, except thin-bedded
Shaly limestone, black, slabby, fossiliferous, interbedded with thin limestone, containing black and gray chert lenses, fossiliferous
Limestone, black, fine-grained, massive beds, abundant nodular black and gray chert lenses
Limestone, gray, coarse-grained, crinoidal, thin lenticular beds, variable thickness
DEVONIAN
Percha shale
Shale, green, almost fissile, abundant small black limestone nodules, lenses, and thin beds, which are highly fossiliferous
Shale, green and black, fissile, poorly exposed on hill slope. Thickness is approximately 45 feet greater than illustrated

Figure 7

correspond to an end member of the chlorite group commonly called "serpentine" (Winchell, 1945, pp 276-279), were found in some of the fractures and in the limestone itself. Several silicified chertlike beds still contain fenestellid bryozoan remains.

The fauna, collected by the author from the middle unit of the Lake Valley limestone, is of Mississippian age and consists chiefly of brachiopods, crinoid fragments, and a few trilobite pygidia and spines. On the basis of this collection, Dr. Weller has suggested that the age of the Lake Valley limestone lies somewhere in the range Kinderhook to Osage. This corresponds to Laudon and Bowsher's (1949) conclusion.

The Lake Valley limestone, which is separated from the overlying Pennsylvanian Magdalena formation by a disconformity, crops out in Ladrone Gulch and near the Lady Franklin mine, northwest of Kingston, also along South Percha Creek, and in large inliers southwest of Emory Pass.

PENNSYLVANIAN SYSTEM

The Magdalena was first proposed as a group name by Gordon (1907-b), who named it for its development in the Magdalena Mountains, New Mexico, where it has been divided into two formations. In the Kingston area, however, the lithologic uniformity of this formation precludes any subdivision except on a faunal basis. For the purpose of description, the Magdalena has been arbitrarily divided into units with very similar characteristics. Since the lithology at any stratigraphic horizon varies considerably, these units must be regarded as integrations of a generalized nature. For the exact details the reader is referred to Sections I, III, and IV.

The basal unit consists primarily of shale and shaly limestone. The shale, which generally weathers brown, may be gray, yellow, brown, green, or black, and is blocky, slabby, or fissile. The shaly limestone is gray to black, thin-bedded and nodular, with some gray or black chert lenses. Some limestone beds contain abundant small fusulinids. In Section I and in several other localities, this unit also contains a gray fine-grained well-cemented blocky orthoquartzite bed. The average thickness of the basal unit is approximately 50 feet.

The distinguishing feature of the next youngest unit, approximately 55 feet thick, is the massiveness of most of the limestone beds. The limestone is gray to black, and contains nodular black and light-gray chert lenses, numerous fossils (especially fusulinids), and, in Section I, lenticular zones with abundant crinoid columnals. Some weathered surfaces are covered with a yellowish-brown siltstonelike material. Locally it ranges to a thin-bedded slabby nodular shaly limestone. Interbeds of gray, greenish-black, and black shale are common.

The succeeding unit is about 200 feet thick and consists of massive- to thin-bedded limestone, containing nodular black and gray chert lenses. The chief unifying characteristic is that the beds are about equally divided between massive limestones, and silty limestones, siltstones, and shales. The shale is gray, green, or black, and fissile or almost so. The silty limestone appears identical to the massive

limestone on a fresh surface. However, in weathering it produces a yellowish-brown, *very* fine-grained, porous-looking surface, and breaks into angular blocks. The he silty limestone encloses gray lenses and large brachiopod-shaped masses that on weathering form slight depressions below the surface of the silty limestone. The differential weathering suggests that the irregular gray limestone lenses and patches are considerably lower in noncarbonate elastic content than the anastomosing yellowish-brown silty limestone portions. Several thin gray siltstone or sandstone beds occur at the base of this horizon in one locality (Section I). Near the top of this unit, in one place (Section III), there is a chert (or silicified) bed. Fossils are common and consist chiefly of fusulinids and brachiopods.

A grayish-green fissile shale bed, about 10 feet thick, is the next unit. It is generally poorly exposed or concealed. The unit overlying the shale is very similar to that which underlies the shale. Its thickness is approximately 80 feet.

The next youngest unit, 120 feet thick, is a gray thin-bedded nodular shaly limestone. It is highly fossiliferous and weathers a yellowish-brown, possibly owing to a high noncarbonate clastic content. It is interbedded with thicker beds of a gray to black, fine-grained limestone. A striking feature of this unit is the presence of lenticular limestone pebble-conglomerate lenses, 5 feet and less thick. These conglomerates are gray and have a matrix consisting of coarse-grained fragmental carbonate detritus and fine black carbonate. The pebbles are well rounded and consist of limestone and fossil fragments. Many pebbles are enveloped by a thin fine-grained black concentric layer, which may have formed in a manner similar to that of mud balls.

Above is a massive gray fine-grained silty limestone unit, 12 feet thick. On a weathered surface it has a yellow-brown color with slight gray depressions, as described above. This unit is overlain by a yellow, slabby to fissile, shale containing sparse limestone nodules which are highly fossiliferous. This shale is approximately 60 feet thick; the exposures, however, are poor.

The uppermost unit in the measured stratigraphic sections (Sec-don III) is 15 feet of gray fine-grained shaly limestone which weathers to a yellowish brown. Above the measured sections there remains an estimated 50-75 feet of a slabby nodular shaly limestone which is concealed in most localities. The total thickness of the Magdalena in this area is at least 650 feet.

The fossils found in the Magdalena consist mainly of foraminifera and brachiopods. Dr. Weller has examined the brachiopod fauna collected by the author and has suggested that their probable range is from middle Pennsylvanian to Permian. However, it is recognized that brachiopods alone are very unsuitable for determining a precise age in the Pennsylvanian (Weller, 1947, p 258). Needham (1937, pp 13-15) has collected fusulinids from near Kingston, New Mexico, and has correlated the lower part of the Magdalena with parts of the Des Moines series of the midcontinent region.

As the term Magdalena is practically synonymous with Pennsylvanian in New Mexico (Thompson, 1942, p 22), various authors

(Thompson, 1942; Kelley and Silver, 1952; see also Read and Wood, 1947) have divided it into smaller formational units. At the present time, however, separation of the Magdalena group into formations in the Kingston area would be unwarranted.

The Magdalena limestone is found in extremely dissected north-south cuestas just west of the town of Kingston. It' is well exposed in road cuts at 3 points along State Highway 180—approximately 2 miles west of Kingston, north of the Gray Eagle mine, several hundred yards east of the Iron Creek campground—and in numerous other localities. In the Kingston area it is overlain conformably by the red beds of the Abo formation.

PERMIAN SYSTEM

The Abo formation was first named by W. T. Lee (see Wilmarth, 1938, p 9) for its exposures in Abo Canyon at the southern end of the Manzano Mountains, New Mexico.

In the Kingston area it is at least 70 percent red shale and at the most 30 percent red siltstone, sandstone, and arkosic conglomerate with very minor thin limestone beds. For the most part the shale is massive and nonresistant, so that its outcrops are poor. Locally the shales and siltstones have a greenish color unevenly distributed throughout the layers, which may be the result of a secondary reduction of the ferric oxides. Several thin nodular shaly limestone and calcareous shale beds are present; these generally have a green color, or greenish tinge.

Numerous thin conglomerate beds occur throughout the Abo formation. These consist of angular to round pebbles, granules, and coarse sand of gray limestone, red shale, and reddish-gray chert cemented by white calcite or a greenish-gray fine-grained limestone. Approximately 1¼ miles east of the mapped area and north of State Highway 180, these conglomerates cap a series of small cuestas within the easily eroded Abo formation. Several thin intraformational conglomerate beds in the Abo can be easily distinguished by their fissile red shale matrix. The pebbles in the intraformational conglomerates consist of gray limestone, red sandstone, and red shale.

The top beds in many localities are considerably different from the underlying portions. At the top, or within 60 feet of the Abo-early andesite contact, is a massive red shale which is similar to the lower parts of the formation. Locally, however, the red shale is overlain by 20 feet of buff to brown, massive, crossbedded orthoquartzite. In Section V at this horizon, a green massive- to thin-bedded siltstone, 36 feet thick, is interbedded with thin shale units. Overlying this is 10 to 25 feet of interbedded black fissile shale and a black and gray shaly limestone. Again at Section V, this black shale horizon seems to be represented by 4 feet of a red and green fissile shale interbedded with a gray nodular limestone. Above this horizon is a white, gray or pink, massive, crossbedded, medium- to coarse-grained orthoquartzite. Coarse

Figure 8. SECTION V. COMPOSITE OF TWO SECTIONS: ROAD CUTS ON STATE HIGHWAY 180, IN SECS. 16 AND 22, T. 16 S., R. 9 W. (UNSURVEYED).

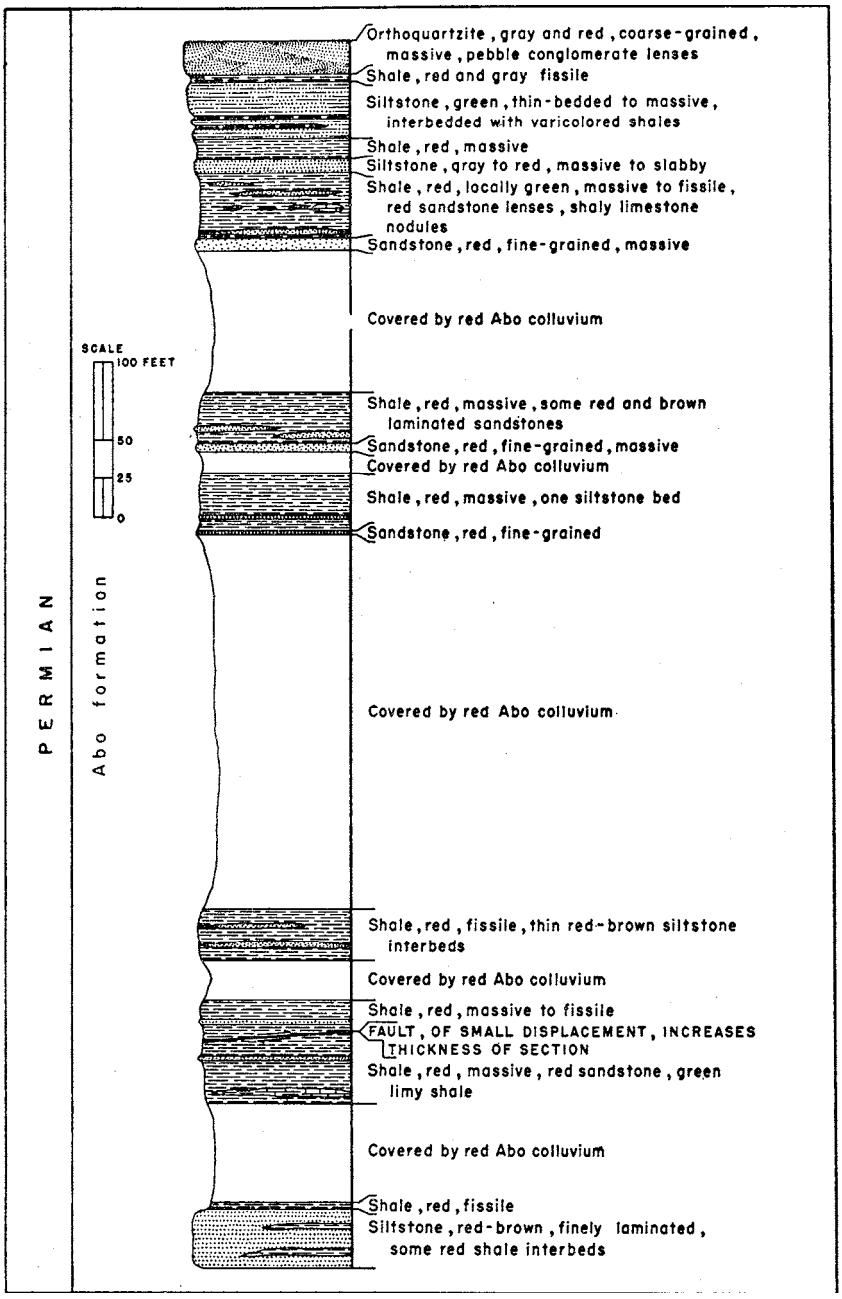
PERMIAN
Abo formation
SCALE
100 FEET
50
25
0
Orthoquartzite, gray and red, coarse-grained, massive, pebble conglomerate lenses
Shale, red and gray fissile
Siltstone, green, thin-bedded to massive, interbedded with varicolored shales
Shale, red, massive
Siltstone, gray to red, massive to slabby
Shale, red, locally green, massive to fissile, red sandstone lenses, shaly limestone nodules
Sandstone, red, fine-grained, massive
Covered by red Abo colluvium
Shale, red, massive, some red and brown laminated sandstones
Sandstone, red, fine-grained, massive
Covered by red Abo colluvium
Shale, red, massive, one siltstone bed
Sandstone, red, fine-grained
Covered by red Abo colluvium
Shale, red, fissile, thin red-brown siltstone interbeds
Covered by red Abo colluvium
Shale, red, massive to fissile
FAULT, OF SMALL DISPLACEMENT, INCREASES THICKNESS OF SECTION
Shale, red, massive, red sandstone, green limy shale
Covered by red Abo colluvium
Shale, red, fissile
Siltstone, red-brown, finely laminated, some red shale interbeds

Figure 8

or fine sand lenses, and conglomerate lenses, 3 inches or less in thickness, of rounded chert and quartz pebbles, are common in the orthoquartzite, which may be friable or well cemented. Near Kingston the orthoquartzite contains some gray, yellow, and purple shaly interbeds. At Section V this sandstone has red and gray shale partings between the massive beds. The thickness of the unit ranges from 15 to 30 feet. These top beds are best exposed in the draws north of State Highway 180, between a quarter and a half mile west of Wright's Cabin campground.

The estimated thickness of the Abo formation is 700 feet. As the red beds are the least resistant of any of the Paleozoic formations, they are poorly exposed and are found mostly in depressions. Their areal extent, however, can be easily determined because of the intense red coloring they impart to the mantle rock. Although in Section V more than 50 percent of the formation is concealed by slope wash, it is still the best exposed section. The Abo formation crops out in and around the town of Kingston, 2½ miles west of Kingston, also just west of the crest of the range, and in several other localities. The Abo is separated from the overlying Tertiary andesite by a very marked erosional unconformity. Where the andesite overlies the Abo red beds, the layering of both formations is approximately parallel. In many localities, however, the Abo formation has been completely removed, so that the Tertiary andesite rests directly on the Magdalena limestone.

In the Kingston area, no fossils were found in the Abo formation. Its coloring is so intensely red, however, that the correlation is considered more certain than the average correlation based on lithology. The Permian age of the Abo formation is well established (see King, P. B., 1942, p 690; Miller and Parizek, 1948; Langston, 1949). Southward, according to Needham and Bates (1943, p 1657), the Hueco limestone is the equivalent of the Abo formation. Darton (1926) has correlated the Abo formation with part of the Supai formation of the Grand Canyon region of Arizona.

Until recently the entire Abo has been considered as basal Permian (Wolfcamp series). Owing to its lithologic character, and the plant and vertebrate fossils which it contains, the Abo is considered to be terrestrial in origin. P. B. King (1942, pp 675-677, 687-690) has presented evidence which, he believes, suggests that the Abo is primarily of Leonard age (lower Permian, but overlying the Wolfcamp series). The evidence for this is that the marine fossils establishing Wolf-camp age are supposed to have come from transitional beds (i.e., interbedded limestone, red and gray shale, and arkosic conglomerates) which actually underlie the Abo and which have been mapped as part of the underlying Magdalena group. King (1942, pp 687-690) also reports that fossil plants from the upper Abo beds studied by C. B. Read constitute a Supai floral assemblage, which is supposedly of Leonard age. Inasmuch as the Abo formation is a lithologic unit and contains very few marine fossils, exact time-stratigraphic correlation with either the marine Leonard or the marine Wolfcamp series would seem impossible. Skinner (1946, p 1871) and Lloyd (1949, pp 30-31) have conjectured that the Abo formation actually crosses the time boundary represented by the Leonard-Wolfcamp contact. Thompson's cross-section (1942, pl

II), and Miller and Parizek's (1948) faunal age determinations suggest that most of the Abo formation in New Mexico is of late Wolfcamp age.

The 60 feet (approximately) of sandstone and limestone described on pp 24, 26, which occur at the top of the Abo red beds in several localities of the Kingston area, are inconsistent with the uniform lithology of the Abo formation as a whole. However, the base of the Permian Yeso formation, which overlies the Abo red beds in many parts of New Mexico, as described by Needham and Bates (1943, pp 1658-1661), is very similar to the shaly limestone and massive orthoquartzite beds found within the upper 60 feet of the Abo formation, as mapped in the Kingston region. It is possible that these upper beds may represent erosional remnants of the Yeso formation, which suggests that sedimentation, as in adjacent regions, continued after formation of the Abo red beds.

SUMMARY OF THE PALEOZOIC STRATA

An integrated picture of the Paleozoic rocks in the Kingston area can be attained by tabulating the stratigraphy in various age groups, as in Table 2. The regional relationship is obviously derived from a study of the geologic literature of New Mexico and omits many details which can be found in the references cited. Cambrian through Mississippian rocks are not found north of the 34th parallel in New Mexico,' whereas near the southern border of New Mexico these rocks attain great thicknesses. From this it appears likely that north of the Kingston area there existed a stable land mass and that to the south there was a deep, or rapidly subsiding, depositional basin (Sonora trough, Schuchert, 1930, fig 1). The presence and character of the Pennsylvanian and Permian rocks throughout the state have led to the conclusion that, during the periods when these rocks were deposited, orogenesis was taking place in north central New Mexico (Melton, 1925; and others), marine waters advanced over most of the state, and finally retreated from most of New Mexico.

Compositional differences (table 2) between the upper and lower Paleozoic rocks are qualitative estimates based on the field occurrence and to a lesser extent on microscopic determinations. The major constituents of the pre-Devonian rocks are limestone, dolomite, and sand-stone. Devonian and later Paleozoic rocks, on the other hand, consist primarily of limestone and shale. The presence or absence of dolomite, and the abundance of shale, are the most pronounced differences between these two groups.

Under sedimentary facies (table 2), supposedly the orthoquartzite-limestone suite represents marine deposition in a relatively shallow sea, which has covered a low and stable part of the earth's crust (Pettijohn, 1949).. The arkose suite is considered to be formed by terrestrial deposition in one area while mountain building in an adjacent area is in its later stages (ibid). Although the Permian red beds in the Kings-

1. Recently Read and Wood (1947, pp 229, 231-32, 235) have suggested that some thin strata in northern New Mexico formerly mapped as Pennsylvanian may actually be Mississippian, or even Devonian.

ton area may not be true arkoses, most geologists would agree that they are probably terrestrial deposits, and that for this reason they fit best in the arkose suite.

Finally, the Paleozoic sediments may be grouped (table 2) according to their behavior with respect to the igneous intrusions in the mapped area. Cambrian through Silurian rocks (mostly carbonates and sand-stone) were apparently much more rigid and impermeable with regard to the igneous intrusion than the overlying Devonian through Permian rocks (mostly limestone and shale). The mechanical behavior of the Paleozoic sediments is presented in detail in the sections on the major structural features and the quartz monzonite porphyry.

TABLE 2. CLASSIFICATION OF THE PALEOZOIC STRATA IN THE KINGSTON AREA

CLASSIFICATORY CRITERION	CHRONOLOGIC GROUP	REMARKS
Regional relationship	Cambrian to Mississippian	Stable positive area to north and Sonora trough to south
	Pennsylvanian to Permian	Orogeny to north, maximum marine inundation, followed by regression of sea
Composition	Cambrian to Silurian	Limestone, dolomite, sandstone, some shale
	Devonian to Permian	Limestone, shale, sandstone, no dolomite
Sedimentary facies	Cambrian to Pennsylvanian	Orthoquartzite-limestone suite
	Permian	Arkose suite
Mechanical behavior with respect to igneous intrusives	Cambrian to Silurian	More rigid and resistant
	Devonian to Permian	Less rigid and resistant

Tertiary Sequence

INTRODUCTION

General chronology. The sequence of rock units younger than the Paleozoic sediments is, in order of decreasing age:

1. Fanglomerate deposit. This is found only in one locality.
2. Andesite, latite, and their corresponding quartzose counterparts occurring as flows, tuffs, and agglomerates.
3. Quartz monzonite porphyry intrusives.
4. Extrusive tuffaceous rhyolite, intrusive rhyolite porphyry, rhyolite dikes, and rhyolite vitrophyre dikes and irregularly shaped masses.
5. Arkosic sandstone, conglomerate, and tuff beds.
6. Late andesite flows and agglomerates.
7. Early gravel deposits. This unit is partly contemporaneous with the late andesite of item 6 (above).

The ages of these rock units can only be estimated by comparison with nearby regions and with respect to the regional picture which has been formed concerning the Tertiary history of the western part of the United States. Volcanic rocks of possible Cretaceous age have been de-scribed (Paige, 1916, p 7) in the nearby Silver City region. According to many studies their distribution is limited and they have been altered considerably in contrast to the more widespread and more unaltered volcanic rocks listed above. In the Rocky Mountain region of the United States, according to Callaghan (1951), the volcanic rocks may be divided into three series, of which the first two are Tertiary, but older than latest Miocene, and the third ranges in age from Pliocene to post-Wisconsin. The rock units of items 2, 4, and 6 (above) may correspond, respectively, to these three series. In the NE¼, sec. 13, T. 16 S., R. 8 W., approximately 5 miles east of the mapped area on State Highway 180, there are Tertiary lake beds with a conifer flora. This flora has been identified (Brown, R. W., personal communication) as between early Miocene and early Pliocene in age. Reconnaissance studies of the lake beds and the volcanic rock which overlies the lake beds suggest that, in terms of stratigraphic position, the arkosic sand-stone, conglomerate, and tuff listed above (item 5) are of approximately the same age. In addition, Knechtel (1936) has reported the Pliocene age of the Gila conglomerate in southeastern Arizona, with which these early gravels might tentatively be correlated, with respect again to their stratigraphic position and distribution. These age assignments, al-though inconclusive, seem reasonable in view of the present-day data.

The post-Permian pre-Tertiary land surface. Some generalized conclusions concerning the land surface may be drawn on the basis of the following evidence:

1. Post-Abo Permian sediments have been found in many localities in Sierra County, New Mexico (Harley, 1934, pl 2).
2. Cretaceous sediments have also been reported (Harley, 1934,

pl 2; Spencer and Paige, 1935, pp 28-31) in regions surrounding the mapped area.

3. In the mapped area the earliest Tertiary rocks overlie either the Pennsylvanian Magdalena limestone or the Permian Abo formation, but no older formation.

4. The angle between the planar structures of the earliest Tertiary rocks and the nearest underlying Paleozoic sediment varies from 4 to 65 degrees. South of Kingston and northeast of Iron Creek, the structure in both rocks is nearly parallel.

5. In a road cut, half a mile south of Emory Pass, a boulder deposit occurs between Paleozoic red beds and the oldest Tertiary volcanic rocks. This deposit contains both red shale and sandstone fragments of the Abo formation and altered fragments of some volcanic rock. The boulders and cobbles are subrounded, slightly brecciated, hematite-stained, and show some slickensided surfaces. The matrix consists of coarse sand and small shale fragments. There are two reasons for interpreting this deposit as a local fanglomerate, along which postdepositionally some movement or beddingplane faulting occurred, rather than as a fault breccia: (a) the high degree of roundness of some of the larger fragments, and (b) the boulders do not appear to be derived from the volcanic rocks in the immediate vicinity.

Items 1, 2, and 3 (above) suggest that the pre-Tertiary rocks of this area had been considerably eroded. Items 3 and 4 imply that there was some tilting, folding, and/or faulting in pre-Tertiary time. The fanglomerate described under item 5, may not be pre-Tertiary, because the volcanic rock boulders which it contains are of unknown age. Since, however, the fanglomerate is found at the base of the volcanic sequence, it is likely that near the beginning of the recorded Tertiary events the regional relief was considerable. The general parallelism (item 4 above) of the pre- and post-Tertiary planar structures in large areas implies that the deformational effects may have been localized as a result of tilting and block faulting.

ANDESITE, LATITE, AND THEIR QUARTZOSE EQUIVALENTS

These rocks occur as flows, tuffs, and agglomerates, and form the earliest volcanic series. In this report this unit has been called the early andesite sequence. The early andesite volcanic sequence crops out chiefly along the central part of the Black Range, and to a smaller extent in the vicinity of Kingston, east of the crest of the Range. In the western part of the area mapped, it does not appear at the surface. The unconformable relationship between this volcanic sequence and the underlying Paleozoic strata has previously been described. Estimated thicknesses of the early andesite in various localities range from 250 to 1,700 feet. Just north of Kingston it is very thin or missing between the younger tuffaceous rhyolite and the Permian Abo formation. This suggests a stratigraphic break between the early andesite and the tuffaceous rhyolite. Their planar structure and bedding are

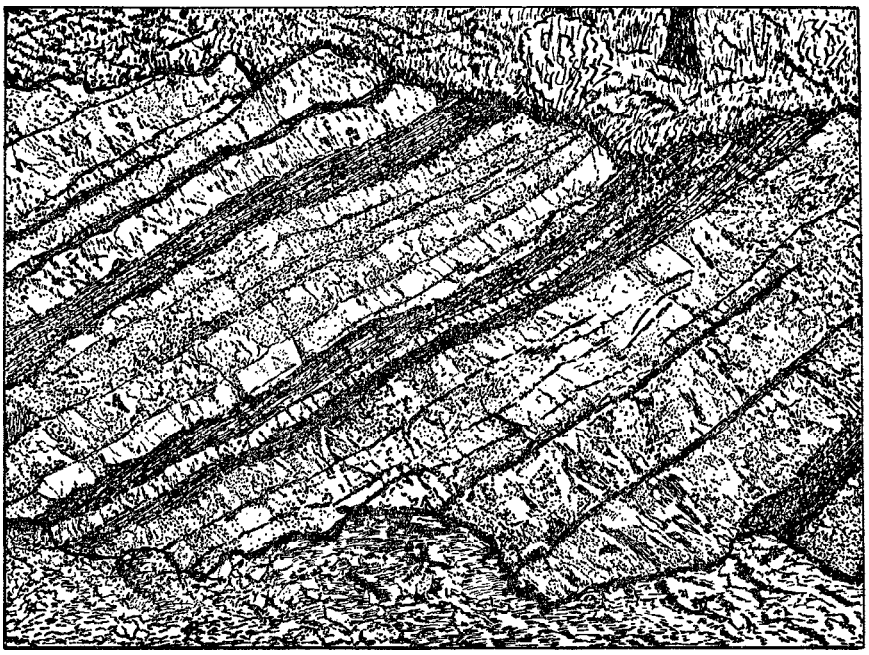

Figure 9
INTERBEDDED FLOWS AND TUFFS OF THE EARLY ANDESITE IN ROAD CUT ONE-HALF MILE WEST OF EMORY PASS. HEIGHT OF OUTCROP IS ABOUT 12 FEET.

nearly parallel in some places; in other areas they exhibit a marked unconformity.

The lower part of the early andesite volcanic sequence consists of well-bedded flows, tuffs, and agglomerates (see fig 9). The flows are a dense bluish black with sparse colorless to white feldspar phenocrysts about 2 mm long. The thickness of the individual flows in the lower part of this unit is in most outcrops 6 feet or less. The terminology used in describing the tuffs and agglomerates, with some modification, is that defined by Wentworth and Williams (1932). Volcanic breccias consist predominantly of sharp angular fragments, whereas the agglomerates contain more highly rounded fragments, though showing no features of water-laid sediments. Interbedded with the flow units are thin beds of a red-violet, fine to coarse, essential or accessory tuff, and thick beds of light-green, gray, or purple lapilli tuff or agglomerate. The fragments in the pyroclastic beds are aphanitic porphyries with very abundant small (1 mm and less) subhedral white phenocrysts, that have been considerably altered. Less abundant, but identical, phenocrysts are also found in the matrix of the pyroclastic rocks.

Above this is a great thickness of massive flows and flow breccias. These rocks are aphanitic, red violet, purple, gray, green, or various combinations of these colors, and contain abundant white subhedral

phenocrysts which may be as large as 1 cm, although most are 2 mm and less. Locally, small hornblende laths which may show an alignment are abundant. Faint color bands and a slabby weathering, present in many outcrops, probably represent a flow banding.

The upper part of this volcanic sequence consists of massive beds of volcanic breccia and agglomerate, and thin to thick beds of essential and accessory tuffs. The grain size extends over the entire tuff range. These beds are red, purple, gray, green, white, black, or mixtures of these colors. The finer-grained black or purple tuff may weather into flattened pieces parallel to the bedding with rounded corners, such that the weathered surface resembles that of a cobblestone street. The phenocrysts of the larger fragments and the matrix are identical to those found in the pyroclastic rocks in the lower part of the early andesite sequence.

The field criteria which distinguish this volcanic sequence from the overlying tuffaceous rhyolite are:

1. Absence of visible quartz phenocrysts.
2. Presence of altered feldspars, i.e., white phenocrysts with a clayey luster and no shiny cleavage on a fractured surface.
3. A darker color, in general.
4. Never more than one feldspar megascopically. In many places white and pink feldspars can be seen in the overlying unit.
5. Locally abundant hornblende laths.
6. Absence of megascopic biotite.

There are exceptions to any single criterion. The combination of them leaves little doubt, however, as to the proper identification. Three-fourths of a mile south-southwest of the town of Kingston, enclosed by a bend in State Highway 180, this volcanic unit forms a small synclinal structure. Here some of the flows contain a considerable amount of very small quartz phenocrysts. This is the only known locality in which the first criterion listed above is not applicable.

Microscopically, the texture of the flows is holocrystalline, seriate porphyritic, and felty or trachytic. It contains corroded euhedral phenocrysts and a cryptocrystalline to aphanitic matrix. The analysis, norm, and mode of a quartz latite specimen from a flow in the lower part of this volcanic unit are given in Table 6 (see 389-A-236). The normative calcite and corundum in this specimen suggest that the original rock was dacitic. For the massive flows comprising the middle part of this volcanic sequence, the average mode of the primary components is (in percentages): andesine, 26.5; hornblende, 8.0; magnetite and ilmenite, 3.0; biotite, 2.0; matrix, 58.5; and small amounts of quartz and apatite. On the basis of the phenocrysts, these massive flows are andesites. How-ever, the composition of the matrix is largely unknown, and in several thinsections the amount of fine-grained quartz in the matrix appears to be considerable; the deviations from this mode may, therefore, be large. The petrographic description which follows deals primarily with the massive flows forming the middle part of this volcanic sequence.

The plagioclase occurs as resorbed and corroded phenocrysts, 5 mm

and less in size, and as fine microlitic laths. The composition of the plagioclase, determined by its extinction angles, is approximately An_{37}. Normal and oscillatory zoning are present. Common features of the larger andesine phenocrysts are myrmekitelike inclusions which are found throughout the grain, as a central core, or in a concentric zone about the central part. The material of the inclusions appears similar to the groundmass. Commonly, plagioclase develops thin clear outer rims which may display euhedral terminations. These phenocrysts commonly are clumped together and partly enclose one another.

The hornblende occurs as lath-shaped prisms with a pseudohexagonal cross-section. Its pleochroism is pale yellow, yellowish green, and green, from alpha to gamma, respectively. Its optic angle ($2V\alpha$) is approximately 85 degrees and r <v. Each hornblende grain is enclosed by a thin opaque hematite rim. Some of the hornblende has been partially resorbed and corroded.

.Biotite is pleochroic from dark brown to tan. It is rimmed with, and partially altered to, hematite. Locally the hornblende has been replaced by biotite. Most of the apatite needles are found within the biotite.

The matrix is cryptocrystalline to very fine-grained. Plagioclase microlites form the most easily recognized constituents. Numerous small anhedral magnetite and ilmenite grains are found in the groundmass. Very fine-grained quartz, which in several sections may be present in amount sufficient to change the rock name from andesite to dacite, occurs in the matrix. Some of the cavities in the matrix have been filled in concentric zones by quartz, opal, and several zeolites.

The common alteration and replacement minerals found in the flows are calcite, sericite, hematite, limonite, and leucoxene, in order of decreasing abundance. Locally the alteration is so intense that no primary minerals can be identified. This is especially true in the massive flows and flow breccias comprising the middle part of the early andesite sequence.

The microscopic texture of the tuff beds in the early andesite sequence is very similar to that of a graywacke. The tuff consists of a glassy to cryptocrystalline or fine-grained matrix, which may be clouded or even opaque. In some parts, however, eutaxitic banding, a felty texture, or both may be predominant in the matrix. The phenocrysts are seriate, locally broken, euhedral to subhedral, resorbed and corroded, and are composed chiefly of lath-shaped plagioclase. The rock fragments vary in size from fine-grained upward, are round to subround, and have the same texture and composition as the matrix, which shows flow textures.

Analyses, norms, and modes, which are probably typical of the pyroclastic rocks of this earliest volcanic sequence, are presented under NL2 and L2 in Table 6. On the basis of their chemical composition, some of these tuffs are classified as quartz latites.

Most of the phenocrysts in the quartz lathe tuffs are plagioclase, with optical properties corresponding to compositions ranging from An_{35} to An_{50}. The plagioclase is subhedral, twinned, zoned, fractured, broken, tabular, and slightly embayed and corroded by the groundmass. Many crystals enclose myrmekitelike masses, as described above.

In the tuff modes presented in Table 6, potash feldspar has not been counted separately from the plagioclase (An_{35}-An_{50}). The matrix and some of the phenocrysts are clouded intensely with fine hematitic dust; moreover, the phenocrysts in general are separated from one another by groundmass, so that in any counting process it is not possible to subdivide the feldspar without determining the optical properties of every untwinned feldspar phenocryst. Several U-stage determinations suggest that a small amount of potash feldspar has been included in the modal plagioclase.

Quartz forms small angular grains, 1 mm and less in size. Some of the grains show a slight rounding, possibly owing to resorption. Magnetite (and possibly ilmenite) is present as small euhedral to anhedral grains. A colorless pyroxene, which has been almost completely altered and replaced, is identified as pigeonite on the basis of the optic angle ($2V\gamma$), which is less than 40 degrees, and the extinction ($\gamma \wedge c$), which ranges from 21 to 35 degrees.

The matrix comprises at least 50 percent of the rock. It is consider-ably clouded, almost opaque where hematite (and leucoxene?) abounds. The matrix commonly contains a few small fragments of glass or devitrified glass.

Numerous secondary alteration minerals, as shown in Table 6, are calcite, sericite, chlorite, hematite and leucoxene, epidote, and one or more minerals which have been called zeolites. Finely divided hematite and leucoxene render thinsections opaque. Calcite forms small, irregular sutured grains within plagioclase and pyroxene, around irregular plagioclase and pyroxene remnants, and in the groundmass. Large phenocrysts, consisting only of calcite and sericite, are interpreted as complete replacements of the above-mentioned phenocrysts. Minute sericite shreds are also prominent in the feldspar, around and within the pyroxene, and in the matrix. Locally the chlorite attains prominence as a part of the matrix, associated with the pyroxene, and to a small extent on the perimeter and along the cleavage of the feldspar grains. In one specimen, some shard-shaped masses have a peripheral zone of anhedral quartz with a center of radially fibrous chlorite. Epi-dote occurs as sparse anhedral grains associated with calcite and chlorite in the replacement of plagioclase and pyroxene. In several thinsections the feldspar has been replaced by very fine-grained irregular masses which may be one or more zeolites. Their properties are:

1. Some parts have an undulatory or radial extinction.
2. Maximum birefringence of about .010.
3. Uniaxial negative or biaxial with a small 2V.
4. Some grains show two cleavages at approximately 88 degrees, and symmetrical extinction.
5. The indices relative to calcite and plagioclase are such that $n > 1.486$, $N < 1.548$. Grains immersed in oil show indices between 1.515 and 1.530.

Since the properties do not fit any of the common zeolites, it is possible that more than one mineral may be present. The silicic nature

of these rocks suggests that this mineral may not be, in fact, a zeolite. Item (1) above, and the symmetrical extinction, would seem to preclude the presence of a high-temperature feldspar. At any rate, because of its properties, small size, and amount, a tentative classification as "zeolites" has been deemed sufficient.

Compositional differences between the feldspar phenocrysts and the normative feldspar make it likely that equilibrium conditions were not attained during crystallization. Corrosion and resorption of the phenocrysts suggest that crystallization began intratellurically. The myrmekitelike inclusions in the feldspar phenocrysts are almost diagnostic of the earliest volcanic sequence. The intensive secondary alteration and replacement is a diagnostic feature, inasmuch as it occurs in no younger volcanic rock in the area.

QUARTZ MONZONITE PORPHYRY

In the mapped area (pl 1), quartz monzonite porphyry is found east of the longitude of the Grandview mine. The name quartz monzonite is used in spite of the fine-grained nature of this rock unit, in order to differentiate it clearly from the comparable extrusive rocks of this region.

The quartz monzonite porphyry truncates the early andesite and all older rocks, and is, in turn, cut by younger rhyolite dikes. That some parts of the early andesite volcanic sequence may be the extrusive equivalent of the quartz monzonite is suggested by the fact that hand specimens are similar, the early andesite sequence was the youngest rock unit at the time the quartz monzonite was intruded, and locally the lower part of the andesite sequence has been intruded by the quartz monzonite.

Approximately 1½ miles east of the mapped area, in the NE¼ sec. 16, T. 16 S., R. 8 W., the quartz monzonite porphyry transects a fault with small displacement in the Mississippian and Devonian sediments. Many of the fault zones in the Kingston area now contain quartz monzonite dikes. Therefore, it seems probable that much of the faulting in this area occurred before or during the quartz monzonite intrusion.

From an inspection of the areal distribution (see pl 1) of the quartz monzonite masses, it may be inferred that several factors have controlled the loci of igneous emplacement. The quartz monzonite may have vertical or nearly vertical contacts, and may truncate the bedding of the enclosing sediments. Such dikes are most numerous near the Gray Eagle mine and along Middle Percha Creek (see pl 1). In addition, some of these dikes are found in the fault zones (east of Kingston, pl 1).

West and south of Kingston, along Drummond Gulch, Southwest Canyon, and Middle and South Percha Creeks, larger masses of quartz monzonite have either vertical or horizontal contacts with the Paleozoic sediments and, in addition, enclose planigraphically some large masses of the sediments. In Drummond Gulch several large planigraphically enclosed masses of the Lake Valley limestone have their bedding approximately parallel to each other.

The Paleozoic sediments consist primarily of massive carbonate

rocks, of which the upper units, Devonian through Pennsylvanian sediments, are characterized by large amounts of shale. The Devonian Percha shale and the thin shale unit at the base of the Pennsylvanian Magdalena limestone are the most prominent shale horizons. At the above localities (see pl I), the quartz monzonite porphyry overlies or underlies stratigraphically the Mississippian Lake Valley limestone, which separates these two prominent shale horizons. Here the shale units may be partly or completely missing. Some thin horizontal sheets of quartz monzonite were found in the red shales of the Abo formation, but their size and distribution are minor in comparison with those found at the Percha and basal Magdalena shale horizons.

On Plate 1, the Precambrian through Silurian rocks do not show the same degree of irregularity in their contacts with the quartz monzonite as do the Upper Paleozoic rocks. The Cambrian through Silurian sediments apparently acted as single rigid blocks, competent enough to resist any sill-making tendencies of the magmatic intrusion. This is not the case with the Devonian through Permian sediments.

Some of the localities and horizons at which the quartz monzonite forms a partly conformable mass within the Paleozoic strata are listed below:

1. One and one-half miles south of Kingston, approximately at the basal Magdalena shale horizon.
2. In Drummond Gulch, at the basal Magdalena shale horizon.
3. A quarter of a mile south of the Gray Eagle mine, overlying the Fusselman dolomite.
4. A quarter of a mile northeast of the Gray Eagle mine, at the Percha shale to basal Magdalena shale horizons.
5. Two miles southwest of Kingston, at or over the Percha black shale horizon.
6. In Middle Percha Creek, 2½ miles west of Kingston, within the Abo red shales.
7. One and one-half miles northwest of Kingston, at the Percha shale horizon.

Two possible hypotheses concerning the shape of the quartz monzonite intrusive are considered, namely:

1. The quartz monzonite is a large intrusive mass which would increase its dimensions in depth, as suggested by Harley (1934, p 99). The large limestone masses are xenoliths or roof pendants which were floating or suspended in the magma.
2. The horizontal masses of quartz monzonite are the result of a lateral spreading of the magma from high-angle fault or fracture zones into certain favorable sedimentary horizons.

The density variations in sediments and glassy igneous rocks (Birch, et al., 1942, pp 16-25) show that the large floated xenoliths required by the first hypothesis might be possible. However, the Precambrian through Silurian rocks are not interpenetrated by the quartz

monzonite to the same degree as the younger Paleozoic sediments. No possible xenoliths or roof pendants of the Precambrian through Silurian rocks were found.

Therefore, the second hypothesis, outlined above, seems to the author to offer the more likely explanation. The almost parallel orientation of sediments enclosed by the quartz monzonite, and the presence of several thick conformable igneous masses which are both floored and roofed, strengthens this interpretation. Along Middle Percha Creek, persistent small intrusive masses (see pl 1) form discordant dikes near their western terminus and sills to the east. Such intrusions are not unknown in the western United States (see Balk, 1948, p 124). This conclusion imparts an orderly interpretation to the distribution of the quartz monzonite porphyry and has been followed in drawing the geologic cross-section (see pl 1). However, several small erratically oriented blocks of sediments which have been mapped might best be explained as a result of stoping, since magmatic pulsations in a -near-surface intrusive of this kind might easily loosen large rock blocks (Balk, 1948, p 125). Possible causes of this lateral spreading of the quartz monzonite will be discussed in a later section.

Megascopically the unaltered quartz monzonite is a gray aphanitic porphyry with abundant white euhedral feldspar phenocrysts, 1 cm and less in maximum diameter. Small phenocrysts (2 mm and less) of hexagon-shaped biotite flakes and prismatic hornblende laths are common. Since most of the rock has been altered to epidote-chlorite aggregates, the average specimen is green.

The outcrops are massive, well-jointed, limonite-stained, and show spheroidal weathering. Some of the joints are coated with green epidote veneers. Numerous zones within the quartz monzonite porphyry and many of the contacts are brecciated, and silica, calcite, and epidote have locally replaced portions of the breccia matrices.

Microscopically the rock is holocrystalline, porphyritic, with a very fine-grained (about 0.2 mm) xenomorphic-granular groundmass, which in some of the thinner veins contains feldspar microlites. A delicate planar structure is apparent within 1 inch of the contact. This rock is altered so intensely that its primary composition could be estimated only in 5 of the 27 thinsections examined. The minerals are listed in Table 3.

The feldspar in the quartz monzonite forms large (2 mm) glomero-porphyritic aggregates and phenocrysts, which are partially rounded and embayed by the groundmass. Locally plagioclase overgrowths have increased the idiomorphism of the rounded phenocryst nuclei. The resorption or rounding may be the result of the pressure decrease after intrusion of the magma to shallow depth (Bowen, 1928, p 183). Normal zoning is found in some of the less altered plagioclase. In general, the smaller the phenocryst the more euhedral.

Table 4 presents the significant optical properties of the feldspars in the quartz monzonite porphyry. The intermediate index was measured in immersion oils, and the remaining optical properties were determined in thinsection on the universal-stage (Emmons, 1943). Fair-bairn and Podolsky (1951) have measured the precision and accuracy

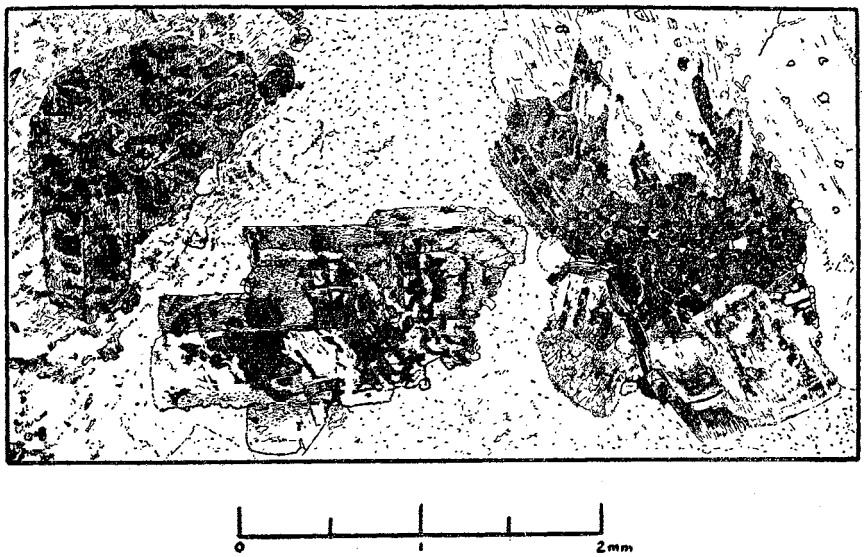

Figure 10

PLAGIOCLASE PHENOCRYSTS IN THE QUARTZ MONZONITE PORPHYRY. THE ISLAND-LIKE BLACK AREAS ARE FELDSPARS WITH OPTICAL PROPERTIES DIFFERENT FROM THE ENCLOSING PHENOCRYST. SEE TEXT AND TABLE 4. CROSSED NICOLS.

of universal-stage optic-angle (2V) determinations. Their maximum error of 2.8 degrees for plagioclase would probably be applicable to the optic-angle (2Vα) determinations in Table 4. The occurrence of the feldspars has been tabulated into four groups which have been labeled P, G, and E, where P indicates a phenocryst, G a part of the ground-mass, I an islandlike relict of a feldspar in a phenocryst, and E the rest of the material of the feldspar phenocryst enclosing the islandlike relict. The composition of the plagioclase, with the exception of the high-temperature form, was determined by the optical properties, utilizing charts prepared by Kennedy (1947). The composition of those plagioclases exhibiting small optic angles (2Vα) and large extinction angles was determined, very crudely, by using the graph which Tuttle and Bowen (1950, fig 4) have presented.

Many phenocrysts contain small poikilitic inclusions of feldspar, which are in optical continuity with each other and have a different extinction from the enclosing phenocryst. Such islandlike remnants are illustrated in Figure 10. The data, determined on these islandlike remnants (I) and on the corresponding enclosing material (E), are summarized in lines 5 through 12 of Table 4. Unfortunately, the grain size and rock alteration are such as to preclude X-ray verification of the interpretations listed in Table 4, so that the conclusions must not be regarded as certain.

TABLE 3. MINERALS OF THE QUARTZ MONZONITE PORPHYRY

PRIMARY MINERALS AND ABUNDANCES		SECONDARY MINERALS
	Percent	Calcite
Plagioclase (An_{30-38})	44	Plagioclase (An_{5-17})
Orthoclase	27	Chlorite
Quartz	16	Sericite
Brown biotite	4	Quartz
Hornblende	2	Green biotite
Magnetite	3	Epidote
Apatite	x	Pyrite
Sphene	x	Hematite

x Indicates present. Here, secondary minerals include both alteration and replacement products.

The conclusions to be drawn concerning the feldspars are that:

1. The anomalous properties of the feldspars listed in Table 4 suggest that both high- and low-temperature forms are present.
2. Potash feldspar and two plagioclases, of approximate composition An_{30-36}, and An_{5-17}, are present.
3. The more albitic plagioclase (An_{5-17}) in the groundmass and enclosing the islandlike relicts seems to be best explained as a low-temperature replacement product following the crystallization of the quartz monzonite magma.

Studies of the differences in the optical properties of the feldspars in coarser-grained plutonic rocks less altered than the quartz monzonite porphyry, might provide, when combined with X-ray data, a valuable criterion for determining the origin of plutonic rocks (see Fairbairn and Podolsky, 1951, p 832). Detailed optical studies of the feldspars were carried out for this reason, although the Tertiary age and shallow depth of the quartz monzonite intrusions leave little doubt as to the igneous origin of this rock.

Quartz, which is less than 5 percent in some thinsections, occurs almost exclusively in the groundmass. Only two quartz phenocrysts were noted in the 27 thinsections examined. In the matrix the quartz is anhedral and larger groups of quartz grains enclose poikilitically small feldspar laths. Therefore, the quartz was probably the last primary mineral to crystallize.

The brown biotite is anhedral, corroded and almost completely altered to a bleached biotite, so that only in a few grains can a faint-brown to colorless pleochroisrn be noticed. Hornblende laths could be determined in only one thinsection; however, in the remainder alteration and replacement have not destroyed the lath-shaped forms or the pseudohexagonal cross-sections. Of the remaining minor constituents, apatite and sphene occur as small euhedra, and magnetite as small anhedra. Magnetite and apatite are common as inclusions in the biotite.

TABLE 4. OPTICAL PROPERTIES OF FELDSPARS[a] OF THE QUARTZ MONZONITE PORPHYRY

Number of Thin-sections	Number of Grains Measured	Occurrence[b]	Index (± 0.004)	2Vα	Maximum Extinction ⊥ (010)	Average Composition	Interpretation
2	8	P	1.525	66-76	0	Orthoclase	Low potash-feldspar
1	2	P	1.525	46	0	Sanidine	High potash-feldspar
2	16	P	1.545	83-88	15-17	An_{33}	Low-temperature plagioclase
1	1	P	1.545	78	18	An_{30}	High-temperature plagioclase
1	2	I	1.545	77	—	An_{30}	Relict of high plagioclase
		E	1.545	89	—	An_{36}	Low-temperature plagioclase
2	4	I	1.525	54-58	0	Sanidine	High potash-feldspar relict
		E	1.537	94	—	An_{14}	Replacement plagioclase
2	4	I	1.525	16-25	0	Sanidine	High potash-feldspar relict
		E	1.537	90-95	10-13	An_{13}	Replacement plagioclase
1	30	I	1.525	<30	—	Sanidine	High potash-feldspar relict
		E	1.535	92-100	16-18	An_{5}	Replacement plagioclase
2	3	P	1.535	—	14-16	An_{6}	Replacement plagioclase
2	2	G	1.525	67-70	0	Orthoclase	Low potash-feldspar
1	2	G	1.525	40-44	0	Sanidine	High potash-feldspar
1	3	G	1.545	80-84	12	An_{30}	Low-temperature plagioclase
1	4	G	1.537	92-93	—	An_{16}	Replacement plagioclase
1	1	G	1.537	98	—	An_{9}	Replacement plagioclase
1	3	G	1.537	86-95	—	An_{17}	Replacement plagioclase
1	2	G	1.537	93-97	—	An_{13}	Replacement plagioclase

a Explanation in text.

[b] P indicates a phenocryst, G a groundmass grain, I an islandlike relict of a feldspar in a phenocryst, and E the remaining phenocryst material enclosing the islandlike relict.

Minute fractures in the quartz monzonite porphyry have been filled with calcite, quartz, chlorite, and epidote. The central parts of some of the fractures containing chlorite and epidote are filled with an albitic plagioclase. This suggests that the replacement plagioclase (An_{5-17}) formed later than the chlorite and epidote. Similar replacements are commonly regarded as deuteric in origin (see Buddington and Callaghan, 1936). Secondary minerals are concentrated particularly in the vicinity of fractures.

The secondary minerals, excluding plagioclase, have replaced considerable parts of the feldspar, brown biotite, hornblende, and matrix. The (0112) glide-plane lamellae of the calcite are prominent in some places and have been transected by minute chlorite shreds, suggesting the relative ages of the calcite and chlorite. Some of the original plagioclase has been replaced parallel to the cleavage directions by quartz and other materials, so that where replacement was most effective the plagioclase is divided into rounded rectangular patches separated by quartz. The green biotite occurs as small shreds with a radial or fibrous habit, maximum interference color of first-order red, a positive elongation, and a green to colorless pleochroism. It is very fresh in appearance and might be called chlorite, except for its birefringence. Hematite clouding is common throughout the rock, and as stringers in, and rims around, altered biotite and hornblende. Pyrite grains are best seen in the hand specimens, although a few were noticed in thinsection.

The petrographic work on the feldspars has verified the igneous origin of quartz monzonite. The absence of quartz phenocrysts, and the secondary alteration and replacement in the intrusive quartz monzonite, are important criteria for differentiating this unit from later intrusive rocks. In addition, the absence of intense alteration and sulfide mineralization in all later rocks is evidence that alteration and ore deposits were formed at or near the end of the quartz monzonite porphyry intrusion.

CONTACT METAMORPHISM AND MINERALIZATION

There is very little obvious contact metamorphism near the quartz monzonite porphyry intrusions. Within the quartz monzonite, directly at the contact just north of the Gray Eagle mine, there are very abundant small (0.5 mm) euhedral diopsidic pyroxene grains. In the adjacent limestones there are large, elongated (18 inches and less) light-green chert-nodulelike masses. Under the microscope these soft masses were determined as fine intergrowths of calcite and serpentine. West of the crest of the range, many of the chert nodules in the Lake Valley limestone have a rim of fibrous wollastonite. Here, some of the fractures are lined with small dodecahedral yellowish-brown garnet crystals, whereas in the recrystallized calcite there are sparse large (up to 3 inches) rounded reddish-brown garnets. One siliceous bed is composed of very finely intergrown quartz, calcite, wollastonite, and clay alteration products. The limited occurrence of these metamorphic minerals suggests that metamorphism was effective only in very small pockets

and fractures, which emphasizes again the near-surface nature of the quartz monzonite intrusion.

Considerable faulting occurred before the major ore deposits and the secondary minerals in the quartz monzonite porphyry were formed. The evidence for this is that fault breccias of the quartz monzonite and all older rocks may have their matrices filled or replaced by quartz, calcite, and minor amounts of copper, lead, and zinc ore minerals. In addition, because the sulfide deposition is greatest where the secondary minerals are significant in amount, it seems probable that they were formed almost at the same time.

Ore deposits of the Kingston area have been described in moderate detail by Harley (1934) as consisting largely of copper, lead, and zinc sulfides, and their related oxidized minerals; the oxides, carbonates, and silicate of manganese; silver, either as a separate mineral or combined in other minerals; minor gold; and alabandite. Two varieties of ore deposits are found: nearly vertical veins and breccia zone replacements, and tabular bodies of replaced limestone, which were once overlain by a shale layer, in most places the Percha shale.

The rocks younger than the quartz monzonite porphyry have not been mineralized extensively. In the tuffaceous rhyolite, there are sparse opaline veins. One mile east of the Gray Eagle mine, cavities in a white rhyolite dike are lined with purple octahedral fluorite crystals.

RHYOLITIC IGNEOUS ROCKS

TUFFACEOUS RHYOLITE

This unit has the largest areal extent of all the formations. Throughout the western part of the area, it is exposed for a distance of approximately 8 miles along State Highway 180 (see pl 1). Along the crest of the range, a short distance north of the State Highway, it forms the highest topographic features. In the vicinity of Kingston and east of the mapped area, the tuffaceous rhyolite crops out over smaller discontinuous areas, which presumably are erosional remnants of a once more extensive volcanic sheet.

The tuffaceous rhyolite is separated from the underlying early andesite volcanics in most places by an angular unconformity varying from 11 to 39 degrees. Approximately 1 mile north-northwest of the Gray Eagle mine, the planar structures of both these formations are essentially parallel. A half mile northwest of Kingston, an agglomeratic part of the tuffaceous rhyolite overlies the red beds of the Abo formation. In most of the mapped area the tuffaceous rhyolite is the surface unit. Near the western map boundary, however, it is overlain with approximate conformity by the arkosic sediments and tuffs, and the late andesite volcanic sequence.

The tuffaceous rhyolite forms a tabular body with an estimated minimum thickness of 1,300 feet. It is exceedingly uniform, devoid of marker horizons, extremely brecciated in places, and traversed by abundant joints. The large mass of tuffaceous rhyolite in the western part of the area is presented in the cross-section and map (pl 1) completely unmarred by faults, although this would indicate a thickness

measurable in miles. Faulting could not be detected here, but is suggested by the 1,300 to 1,800 feet thicknesses of some of the smaller tuffaceous rhyolite masses to the east.

Contrasted with earlier formations in the Black Range, the tuffaceous rhyolite is at the surface over large, continuous areas, and this suggests that the range had undergone most of the faulting before the rhyolite was formed. The faults which transect the tuffaceous rhyolite deviate very little from the north-south regional trend in New Mexico.

In the western part of the mapped area, the planar structures in the rhyolite dip to the west and southwest at a variable angle rarely greater than 55 degrees. Along the crest of the range, the dip is to the north or northeast at an angle of 30-70 degrees. In the vicinity of Kingston the planar structures dip eastward at 30-50 degrees.

Two structure elements produce the linear and planar structure of this rock. Cavities, presumably formed by gas, are sparse throughout the rock unit, but in numerous places abundant cavities, 6 inches and less in length, are flattened, elongated, or both, so that one may measure a planar or a linear structure. Within the groundmass of the tuffaceous rhyolite, which has a uniform color over a limited area, one finds lighter-colored irregular lenticular areas. The long dimensions of these lenses, which range from several feet to less than an inch in length, are approximately parallel and produce a second type of planar element. Under the microscope, the contacts of these lenses with the normal groundmass are invisible, though occasionally slight differences in the amount of hematitic clouding mark the lens borders.

Locally, steep surfaces of the tuffaceous rhyolite faintly resemble a rock with columnar jointing. However, sheetlike planar jointing is very common. These joints within a limited area are approximately parallel and are spaced 10 inches or less apart. Careful inspection of many of these joint surfaces reveals that a few contain small slickensided areas. Most of the joints vary in dip from 55 to 90 degrees and show no preferred strike, nor any systematic relationship to the planar structures.

Most of the tuffaceous rhyolite is a massive gray, violet-gray, white, pink, or brown aphanitic porphyry. The phenocrysts comprise approximately 13-69 percent of the rock and consist of quartz, feldspar, and biotite. Their size is 4 mm and less. The quartz is commonly dipyramidal. Much of the feldspar has a silken luster and is white and/or pinkish white.

A striking feature of this rock is the common presence of angular to rounded xenoliths varying greatly in size. Most of the xenoliths, which consist primarily of fragments of the early andesite volcanic sequence and rarely of red shale fragments, are distributed uniformly throughout the entire tuffaceous rhyolite unit. These xenoliths are 30 mm and less in size. In several areas the xenoliths assume such importance that they have been mapped as separate zones (pl 1). This will be discussed in detail in a later section.

No glass or glassy zone was found at the base of the tuffaceous rhyolite. In one locality, on a weathered surface, a black eutaxitic banding is prominent, which resembles glass lenses, but is actually

the result of a darker weathering of parts of the groundmass. The concentration of foreign particles appears to increase near the base of the tuffaceous rhyolite, and in thinsection the matrix contains more darker-colored well-altered material, possibly indicating that surface material was incorporated into the .base of the tuffaceous rhyolite. The predominant basal unit, with an estimated maximum thickness of 70 feet, is made up of agglomerate and lapilli to fine tuff beds. The fragments in these basal beds are 3 feet and less in diameter and consist of subangular to round tuffaceous rhyolite. Tuffaceous rhyolite of a differing color forms the matrix. Locally the fragments are as round as those of a basal conglomerate. Interbedded with the agglomerates are gray to white .tuff beds, 6 feet and less in thickness, and of varying grain size.

Three-fourths of a mile south of the B in the cross-section line on the map (see pl 1), there are some interbedded tuffs and agglomerates. This is the only locality in which bedded pyroclastic rocks are found within the 'main mass of the tuffaceous rhyolite. These bedded pyroclastic rocks do not resemble those found at the base of the tuffaceous rhyolite.

In the western part of the tuffaceous rhyolite, near the stratigraphic top, there are sparse black glass lenses. In most localities, the upper part of the tuffaceous rhyolite consists of white, porous or clayey tuff, and a few agglomerate beds. This tuff is massive, or very fine-grained and thin-bedded, and resembles the tuffaceous rhyolite, except for its altered and crumbly matrix. These tuff beds have been mapped as part of the overlying arkosic sandstone, conglomerate, and tuff unit.

Microscopically, the tuffaceous rhyolite consists of a glassy to cryptocrystalline matrix. Devitrified groundmass has a radial or spherulitic texture, as defined by Marshall (1935). No glass shards or shreds are discernible. However, in the tuff beds at the base and the top of the tuffaceous rhyolite, and in accessory fragments in the xenolith zone, a plumose texture may be present (Marshall, 1935). The plumose texture, which appears to be formed by glass shards and shreds, can be compared easily with the texture which is found in the larger part of the tuffaceous rhyolite by inspection of Figure 11. Similar examples of plumose texture are illustrated by Gilbert (1938), Mansfield and Ross (1935), and Marshall (1935). The matrix of the glassy lenses is massive and locally shows a eutaxitic structure. The glass has an index of refraction of 1.497 (+0.002). It contains considerable amounts of finely ground crystalline rock flour. The eutaxitic banding is shown by slight color differences between those parts of the glass with much rock flour and those with little or none.

The phenocrysts are seriate, subhedral, fractured, bent, rounded, and embayed by the groundmass. They constitute 13 to 69 percent of the rock (see fig 12). Table 5 presents the average mode of the tuffaceous rhyolite.

Sanidine phenocrysts have an optic angle ($2V\alpha$) of 30 degrees or less and the following refractive indices ($\pm$ 0.002): α=1.516, β=1.522, γ=1.523. Some plagioclase is completely or partially enclosed by the sanidine. Two types of sanidine occur in the tuffaceous rhyolite,

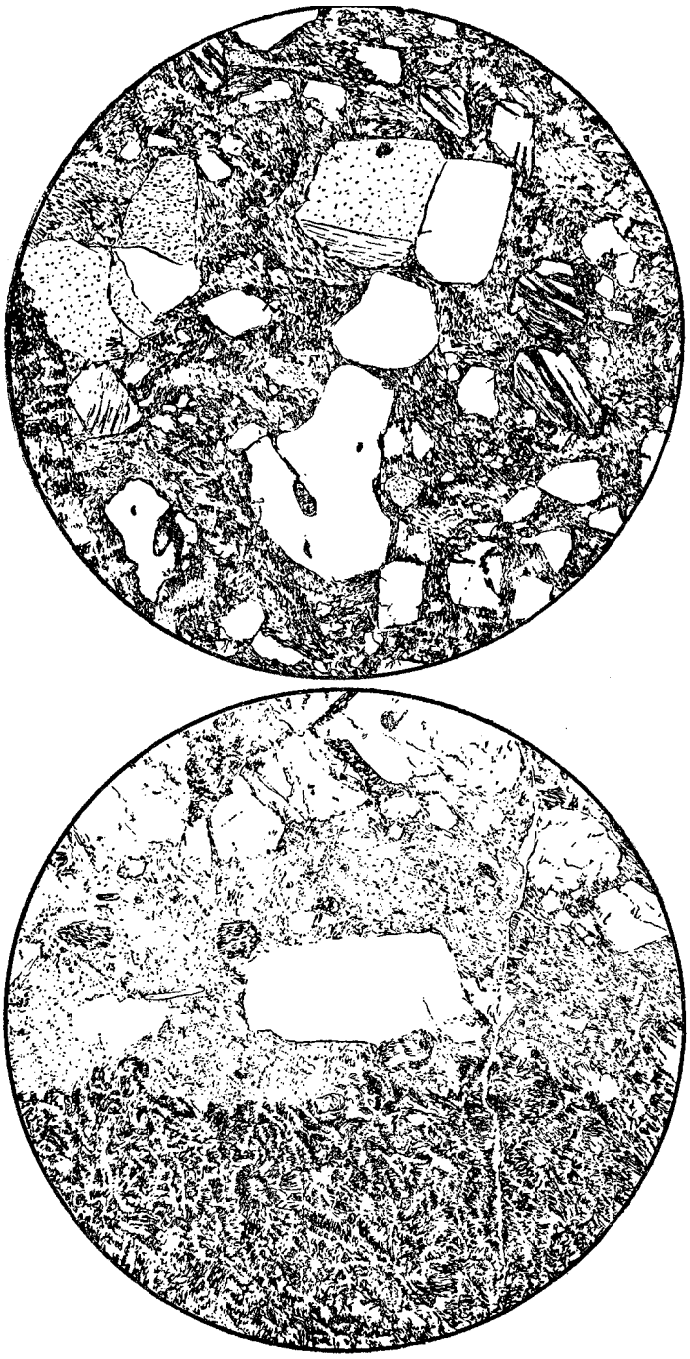

Figure 11 (left). PLUMOSE TEXTURE IN XENOLITH ON LEFT, NORMAL TEXTURE OF TUFFACEOUS RHYOLITE ON THE RIGHT.

Figure 12 (right). ROUNDED, CORRODED, AND FRACTURED PHENOCRYSTS IN TUFFACEOUS RHYOLITE. DIAMETER OF FIELD IS 4 MM.

TABLE 5. AVERAGE MODES OF THE RHYOLITIC ROCKS

	Tuffaceous Rhyolite	Rhyolite Porphyry	Rhyolite Dikes
Number Averaged	15	8	3
Mineral			
Quartz*	15.8	16.4	3.7
Sanidine	14.7	23.1	6.0
Plagioclase (An_{10-35})	10.1	17.7	1.0
Biotite	1.1	2.5	0.3
Matrix	55.6	40.2	88.9
Rock fragments	1.5	—	—
Hornblende	x	—	—
Pyroxene	x	—	—
Magnetite and ilmenite	0.2	0.2	x
Apatite	x	x	x
Sphene	x	x	x
Zircon	x	x	x
Rutile	x	x	—
Hematite and leucoxene	x	x	x
Bleached biotite	x	x	—
Sericite	x	x	x
Chlorite	x	x	—
Albite	0.4	x	—
Calcite	x	x	—
Epidote	—	x	—
Vein quartz	—	—	x

x Indicates present.

* Includes possible tridymite and cristobalite.

although a single thinsection contains only one kind. The one variety is uniform in appearance, whereas the other is made up of irregular shreds, which are most apparent at or near extinction because of slightly different extinctions (see fig 13). Optically, except for the extinction, these shreds are identical. Secondary overgrowths of albite enclose the sanidine rarely.

Plagioclase, in general, forms smaller phenocrysts than sanidine. Rarely, it encloses small biotite flakes. The optical properties, except for the indices of refraction, are of little value in determining composition. This is to be expected, because high-temperature plagioclase occurs commonly in volcanic rocks. In immersion oils the intermediate index ranges from 1.53 to 1.55. This corresponds to a composition ranging from An_{10} to An_{35}. In a single thinsection, the composition appears to be quite uniform. The zoned plagioclases have, as a rule, an index greater than that of balsam (1.54±), whereas the unzoned plagioclases have a smaller index. Very rarely, one finds plagioclase with myrmekitelike inclusion zones similar to those found in the flows of the early andesite volcanic sequence.

The biotite flakes are bent and crumpled, and show the most alteration of any of the phenocrysts. Many of the brown biotite phenocrysts have been partly bleached peripherally and along cleavage cracks

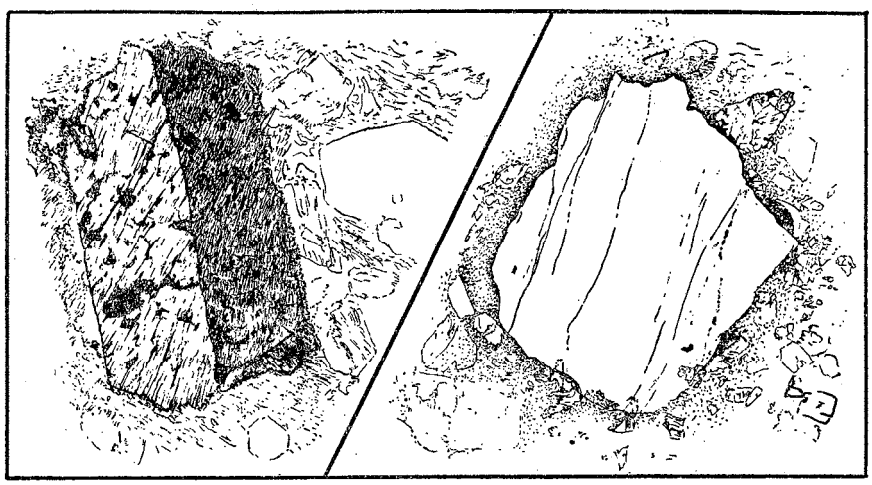

Figure 13
THE TWO VARIETIES OF SANIDINE PHENOCRYSTS FOUND IN THE TUFFACEOUS RHYOLITE. THE ONE VARIETY APPEARS CLEAR AND HOMOGENEOUS, AND THE OTHER IS CLOUDED AND SHOWS SHREDLIKE AREAS OF SLIGHTLY DIFFERING EX- TINCTION. PHENOCRYSTS ARE ABOUT 2 MM LONG.

to a colorless biotite. Hematite rims are common around biotite: The pleochroism in most of the grains varies from brown to colorless, al-though yellowish-green and olive-brown colors are rarely to be noted. Some of the grains have been oxidized to a deep red, either peripherally, along the cleavages, or throughout. Within the same thinsection, some biotite flakes may be oxidized to a red color, whereas others are still brown. In contrast, biotite in the xenolith zones displays a normal brown and shows no trace of a red oxidation color.

The occurrence of sparse common green hornblende in a rock of this nature is regarded as unusual. Although the hornblende is only an accessory mineral, it was present in every thinsection examined. The grains are subhedral, rounded, and embayed. Identification of the hornblende is based on its maximum extinction of 15-21 degrees, birefringence of approximately 0.023, a pleochroism ranging from a green or brownish green to a colorless or very pale yellowish-green, the amphibole cleavage, and an optic angle ($2V\alpha$) of approximately 60 degrees. Several very rare pyroxene grains form relicts enclosed by the hornblende. Because of the optical continuity of the pyroxene relicts, this suggests a replacement of the pyroxene by the hornblende.

It was desirable to know to what extent the green hornblende may have been oxidized to basaltic hornblende. Three small phenocrysts of hornblende were each divided into two parts. One of these parts in each case was maintained at a temperature of approximately 850°C for a 3-hour period. Subsequent comparison of both parts of the phenocrysts reaffirmed the pronounced changes which have been described

in detail by Barnes (1930) and others. After heating, the phenocrysts had a parallel extinction, birefringence greater than 0.050, and a pleochroism ranging from an orange brown to a pale orange.

One of the heated phenocrysts was obtained from a specimen containing lenses of a black glass, which was collected at the extreme top of the tuffaceous rhyolite in the western part of the area (see pl 1). A second specimen came from the xenolith zone, and a third from a position approximately halfway between these two localities (see pl 1). The change in the hornblende of each of these phenocrysts was identical.

The hornblende in many places encloses small biotite grains of reddish-brown color in random orientation. In only one grain did the biotite inclusions have a common orientation and elongation parallel to the hornblende cleavage. Magnetite and apatite inclusions are numerous in both the biotite and hematite. The possible temperature significance of the hornblende and biotite will be discussed at the end of this section.

The mineral which has been called albite (see table 5) occurs in fractures in the rock, enclosing sanidine as an overgrowth, and replaces sanidine and plagioclase phenocrysts along fractures, cleavages, and in irregular areas. It is fine-grained, and common in only a few thin-sections. Its properties are: (1) indices greater than sanidine and less than plagioclase phenocrysts and balsam, (2) simple and polysynthetic twinning, (3) maximum extinction of 16 degrees, (4) higher birefringence than either sanidine or plagioclase, and (5) an optic angle ($2V\alpha$) of 110 degrees.

Chemical analyses from the xenolith zone, listed under R2 and V2 in Table 6, are probably representative of the tuffaceous rhyolite.

The properties of the tuffaceous rhyolite correspond closely to those of nuées ardentes (Lacroix, 1904), welded tuffs (Iddings, 1899), or sillars (Fenner, 1948). There are some differences, however, which may be of genetic significance. The tuffaceous rhyolite, for example, has abundant accidental xenoliths, which in the xenolith zones are extremely large. Such fragments are unknown in nuées ardentes, although they are not uncommon in explosively ejected material, according to Lacroix (1904, p 206). Moore (1934, p 374), listing the criteria for a welded tuff deposit, states, "Material from one magma and no extraneous material." Fenner (1948) described a rock unit under the heading "Abnormal Tuff" because it contains large amounts of extraneous matter.

It is believed that, in general, planar structures in a welded tuff are not caused by flow, but rather by compaction of the originally loosely deposited particles, so that gas cavities are rare. The linear gas cavities in the tuffaceous rhyolite could not have been produced by compaction alone, but require a flow. In addition, the planar structures of the xenolith zone, shown by the lighter-colored lenses, bend around the xenoliths in a flowlike manner, even within small outcrops, so that the possibility that this structure was formed by compaction seems remote. Mansfield and Ross (1935) have illustrated a megascopically massive obsidian which still shows microscopically structures of glass shards and shreds. 'Nothing of this sort has been found in the vitro-

Plate 2: Spheroidal masses of lighter carbonate and spheroidal cavities in the Montoya limestone. See text. Ladrone Gulch.

A.

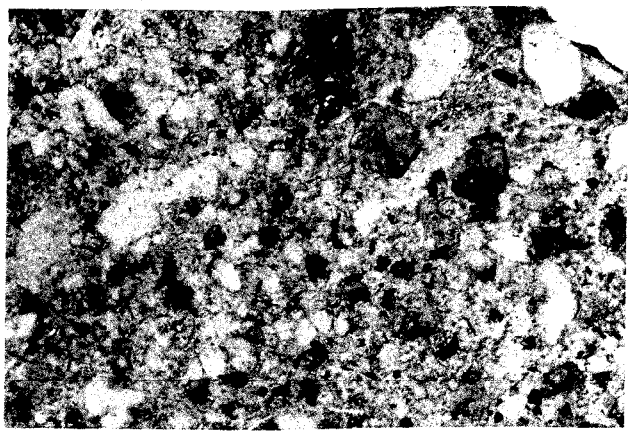

B.

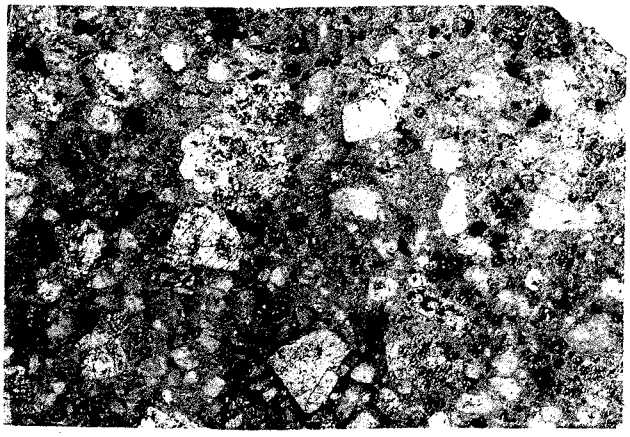

Plate 3: A. Enlarged polished surface of tuffaceous rhyolite.
Enlarged 3X with respect to B.

B. Polished surface of rhyolite porphyry. About actual size.

phyres or glassy lenses of the tuffaceous rhyolite. No pumice fragments, collapsed or otherwise, were detected in more than 90 thinsections or in the field.

The largest percentage of phenocrysts described in a welded tuff is 25 (Mansfield and Ross, 1935), whereas the tuffaceous rhyolite contains an average of 40 percent. This may have affected the properties considerably. Perret (1934) has shown that nuées ardentes and gas-free lava do not tend to be extruded at the same time. However, ferret's Chart I shows that the cyclical alternation of these two extrusive phases is so short that the processes may be considered simultaneous. Fenner (1937) emphasizes the fact that volcanic material may be deposited by a great variety of processes. Ross and Smith (Smith, Robert L., personal communication) would probably use the term "welded tuff" to designate a volcanic deposit of this kind, and specify that it consists of "ash flow tuffs" and "ash fall tuffs." On the basis of the abundant accidental xenoliths, and the deduced origin of at least part of the planar and linear structure, it is concluded that a large part of the tuffaceous rhyolite actually flowed, using the term flow in its elementary sense and not in terms of modern rheology. The name tuffaceous rhyolite was chosen to signify both particulate flows and pyroclastic material.

Kozu and his coworkers (see Gilbert, 1938, p 1856) have shown that at atmospheric pressures biotite transforms from a brown to a red color beginning at 400°-500°C and continuing almost to 1,000°C. On this basis the temperature at the time of deposition of the tuffaceous rhyolite was greater than 400°-500°C. Because the dipyramidal quartz and sanidine phenocrysts are corroded, one might conclude that the temperature was greater than 870°C (Rogers and Kerr, 1942, p 184), and equal to or greater than 1,063°C (Bowen and Tuttle, 1950, p 496), respectively, for each of these minerals. However, the melting point of the sanidine (Bowen and Tuttle, 1950), and probably of the quartz, would have been considerably lowered by the presence of water and other constituents in the liquid phase.

The presence of common green hornblende may indicate a temperature less than 850°C, because this is the transition temperature at which common hornblende readily changes into basaltic hornblende in a dry laboratory system open to the atmosphere (Barnes, 1930). However, Barnes found that a lack of oxygen might prevent the transition from green to brown hornblende. In nature, brown basaltic hornblende is common in basalts. Does a basaltic lava flow have more available oxygen than a particulate rhyolitic flow or nuée ardente? If so, the hornblende will have no temperature significance. Yet sufficient oxygen was present to change some of the biotite from brown to red. With more data concerning these oxidizing transformations, the biotite and hornblende might be used as a geothermometer for volcanic rocks; they might also, by inference, provide the basis for estimating the minimum temperature at which a magma may exist.

One or more of the following explanations may account for the green color of the hornblende:

1. The temperature at the time of extrusion was below 850°C. Jaggar's (1917) measurements of the Kilauean lava immediately below

the surface show a temperature range from 750° to 850°C. Possibly basaltic Kilauean lava might have a higher temperature than many acidic tuffs and flows. Most measured volcanic temperatures, however, are higher than 850°C (see Barth, 1952).

2. The oxygen concentration may have been too low to oxidize the hornblende.

3. After or during cooling, the hornblende may have changed back into the green variety. Where the green hornblende is enclosed by, or adjacent to, glass lenses, this requires a transformation in spite of extreme quenching.

RHYOLITE. PORPHYRY

This rock has its largest areal extent north and south of State Highway 180 in the vicinity of Iron Creek, west of the crest of the Black Range. Smaller outcrops are found south of the xenolith zone, and in several other localities.

West of the crest of the range, at contacts with the early andesite volcanic sequence, both the phenocrysts and groundmass in the rhyolite porphyry are abnormally fine-grained. Both the early andesite and the rhyolite porphyry are altered considerably near their contacts, so that they break into loose debris very readily. Sparse thin quartz veins are present in the early andesite near the rhyolite porphyry, and a few small fragments of the early andesite sequence may be found in the rhyolite porphyry near the contacts. The contacts are vertical or very steep for the most part and trend primarily in a north-south direction. Therefore, the rhyolite porphyry forms large irregular dikelike masses of a general north-south trend, which have been intruded into the early andesite sequence. The east-west cross-section of these dikelike masses is interpreted as funnel-shaped (see pl 1), because southward, and topographically higher, the rhyolite porphyry has a greater areal extent.

Southwest of Iron Creek the contact between the tuffaceous rhyolite and the rhyolite porphyry appears to be gradational, although the exposures in this locality are not too good. Elsewhere the contact between these two rock units, although clearly marked topographically, contributes nothing to a knowledge of their age relations.

The rhyolite porphyry is a massive pink, cream, gray, or light-brown aphanitic porphyry. The seriate phenocrysts, comprising approximately 60 percent of the rock, are very striking, because of the large size which they attain. The maximum dimension of the phenocrysts is of the order of 4 inches. In hand specimens sanidine and quartz form the larger, most euhedral, and most abundant phenocrysts, while plagioclase and biotite are smaller and apparently less abundant. The quartz grains display rarely a dipyramidal habit, and in many places sanidine and plagioclase phenocrysts are enclosed by quartz. Locally this rock has a planar structure which appears to vary randomly from outcrop to outcrop. The rhyolite porphyry weathers spheroidally and crumbles into pebbles and granules.

Microscopically the rhyolite porphyry resembles the tuffaceous rhyolite closely. Both contain the same minerals, although the relative

proportions differ slightly (see table 5). The rhyolite porphyry is more altered in general and has fewer fractured phenocrysts. Phenocrysts of the porphyry are more rounded and embayed, and secondary over-growths on the corroded grains are more common. The matrix is very fine-grained xenomorphic-granular, but not cryptocrystalline or glassy, as in the tuffaceous rhyolite. Xenoliths are almost unknown in the rhyolite porphyry. Most of the sanidine phenocrysts in the rhyolite porphyry are composed of irregular shreds, as described under the tuffaceous rhyolite. No red biotite was found in the rhyolite porphyry. These differences between the intrusive rhyolite porphyry and extrusive tuffaceous rhyolite seem to be consistent with the differences in the loci of crystallization and the consequent pressure, temperature, and cooling conditions.

The petrographic similarity of these two rocks in every other aspect is so great that further repetitive description is omitted. The difference is of degree rather than kind. Plate 3, by eliminating the grain size differences, allows a direct comparison of the tuffaceous rhyolite and rhyolite porphyry, since the tuffaceous rhyolite has been enlarged relative to the rhyolite porphyry. For these reasons, it is concluded that the tuffaceous rhyolite and rhyolite porphyry are consanguineous. In addition, the high stratigraphic horizon intruded by the funnel-shaped rhyolite porphyry, the suggested gradational contact southwest of Iron Creek, and the petrographic similarity, between the tuffaceous rhyolite and the rhyolite porphyry suggest that the rhyolite porphyry now occupies one of the feeding zones through which much of the extrusive rhyolitic material passed.

Approximately 1½ miles north-northwest of the Grandview mine, there are several poorly exposed lenses of a medium-grained, tan rock enclosed by, and forming a moderately sharp contact with, the rhyolite porphyry. Microscopically this rock is xenomorphic-granular and is conspicuous by its lack of groundmass (see fig 14). It contains the same minerals as the enclosing rock, although the relative proportions are quite different. This is not unexpected, since it has no matrix.

The mineral constituents and the geologic location make it probable that the even-grained xenomorphic-granular phase is related to the surrounding rhyolite porphyry. In addition, the high-temperature minerals prove that crystallization occurred from an igneous melt. This is of great interest, for Drescher-Kaden (1948) has emphasized the difference between positive igneous textures (glasses and porphyries) and plutonic rock textures (e.g., xenomorphic-granular).

SMALL RHYOLITIC INTRUSIVE MASSES

The smaller dikes and sills east of the longitude of the Grandview mine may be divided into three varieties. These are rhyolite porphyry, green vitrophyre, and normal rhyolitic dikes and sills. The rhyolite porphyry dikes are identical with the larger rhyolite porphyry masses both megascopically and microscopically, and need not be discussed further.

Megascopically, the normal rhyolitic dikes look like white unglazed porcelain, with abundant phenocrysts approximately 1 mm in

Figure 14 (left). XENOMORPHIC-GRANULAR PHASE OF RHYOLITE PORPHYRY. MINERALS PRESENT ARE QUARTZ, SANIDINE, BIOTITE, AND MAGNETITE. CROSSED NICOLS.

Figure 15 (right). PERTHITE (GRAY, RAGGED APPEARANCE) AND QUARTZ (MOSTLY WHITE) WITH SPHERULITIC FRINGES OF SODIC PLAGIOCLASE IN RHYOLITE SILL IN DRUMMOND GULCH. CROSSED NICOLS.

DIAMETER OF FIELD IS 3 MM.

size. These dikes show a banding or flow structure parallel to their contacts. Locally the matrix is composed of a brown glass, and here the phenocrysts are surrounded by small concentric rims of devitrified glass.

The average mode of the normal rhyolitic dikes is listed in Table 5. Microscopically, the matrix ranges from glass to very fine-grained quartz and acid feldspar. The index of the glass is 1.485 (±0.002).

The phenocrysts are subhedral, rounded, embayed by the ground-mass, and in several instances are fractured and broken. Their proper-ties are closely identical to those described under the tuffaceous rhyolite. The phenocrysts comprise only about 10 percent of the rock. Plagioclase (An_{10-35}) is much scarcer relative to the quartz and potash feldspar (see table 5), and no albitization of the feldspars was found.

A sill, 20 feet thick, occurs approximately 1 mile southwest of the Gray Eagle mine. In hand specimens this rock is gray, with a flow structure indicated by green and pink banding near the contacts. The phenocrysts are about 1 mm in length and many have a small concentric shell of a lighter-colored material, so that this rock is apparently identical with the other small intrusive rhyolitic masses. In thinsection (see fig 15), however, it differs in that the potash feldspar is perthite, and radial and spherulitic growths of an albitic plagioclase are common.

The minerals in this sill are quartz, perthite, albitic plagioclase, biotite, and the same accessory minerals found in other rhyolitic rocks of this area. The phenocrysts are subhedral, rounded, and embayed by the groundmass. Plagioclase of the perthites forms elongated shreds and irregular patches. The maximum extinction of the plagioclase part of the perthite is 14.5 degrees, which corresponds to a composition of An_5. Most of the phenocrysts are surrounded by the spherulitic albitic plagioclase, and they seem to have acted as nuclei for the crystallization of the albitic plagioclase. Small skeleton crystals have been enclosed by the spherulitic plagioclase. The groundmass of this rock consists of anhedral interlocking quartz, perthite, biotite shreds, and secondary sericite. Much of the feldspar is euhedral and is enclosed by the quartz.

The perthitic intergrowths suggest that the temperature of this sill was lowered much more slowly than that of other rhyolitic rocks in this region. The possibility of a secondary origin for the perthites seems to be precluded by the corroded phenocrysts, the spherulitic growths, and the occurrence of this sill in unmetamorphosed Carboniferous sediments.

Small green vitrophyre dikes are found in the area. For the most part, the outcrops consist of loose piles of glass rubble. Several excellent road cuts (see figs 16-17) demonstrate that the vitrophyre forms dikes. The dikes are partially devitrified along their contacts. Most of the green glass has a well-developed system of fractures approximately parallel to the contacts. In addition, many randomly oriented fractures are present. The glass tends to split along the dull fractures rather than to form vitreous conchoidal surfaces. It has an index of 1.494 (±0.002), shows very little devitrification except at its contacts, and contains small skeleton crystals of sanidine.

Approximately 10 percent of the rock is phenocrysts (2 mm and less in length), of which quartz, sanidine, and granophyric intergrowths

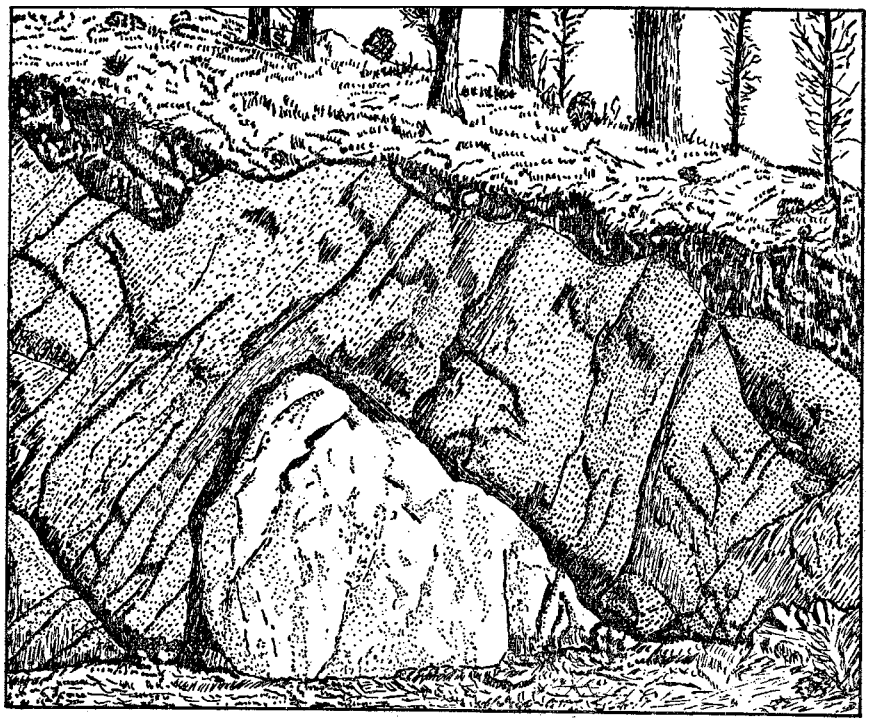

Figure 16
UPPER TERMINATION OF A GREEN VITROPHYRE DIKE IN ANDESITE, A QUARTER OF A MILE WEST OF EMORY PASS IN A ROAD CUT. WIDTH OF DIKE AT BASE OF OUTCROP IS 6 FEET.

of these two minerals are the most abundant. These phenocrysts are rounded and very intimately embayed by the groundmass (see fig 18), although skeleton-crystal growths and subhedral crystals are common (see figs 19-20). Acidic plagioclase, with an estimated composition of An_6 (based only on high-temperature optics, utilizing data of Tuttle and Bowen, 1950), biotite, and sphene are rare, and one magnetite grain was observed. The biotite is pleochroic from brown to colorless and shows no trace of oxidation to red.

The granophyric intergrowths vary from cuneiform to irregular globules or myrmekitelike masses. The corrosion pattern of quartz or sanidine phenocrysts displays a remarkable similarity to some of the granophyric intergrowths (see fig 22). Of all the granophyric grains (25) measured on the universal stage, there is no recognizable systematic relationship between the optic axis of the quartz and the cleavage planes of the sanidine. The quartz-sanidine contacts of cuneiform or very fine myrmekitelike intergrowths are completely clear. In contrast, the quartz-sanidine contacts of the irregular globular and coarser

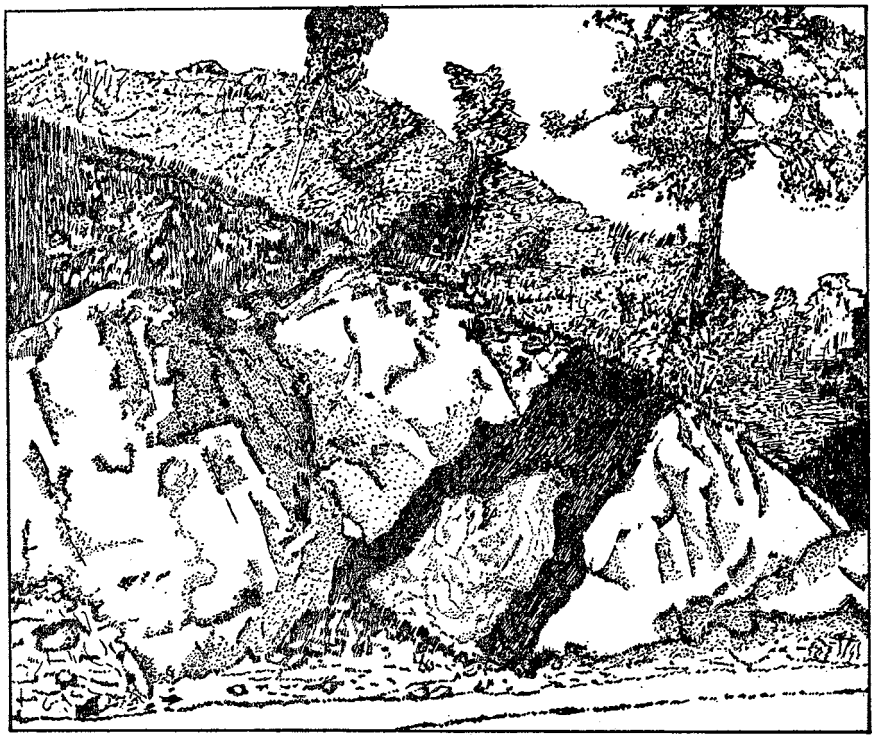

Figure 17
LENS-SHAPED GREEN VITROPHYRE ENCLOSED BY STONY RHYOLITE DIKE (COLORED BLACK IN SKETCH) IN ANDESITIC TUFF. DIKE WIDTH IS ABOUT 6 FEET. ROAD CUT ABOUT HALF A MILE WEST OF EMORY PASS.

myrmekitelike intergrowths contain traces of a dusty material, which resembles the part of the glassy matrix where crystallites have formed. A main core of quartz, sanidine, or plagioclase may be present (see fig 21). The material comprising the core, with the exception of plagioclase, has the same orientation as the corresponding material in the granophyric overgrowth. The material which does not form the core has, in most cases, a common optical orientation only over limited parts of the granophyric intergrowths; therefore, one mineral phase of most intergrowths may be divided into three or four separate grains on the basis of optical discontinuity. Some of the coarser intergrowths enclose a rounded or corroded plagioclase grain. In addition to single granophyric grains, aggregates of several grains are common. The contacts of the grains comprising the aggregates are irregular, although where the individual grain extends into the groundmass it may be almost euhedral. Where individual granophyric grains of an aggregate have central nuclei, and each nucleus is composed of a single mineral

Figure 18 (left). CORRODED GRANOPHYRIC GRAIN (A) AND CORRODED QUARTZ CRYSTAL (B) IN A GLASS MATRIX. CORROSION EMBAYMENTS IN QUARTZ ARE PARTLY FILLED WITH SANIDINE (C).

Figure 19 (right). PHENOCRYST AGGREGATE IN GLASS MATRIX. NOTE SKELETON GROWTH ON SANIDINE CRYSTALS AND FRINGE-LIKE OVERGROWTHS OF SANIDINE ON QUARTZ.

DIAMETER OF FIELD IS 3 MM.

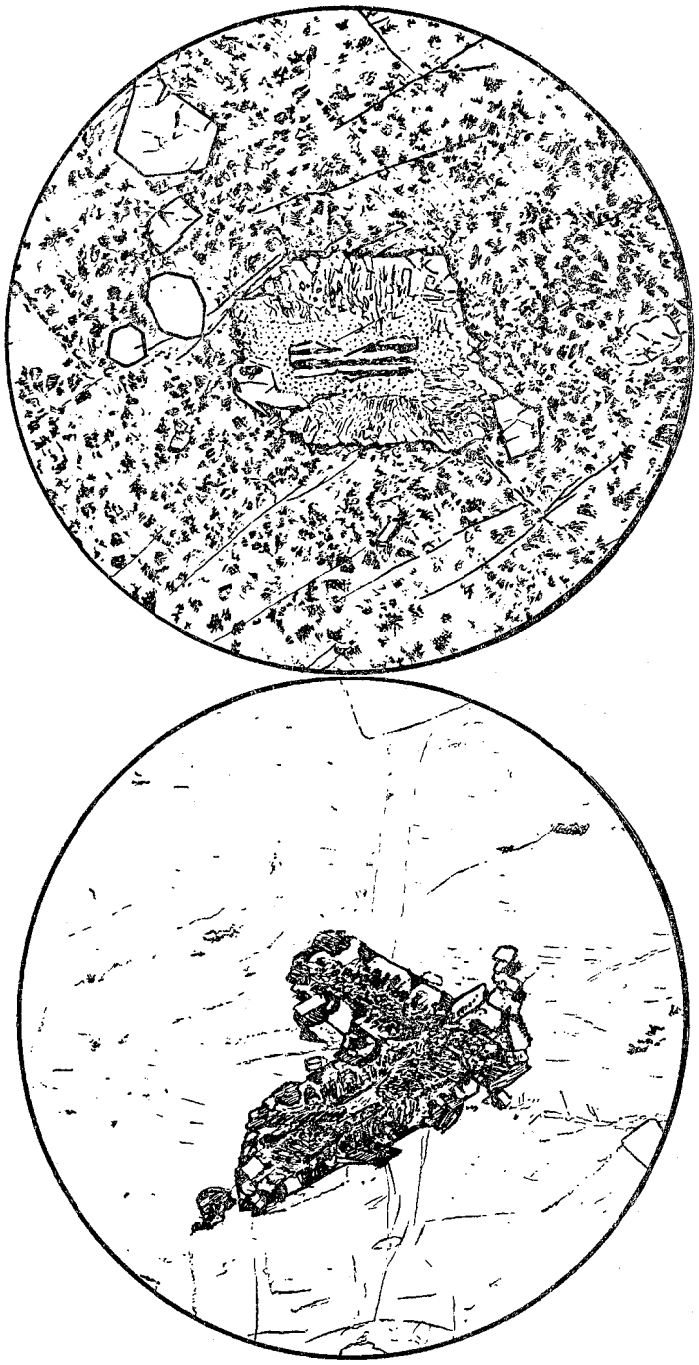

Figure 20 (left). INTERGROWTH OF TWO SUBHEDRAL GRANOPHYRIC GRAINS IN A GLASS MATRIX.

Figure 21 (right). PLAGIOCLASE CORE WITH SANIDINE OVERGROWTH SURROUNDED BY GRANOPHYRIC OVERGROWTH IN A GLASS MATRIX. NOTE CLEAR EUHEDRAL SANIDINE CRYSTALS.

DIAMETER OF FIELD IS 3.5 MM.

Figure 22
CORRODED QUARTZ PHENOCRYSTS PARTLY FILLED WITH SANIDINE OVER-GROWTHS IN A GLASS MATRIX.

DIAMETER OF FIELD IS 4 MM.

phase and separated by two distinct micrographic intergrowths, the grains appear to have grown toward each other until they were in contact.

Skeletal crystal growths of sanidine on large sanidine phenocrysts are common. The quartz commonly has secondary overgrowths, not in optical continuity, of a mineral believed to be sanidine. The over-growths are very fine-grained, spherulitic in appearance, uniaxial negative or biaxial negative with a small 2V, with an index less than quartz, greater than that of the matrix, and approximately equal to sanidine, and with an interference color of first-order gray.

On the basis of the above data the following conclusions are drawn concerning the green vitrophyric dikes:

1. The rounded phenocrysts indicate a period of corrosion and resolution. Inasmuch as most crystallized silicates are denser than the corresponding liquids, and as the crystallization process is generally exothermic, the decreased pressure on the igneous melt following in-

trusion into a higher level of the earth's crust would (in accordance with the Clausius-Clapeyron equation; see MacDougall, 1947, p 119) produce a resorption without an increase in temperature.

2. Because a conspicuous number of the fractures are parallel to the contacts of the green vitrophyres, and because the surrounding rocks show no excessive fracturing, these fractures are interpreted as cracks developed during cooling. The loci of the fractures parallel to the contacts may be due to a residual weakness caused by a shearing between various flow layers during intrusion. In a crystalline rock, slight compositional differences may produce a flow layering (Balk, 1948, pp 48-49). In a glass, slight compositional variations do not change the properties sufficiently to show flow layers, unless many inclusions are present or devitrification is considerable.

3. The phenocrysts in the glass are the result of a primary crystallization from the magma now represented by the glass. In spite of the corroded phenocrysts, the skeleton crystals and skeleton-crystal over-growths establish this. Also, the absence of any minerals which crystallize at higher temperatures eliminates the possibility that the phenocrysts are xenoliths which the glass incorporated from the rocks through which it passed.

4. There is a strong tendency for isolated phenocrysts suspended in a solution to adhere to one another when they come into contact, even in a melt with approximately 10 percent phenocrysts, as in the green vitrophyric dikes. In the other rhyolitic rocks of this region, where the phenocryst percentage is greater, this tendency is even more marked. The failure of many igneous rocks to show idealized crystallization sequences may be due to the aggregation tendency even in the early stages of crystallization.

Recent studies of plutonic rocks have included the origin of granophyric intergrowths. Primary crystallization from a melt, with or without a eutectic, or secondary crystallization by means of metasomatism, hydrothermal solutions, or related processes, are the two groups of hypotheses currently proposed. An excellent summary of the literature and various hypotheses on this subject is included in Drescher-Kaden's (1948) monograph, to which the reader is referred. In view of current interest it is proposed to discuss the previously described occurrence of granophyric texture in some detail.

The only other reported occurrence of granophyric phenocrysts in a glassy matrix is found in the African rift valleys, (N. L. Bowen, personal communication). Similar phenocrysts have been found, however, in lava flows (Iddings, 1899; cf pls LII and LIV). The crystallization of granophyric intergrowths in the vitrophyre may be a eutectic process. The estimated silica range of the glass, based on the refractive index (George, 1924, p 265), is not too dissimilar from the silica range of the silica-potash feldspar cotectic in the system $NaAlSiO_4$-$KAlSiO_4$-SiO_2 (Schairer, 1950). Evidence that this is not a eutectic crystallization is the fact that no skeletal crystals or overgrowths of quartz are found in the thinsections, whereas sanidine overgrowths and skeleton crystals are common.

The two varieties of mineral contacts described above must also be considered. The similarity of the corroded and embayed quartz phenocrysts partly filled with sanidine to the coarser granophyric inter-growths whose contacts are marked by included groundmass is very apparent (see figs 18, 19, and 22). Finally, the tendency of the phenocrysts to form grain aggregates may be significant.

A coherent picture of this crystallization can be formulated if one assumes that a natural silicate melt deviates slightly from homogeneity. This deviation is of the same order of magnitude as the equilibrium distribution of material in a polycomponent solution in a thin tube under the influence of a gravitational field. The picture is as follows:

1. The average composition of the melt is that of a eutectic or almost eutectic mixture.
2. Localized volumes of the melt deviate slightly from the average composition.
3. Quartz, sanidine, and granophyric intergrowths of the cuneiform or fine myrmekitelike varieties crystallize in different parts of the melt as a result of the slight compositional variations.
4. The melt then moves to a locality of lower pressure, presumably nearer the earth's surface.
5. The lowered pressure causes the phenocrysts to be corroded.
6. The movement of the melt improves its homogeneity, and now the composition in the examined section lies slightly on the potash-feldspar side of the cotectic line.
7. Crystallization of sanidine follows, preferentially occurring about some previously existing crystal, so that most of the corroded and embayed quartz crystals are re-formed into granophyric intergrowths.
8. Quenching and the formation of crystallites are the concluding steps.

The foregoing sequence appears to be consistent with all the facts. It indicates that two periods of granophyric growth occurred, and presumably, if crystallization had continued, a third period would also have occurred, when the composition of the melt again reached eutectic proportions. The explanation does not involve any very intricate conditions and probably this process is not unique.

XENOLITH ZONES

These map units are found in the west-central part of the area, primarily in several narrow north-south elongated belts (see pl 1). The size and abundance of the xenoliths assume such tremendous proportions that their distribution may be of significance (see fig 23). As all the tuffaceous rhyolite has numerous xenoliths, the mapped boundaries of this zone are somewhat arbitrary. Lines along which xenoliths cease to be the dominant feature were determined with as much care as possible, and, therefore, it is believed that the general distribution of the xenolithic facies is correctly mapped.

The various rocks comprising the xenoliths are, in order of decreas-

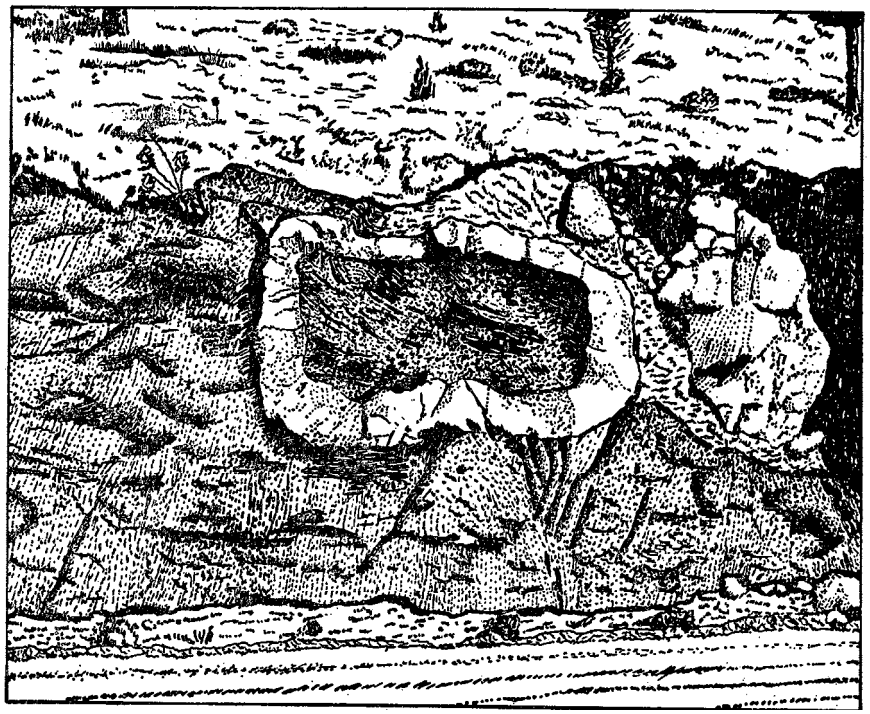

Figure 23
ANDESITIC XENOLITH ENCLOSED BY A STONY RHYOLITE RIM (LIGHT-COLORED) AND PARTLY ENCLOSED BY A BLACK RHYOLITE VITROPHYRE. XENOLITH IS 8 FEET LONG. ROAD CUT IN XENOLITH ZONE.

ing abundance: (1) volcanic rocks of the early andesite sequence, (2) red shale and sandstone of the Abo formation, (3) limestone resembling the Magdalena formation, and (4) blocks of limestone and black fissile shale (one locality only), which resemble the base of the Lake Valley limestone and the Percha black shale, respectively. The early andesite volcanics comprise approximately 90 percent of the xenoliths.

The average diameter of the xenoliths is estimated to be 10-20 feet. Large single exposures of foreign rock approach, however, a maxi-mum length of 80 feet or more. In fact, the size and continuity of some of the early andesite xenoliths is great enough, so that they cannot be shown definitely to be xenoliths and, as a result, the contact between the tuffaceous rhyolite and the early andesite volcanic rocks is interpreted as occurring near the surface in this area (see cross-section, pl 1). The shape of the xenoliths varies from angular to round, and well-rounded xenoliths are quite common.

The smaller xenoliths are contained in a tuffaceous rhyolite matrix; the larger ones, in addition, are intimately interpenetrated by

veins and dikes of tuffaceous rhyolite. Both megascopically and microscopically the tuffaceous rhyolite of the xenolith zone is practically identical with the tuffaceous rhyolite previously described. It differs chiefly in containing only brown biotite (in thinsection) and possibly slightly more glass in the matrix.

The tuffaceous rhyolite in this area has the same two planar structural elements as were described previously for the normal part of the tuffaceous rhyolite. In the xenolith zone, planar structures of the tuffaceous rhyolite have a random orientation (see p11), as do the few bed-ding planes that are measurable in the xenoliths. The planar and linear structures of the tuffaceous rhyolite bend around the enclosed xenoliths and range considerably in their orientation even within a single outcrop. No evidence of a connection between the irregular structures and faulting was found. As these structures do not have any discernible relationship to possible compactional forces modified by faulting, and as the planar structures of the xenolith zone resemble closely those of the remaining tuffaceous rhyolite, it may be concluded that a large part of the structures in the tuffaceous rhyolite is the result of flow.

In the xenolith zone, there are abundant thin veins, dikes, and larger irregular masses (40 feet and less is the maximum dimension) of a black rhyolite vitrophyre (see fig. 23). The chemical composition, norm, and mode of a rhyolite vitrophyre specimen, carefully selected, may be compared with that of a xenolith and the crystalline tuffaceous rhyolite in Table 6 (columns V2, L2, and R2). The megascopic and microscopic texture is identical with that of the tuffaceous rhyolite, with respect to the phenocrysts which the rock contains. Many of the vitrophyre-crystalline rhyolite contacts are marked by a lighter-colored zone (18 inches and less thick) of crystalline tuffaceous rhyolite. The lenticular planar structures in the lighter-colored zone and in the nearby darker tuffaceous rhyolite are parallel to the contact, although some of the thinner vitrophyre dikes truncate the structure of the surrounding tuffaceous rhyolite. Abundant xenoliths, primarily of the early andesite volcanic sequence, are completely or partly enclosed by massive vitrophyre. This aspect will be discussed in some detail in the following section.

In places, the vitrophyre is devitrified, especially along fractures. Thin light-colored veins of devitrified rock penetrate black vitrophyres, both of which have similar phenocrysts and textures. Large spheroidal masses (2 to 3 feet in diameter) of rhyolite vitrophyre appear to be enclosed by the tuffaceous rhyolite as xenoliths. Smaller xenoliths of layered black vitrophyre have a eutaxitic structure parallel to that of the enclosing tuffaceous rhyolite.

The following conclusions are drawn on the basis of the foregoing summary:

1. The great concentration of xenoliths, the lack of sorting, and the wide variation in the amount of enclosing material make it probable that the rocks of these zones do not represent an airborne pyroclastic deposit.

TABLE 6. ANALYSES, NORMS, AND MODES OF IGNEOUS ROCKS OF THE KINGSTON REGION, NEW MEXICO

	Specimen number						
	NL2	L2	R2	V2	389-A-236	389-C-87	389-B-C1
	Analyses[a]						
SiO_2	59.10	62.78	72.82	70.05	58.41	53.55	70.64
TiO_2	0.95	0.78	0.33	0.37	0.78	1.44	0.30
Al_2O_3	13.04	13.09	11.49	12.98	14.44	15.09	13.87
Fe_2O_3	4.32	4.50	1.67	1.41	4.08	3.01	1.79
FeO	1.50	0.67	0.67	0.90	2.02	5.46	0.26
MnO	0.08	0.10	0.06	0.07	0.07	0.16	0.23
MgO	1.81	2.03	0.61	0.68	1.71	5.72	0.72
CaO	5.50	3.29	1.43	2.09	5.58	8.22	1.60
Na_2O	3.65	2.54	2.70	3.98	3.51	2.90	3.00
K_2O	2.60	3.18	5.13	3.57	3.16	1.84	3.96
P_2O_5	0.27	0.19	0.10	0.08	0.27	0.35	0.06
H_2O+	3.72	3.41	2.12	3.13	2.15	1.14	2.77
H_2O-	0.83	3.12	0.54	0.30	0.51	0.28	0.72
CO_2	2.19	0.00	0.00	0.00	2.81	0.71	0.00
Total	99.56	99.68	99.67	99.61	99.50	99.87	99.72
Specific Gravity	2.49	2.41	2.46	2.43	2.69	2.74	2.41

a Analyst, H. B. Wiik, Helsinki, Finland.

TABLE 6 (continued).

	Specimen number						
	NL2	L2	R2	V2	389-A-236	389-C-87	389-B-C1
Norms							
Quartz	20.16	26.16	34.38	28.44	19.98	6.42	33.66
Orthoclase	15.57	18.90	30.02	21.13	18.90	10.56	23.35
Albite	30.92	21.48	23.06	34.06	29.34	24.63	25.15
Anorthite	11.12	14.73	4.17	6.67	8.06	22.80	8.06
Corundum	—	—	—	—	2.24	—	1.73
Pyroxene[b] Wo	0.23	0.35	0.93	1.28	—	4.76	—
Pyroxene[b] En	4.50	5.10	1.50	1.70	4.30	14.30	1.80
Pyroxene[b] Fs	—	—	—	—	—	5.41	—
Ilmenite	1.82	1.52	0.61	0.76	1.52	2.74	0.61
Magnetite	2.32	—	1.39	2.09	4.41	4.41	—
Hematite	2.72	4.48	0.80	—	1.12	—	1.76
Apatite	0.67	0.34	0.34	0.34	0.67	0.67	—
Calcite	4.90	—	—	—	6.40	1.60	—
Modes							
Quartz[c]	3	9	7-14	8-14	6	—	17.7
Sanidine	22	13	10-13	10-13	—	—	22.4
Plagioclase (An_{35-50})			x	x	18	57	—
Plagioclase (An_{10-35})	—	—	10-18	10-18	—	—	19.9
Pyroxene Augite	—	—	x	x	—	—	—
Pyroxene Pigeonite	1	2	—	—	—	31	—
Olivine	—	—	—	—	—	1	—
Iddingsite	—	—	—	—	—	3	—

x Indicates present.

b Normative pyroxene calculated in the manner suggested by Barth (1931).

c Includes possible tridymite and cristobalite.

TABLE 6 (continued).

	Specimen number						
	NL2	L2	R2	V2	389-A-236	389-C-87	389-B-C1
	Modes (continued)						
Biotite	x	x	x-1	x-2	—	—	3.4
Hornblende	—	x	x-1	x	—	—	—
Matrix	55	63	—	—	61	—	32.4
Glass	x	—	—	55.5-59.0	—	—	—
Devitrified glass	x	x	57-61	—	—	—	—
Magnetite and ilmenite	3	2	1	1	3	6	0.6
Apatite	x	x	x	x	—	—	x
Sphene	x	x	x	x	—	—	0.3
Rutile	—	—	x	x	—	—	—
Zircon	—	—	x	x	—	—	—
Rock fragments[d]	—	—	x-1	x-3	—	—	—
Chlorite	3	—	—	—	6	—	—
Hematite and leucoxene	x	x	x	x	x	x	x
Sericite	4	9	—	—	—	—	—
Calcite	5	—	—	—	6	—	—
Zeolites[e]	x	x	—	—	—	—	3.1
Epidote	x	—	—	—	—	—	—

x Indicates present.

d The rock fragments have approximately the same mineral composition as NL2 and L2. Therefore, in these specimens they have not been counted separately.

e See text for mineral properties which have tentatively been interpreted as zeolites.

TABLE 6 (continued).

Description of Specimens
NL2. Quartz latite tuff (II. 4. 2. 4.). Composite sample of bedded tuff of the earliest volcanic sequence from the following localities: 1. Along western boundary of SW¼SW¼ sec. 13, T. 16 S., R. 9 W. (unsurveyed). 2. Center of SW¼NW¼ sec. 18, T. 16 S., R. 9 W. (unsurveyed). 3. Center of sec. 21, T. 16 S., R. 9 W. (unsurveyed). 4. Center of NE¼NE¼ sec. 22, T. 16 S., R. 9 W. (unsurveyed). 5. On State Highway 180, half a mile west of Emory Pass, sec. 16, T. 16 S., R. 9 W. (unsurveyed).
L2. Quartz latite tuff (II. 4. 3. 3.). Xenolith of tuff enclosed in a rhyolite vitrophyre. On State Highway 180, in S¼NE¼ sec. 27, T. 16 S., R. 10 W.
R2. Tuffaceous rhyolite (I. 4. 2. 3.). Crystalline rock enclosing xenolith described above.
V2. Rhyolite vitrophyre (I. 4. 2. 4.). This rock encloses L2 and R2. Location described under L2.
389-A-236. Quartz latite flow (II. 4. 2. 3 (4).). Plagioclase well altered and replaced by calcite, so that originally this rock was probably a dacite. Specimen of the early andesite sequence from: road cut on State Highway 180, approximately three-fourths mile west of Emory Pass, along the E. boundary, NE¼SW¼ sec. 16, T. 16 S., R. 9 W. (unsurveyed).
389-C-87. Andesite flow (II. 5. 3. 4.). Approximately 300 feet north of State Highway 180 and USBM number Z126, at S. boundary, SW¼SE¼ sec. 8, T. 17 S., R. 10 W.
389-B-C1. Rhyolite porphyry, granitoid phase (I. (3) 4. 2. 3.). Rabb Canyon pegmatite area, 2¼ miles northward from juncture of Rabb and Noonday Canyons.

2. The contemporaneity of the xenolith zones and the entire tuffaceous rhyolite is established by the contacts and petrographic similarity.

3. This deposit was formed essentially in place and might be called a vent agglomerate zone. Occurrence within a volcanic rock, distribution parallel to the north-south regional structure, and petrologic similarity to the tuffaceous rhyolite, all lead to this interpretation. Barth (1950) has described similar fissure zones in the volcanic rocks of Iceland, which periodically were reopened by rupturing and so allowed lava to escape. Here the concentration of xenoliths is so high that it does not appear likely that this zone was a major escape route for the rhyolitic volcanics found in the region. An alternate possibility is that the xenolith zone represents the basal phase of the tuffaceous rhyolite, including debris from the surface over which it flowed. Such large amounts of possible surface debris are absent in other localities where the base of the tuffaceous rhyolite is well exposed. This means that local concentrations of possible surface debris would suggest proximity to an orifice or a fissure zone from which igneous material was extruded.

ENDOMORPHIC EFFECTS OF XENOLITHS IN VOLCANIC GLASS

Xenoliths of quartz latite tuff (from the pyroclastic facies of the early andesite volcanic sequence) are very abundant in the rhyolite vitrophyres of the xenolith zone. Their size ranges from a maximum diameter of 20 feet to a small fraction of an inch, and many xenoliths are enclosed in a thin shell of crystalline tuffaceous rhyolite roughly concentric about the xenolith (see fig 23).

The shell of crystalline tuffaceous rhyolite (henceforth called the crystalline rim, or simply rim) appears identical with the massive tuffaceous rhyolite described above. The rim even shows the irregular lighter-colored lenticular patches of groundmass which constitute the planar structure. This planar structure is parallel to the xenolith contact. The massive rhyolite vitrophyre has approximately the same sizes and varieties of phenocrysts as has the crystalline rim. In the outcrop the quartz latite tuff xenoliths do not differ markedly from the quartz latite described above under the heading "Andesite, latite, and their quartzose equivalents," except that their color may be a slightly brighter shade of red.

Microscopic study showed that the crystalline rim and the enclosing vitrophyre have the same texture and composition with respect to the phenocrysts as the tuffaceous rhyolite described above (figs 24-25). However, none of the biotite has been oxidized to a red color. The matrix of the vitrophyre is a very pale-brown glass with an index of 1.497 (±0.002). It shows no devitrification, except very slightly along a few cracks. Locally a eutaxitic structure occurs. The vitrophyre groundmass contains a noticeable amount of small broken fragments of the phenocrysts, and in some lenses this approaches a rock flour or gouge in its fineness. The matrix of the rim is cryptocrystalline, with an overall index of refraction less than that of balsam, and is clouded with oxides of iron. The rim has radial or spherulitic finely intergrown

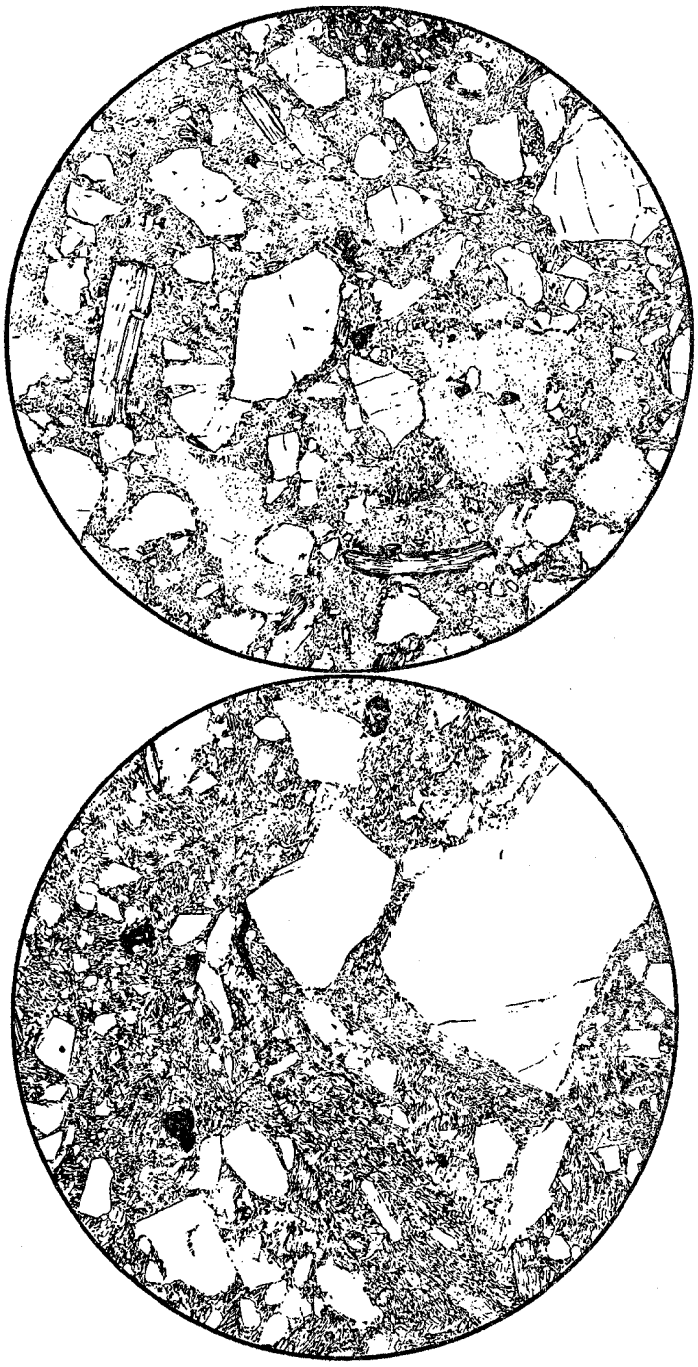

Figure 24 (left). CRYSTALLINE RHYOLITE RIM.
Figure 25 (right). BLACK RHYOLITE VITROPHYRE; MATRIX IS UNALTERED GLASS AND FINE ROCK FLOUR.
DIAMETER OF FIELD IS 3 MM

fibers which locally radiate outward from small broken crystal fragments, slightly larger anhedral quartz grains, and very fine dendrite-shaped intergrown masses.

Petrographically xenoliths of quartz latite tuff differ only slightly from the previously described quartz latite. The groundmass of the tuff xenoliths is more opaque and contains some small secondary spheroidal masses, which consist of an anhedral quartz shell enclosing quartz, quartz and sericite, or quartz and zeolites. Quartz also occurs in several thin veins, with which is associated a brown to colorless, uncorroded, unaltered biotite. The fresh appearance of this biotite is in marked contrast with the corroded and bleached sparse biotite grains found throughout these pyroclastic rocks. Sericite is a common constituent of the tuff xenoliths and occurs chiefly as small grains in the matrix. The sericite also forms radial fibrous aggregates, which are pseudomorphous after a mineral with a square (or nearly so) cross-section. The chemical analyses, norms, and modes of these rocks are listed in Table 6.

It is obvious from the field observations that the size of the crystal-line rim is proportional to the size of the xenolith. It was believed, however, that a more exact idea as to the nature of the proportionality would be valuable. In order to measure the size relations of the xenoliths and crystalline rims, it was necessary to make the following simplifying assumptions:

1. An areal measurement would be directly proportional to the volume of the xenolith.

2. The shape of all the xenoliths is very similar; differences are random and minor in degree. Actually, this assumption appears valid. Most of the xenoliths, especially the larger ones, show a moderate rounding. The small xenoliths are more angular, but because they are also much more abundant, the larger number of obtainable measurements should compensate for this difference in shape, if the variation is random.

3. The cross-sectional shape of the xenoliths falls between that of an ellipse and a rectangle. This also is true as a reasonable first approximation.

On this basis the area may be computed easily by measuring the major axis of the xenolith and by measuring the minor axis approximately bisecting the major one, and at a right angle to it. Then the area of the xenolith is $K(ab)$, where a is the major semiaxis of the xenolith, b the minor semiaxis, and K is a proportionality constant, which, according to the assumptions, is very nearly the same for all the xenoliths and has a value between ,r and 4. Accordingly, a plot of the rim thickness, denoted by r, versus the xenolith size factor (ab) will give a measure of the variation of the size of the xenoliths with the size of the crystalline rims, since K is assumed constant.

The original measurements are listed in Table 7 and illustrated graphically in Figure 26, where they have been plotted on a logarithmic

scale. The straight line (fig 26) was calculated by the method of least mean squares, and has the equation:

$$\log (r) = -0.4009 + 0.4240 \log (ab)$$

The correlation coefficient is 0.97, which has a high significance level. The logarithmic scale was used for convenience in illustrating the measurements on a single graph, and because any deviations from linearity would not involve computations of a second-degree equation. In addition, the few large measurements would not so completely domi-

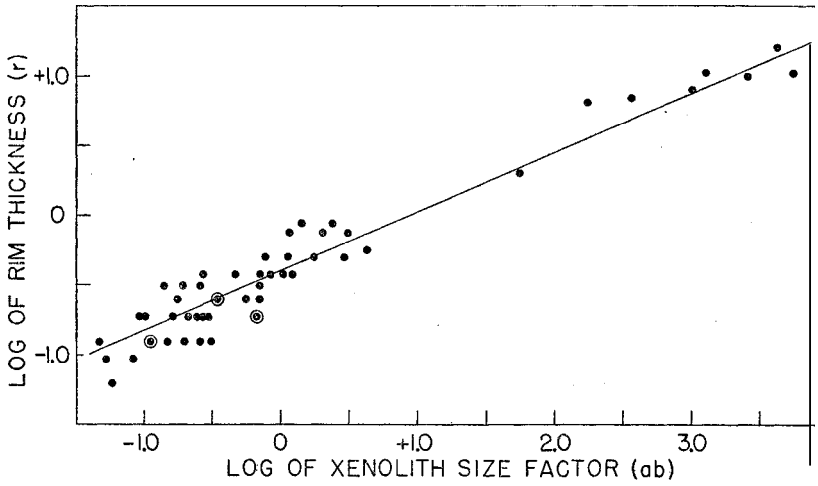

Figure 26. VARIATION OF THE CRYSTALLINE RIM THICKNESS WITH THE XENOLITH SIZE. CIRCLED DOTS INDICATE TWO NEARLY IDENTICAL MEASUREMENTS. SEE TEXT.

nate the determination of the line of best fit. The correlation coefficient on an arithmetic scale is 0.86, still of high significance; however, the straight line of best fit almost completely ignores the larger numerical measurements. The error in the ratio of the size of the crystalline rim to the size of the xenolith, owing to the fact that the measured cross-section is not a principal cross-section, is such that the size of the crystal-line rim will be larger per size of xenolith than it should be, and the slope of the line of best fit will be greater than the true slope. The true relationship, however, may be given by an exponential function of some variety, since this is commonly found to be the case in chemical reactions and in growth processes. Here it is concluded merely that the rim thickness is a function of the xenolith size, and that the rim and xenolith are genetically related.

Analyses V2, R2, L2, and NL2, listed in Table 6, were made in order to ascertain what chemical changes occurred during the crystallization of the matrix of the rim. Analyses V2, R2, and L2 are each composites of three. specimens taken radially outward from the same

xenolith (see table 6) at a distance of 3 feet from the rim, at the rim, and at a distance approximately 3 inches inside the xenolith-rim con-tact. Analysis NL2 represents a composite of many specimens taken at the localities listed in Table 6, and has been called the "normal" quartz latite. It is poor procedure to consider the differences between the xenolith and the "normal" quartz latite when there is no measure of the standard deviation of the latter. Therefore, it is emphasized that the comparison of the xenolith and "normal" quartz latite is given only as a crude first approximation. Now that the differences in composition have been established, contemplated future sampling will remove this objection. Actually, analysis of a quartz latite flow (number 389-A-236 in table 6) suggests that analysis NL2 approaches closely the normal quartz latite.

These changes can be better understood if the analyses are re-calculated in terms of the standard rock cell as defined by Barth (1948), which assumes that the oxygen is constant, so that one may compare changes in the relative molecular amounts of the positive cations with reference to a standard oxygen concentration. This recalculation for the major constituents is presented in Table 8, which also lists the differences between the amounts of the various metallic elements in

TABLE 7. SIZE MEASUREMENTS * ON XENOLITHS AND CRYSTALLINE RIMS

r	*a*	b	*r*	*a*	*b*
2.0	7.75	7.12	.12	.59	.19
.5	1.75	1.0	.12	.53	.38
.09	.34	.25	.19	.88	.75
.12	.25	.19	0.5	1.12	.69
.25	.69	.5	.25	1.12	.50
.19	.38	.25	.25	.56	.31
.12	.62	.5	.75	1.09	1.06
.19	.41	.25	.12	.59	.25
.12	.41	.28	.38	1.56	.69
.88	1.62	.88	.31	1.12	.62
.12	.69	.38	.38	.62	.44
.19	.69	.44	.25	.62	.56
.06	.31	.19	.19	.56	.38
.19	.44	.38	.19	.53	.50
.75	2.50	1.25	.50	1.81	1.62
.75	1.62	1.25	.38	1.31	.62
.31	.44	.38	.56	2.12	2.0
.31	.56	.25	.31	.69	.38
.25	1.25	.56	6.5	16.5	10.5
.38	.88	.81	11.0	45.0	28.0
.88	2.12	1.12	8.0	40.0	25.0
.38	1.12	.75	16.0	138.0	30.0
.19	.56	.44	11.0	90.0	60.0
.50	1.12	1.0	7.0	22.0	16.5
.38	.75	.62	10.0	60.0	42.0
.19	1.0	.69	.09	.28	.19

* The measurements were made in inches and fractions of an inch, and were rounded off to two decimal places for the tabulation. The thickness of the crystalline rim is r, and the major and minor semiaxes of the xenolith are a and b, respectively.

TABLE 8. COMPOSITIONAL DIFFERENCES BETWEEN THE VITROPHYRE, RIM, XENOLITH, AND "NORMAL" QUARTZ LATITE*

	VITROPHYRE		RIM		XENOLITH		"NORMAL" QUARTZ LATITE
ELEMENT	(V2)	(R2)-(V2)	(R2)	(R2)-(L2)	(L2)	(L2)-(NL2)	(NL2)
Si	60.24	+2.88	63.12	+6.75	56.37	+4.32	52.05
Ti	.26	-0.05	.21	-0.33	.54	- .09	.63
Al	13.12	-1.35	11.77	-2.04	13.81	+ .27	13.54
Fe	1.60	-0.09	1.51	-2.00	3.51	- .46	3.97
Mg	.88	-0.10	.78	-1.92	2.70	+ .32	2.38
Ca	1.91	-0.61	1.30	-1.88	3.18	-2.00	5.18
Na	6.61	-2.03	4.58	+0.21	4.37	-1.87	6.24
K	3.93	+1.69	5.62	+1.95	3.67	+0.71	2.96

* Calculated according to the standard rock cell (Barth, 1948). See text for discussion of "normal" quartz latite.

related rocks. In Table 9, the various elements are arranged in order of their increasing abundance in the rim relative to surrounding rocks, and in the xenolith relative to the "normal" quartz latite. The figures should not be regarded in terms of the absolute values, but only with respect to the direction of compositional differences and the order of arrangement of the elements.

It is apparent from Tables 8 and 9 that the rim has been enriched in potash and silica relative to its surroundings, whereas the remaining materials have been decreased relatively. Calcium, titanium, magnesium, aluminum, and iron show a consistent decrease in comparison with the rim surroundings, whereas sodium has increased in the rim relative to the xenolith and decreased relative to the vitrophyre. When the rim is compared with its surroundings (table 9), the magnesium is lower than the iron, and aluminum is lower than silicon. It is interesting to note that, with one exception (i.e., magnesium greater than iron), the same relative order of compositional differences is manifest when the xenolith and "normal" quartz latite are compared (table 9).

Spectrometric analyses, kindly made by Mr. O. Joensuu, of the matrices of the rim and the vitrophyre (table 10) show that the differences in the soda-potash ratios of the matrices are of the same magnitude as the differences in the soda-potash ratios of the vitrophyre and the rim, considering the entire rocks. Owing to the fractured and broken phenocrysts and fine rock flour, the separation of phenocrysts from matrix cannot be regarded as complete, and therefore the data are of value only in indicating the order of magnitude.

Single-crystal X-ray photographs (utilizing iron radiation with a manganese filter) of the sanidine phenocrysts in the vitrophyre and the crystalline rim were taken by Dr. Fritz Laves and the author. This study showed that the sanidine phenocrysts in both rocks consist of sub-

TABLE 9. DIRECTION AND RELATIVE MAGNITUDE OF THE COMPOSITIONAL DIFFERENCES BETWEEN THE RIM AND ITS SURROUNDINGS, AND BETWEEN THE XENOLITH AND "NORMAL" QUARTZ LATITE*

ELEMENT	(R2) — (V2) / (V2)	ELEMENT	(R2) — (L2) / (L2)	ELEMENT	(L2) — (NL2) / (NL2)
Ca	—.319	Mg	—.712	Ca	—.386
Na	—.307	Ti	—.610	Na	—.299
Ti	—.192	Ca	—.592	Ti	—.142
Mg	—.113	Fe	—.570	Fe	—.115
Al	—.102	Al	—.148	Al	+.019
Fe	—.056	Na	+.048	Si	+.082
Si	+.048	Si	+.119	Mg	+.134
K	+.430	K	+.531	K	+.239

* The headings in the second, fourth, and sixth columns refer to the column headings in Table 8. The direction of the differences between the various analyses is given by the sign. A minus sign indicates a decrease in the rim relative to its surroundings, or, in the fifth and sixth columns, a decrease in the xenolith relative to the so-called "normal" quartz latite; a plus sign indicates the opposite. The elements are arranged in order of magnitude.

microscopically unmixed orthoclase and high-albite. The sanidine of the vitrophyre has been unmixed to a greater degree, so that the highalbite parts have a much more pronounced triclinicity. After heating 15 minutes at a temperature of 855°C, the sanidine phenocrysts from both vitrophyre and rim became homogeneous. Both heated sanidines have the same composition $Or_{71}Ab_{29}$ (all sanidine compositions in this report are in mole percent, ± 5 percent).

X-ray powder diagrams of heated sanidine phenocrysts also indicated approximately the same composition (see table 11), utilizing the data of Bowen and Tuttle (1950), and Osten (1951). A powder diagram of unheated sanidine phenocrysts shows (table 11) that the composition based on Bowen and Tuttle's (1950) work differs from that determined with the use of Osten's (1951) data. Since Bowen and Tuttle used pure synthetic minerals which were probably not unmixed, this is not surprising. Osten used natunil minerals which were probably unmixed, and correlated X-ray data with chemical analyses. In a natural mineral the (201) spacings (used by Bowen and Tuttle) of both unmixed phases might not be detected in a powder diagram.

Quartz, potassic sanidine, and sodic sanidine are believed to form the rim matrix on the basis of the X-ray data (table 11). It should be noted that the 4.166 or 4.180 spacing of the potash sanidine does not become apparent until after heating, suggesting that two sanidines were made homogeneous. This is not surprising, as the adjacent quartz lines could easily obscure the 201 lines of a very potassic sanidine. As the 201 spacing (4.047 and 4.054, within the limits of error) does not disappear after 15 minutes at 855°C, it is possible that the potassic and sodic sanidine did not become completely homogeneous and are present, therefore, in the matrix as separate grains rather than cryptoperthites. However, it is also possible that these lines (4.047 and 4.054) were caused by a mineral other than feldspar. One X-ray picture of the matrix material which had been heated for about 24 hours at 900°C was made, in which the powder rod was not allowed to rotate. The uniform, easily measured lines, except for some darker quartz spots, attest to the exceedingly fine-grained nature of the rim matrix. The composition average (table 11) of the homogeneous sanidine in the matrix is identical with that of the sanidine phenocrysts. The fact that neither tridymite nor cristobalite was detected, and the possibility that

TABLE 10. SODA-POTASH CONTENT OF THE MATRICES OF THE RHYOLITE VITROPHYRE AND THE CRYSTALLINE RIM*

OXIDE	WEIGHT PERCENT	
	VITROPHYRE- (V2)	RIM- (R2)
Na_5O	3.7±.2	2.75±.2
K_2O	4.0±.2	5.0 ±.2

* Spectrometric analysis by O. Joensuu, Dept. of Geology, University of Chicago.

TABLE 11. X-RAY DATA ON THE SANIDINE PHENOCRYSTS AND THE MATRIX IN THE CRYSTALLINE RIM

MATERIAL	d[a]	I/I_1	COMPOSITION	SOURCE[b]
Sanidine	4.214	.4	$Or_{87}Ab_{13}$	B
	3.299	.8	Or $(+An)_{76}Ab_{24}$	O
	3.221	1.0		
	1.496	.2	Or $(+An)_{75}Ab_{25}$	O
	1.286	.1		
Heated Sanidine	4.168	.4	$Or_{68}Ab_{32}$	B
	3.281	.8	Or $(+An)_{76}Ab_{24}$	O
	3.192	1.0		
	1.496	.4	Or $(+An)_{71}Ab_{29}$	O
	1.285	.1		
Matrix	4.250	.4	Quartz	—
	4.047	.1	Or_8Ab_{92}	B
	3.344	1.0	Quartz	—
	1.499	.1	Or $(+An)_{77}Ab_{23}$	O
	1.289	.1		
Heated matrix (15 minutes)	4.251	.3	Quartz	—
	4.166	.1	$Or_{67}Ab_{32}$	B
	4.054	.1	Or_9Ab_{91}	B
	3.348	1.0	Quartz	—
	3.273	.4	Or $(+An)_{71}Ab_{29}$	O
	3.204	.4		
Heated matrix (24 hours)	4.258	.3	Quartz	—
	4.180	.1	$Or_{72}Ab_{28}$	B
	3.346	1.0	Quartz	—
	3.274	.2	Or $(+An)_{70}Ab_{30}$	O
	3.207	.2		
	1.492	.1	Or $(+An)_{72}Ab_{28}$	O
	1.282	.1		

[a] Only spacings of feldspar which were used to determine molecular composition and adjacent quartz lines are presented.

[b] Data indicating the variation of lattice spacings with chemical composition for the alkali feldspars have been taken from Bowen and Tuttle (1950), indicated by B, and Osten (1951), indicated by O. Osten's data give the Ab percent of the total Or + Ab + An content.

the potassic and sodic sanidine may form separate grains rather than cryptoperthites, suggest a low crystallization temperature.

Geologic literature contains some evidence that glasses have a much more limited composition than do the corresponding crystalline rocks. This is especially conspicuous if a comparison is made with plutonic rocks (Bowen, 1928, figs 38-39). A comparison of 34 rhyolites and 19 rhyolitic glasses from Johannsen (1932) shows that no glasses have a soda-potash ratio (weight percent) less than 0.47, whereas 14 crystal-

line rhyolites do. Analyses of 33 glasses which George (1924) has studied show a minimum soda-potash ratio of 0.53, and, for most glasses, the ratio is greater than 0.9. R. D. Terzaghi (1935) has compared four volcanic glasses and the devitrified rocks which are supposedly their equivalents. She finds that in the process of devitrification the potash content is increased, whereas the soda content decreases, and concludes, "Devitrification and alteration involving replacement or selective leaching or both, are two closely related processes." The above authors obtained most of their data from Washington's tables of chemical analyses, and there may be some duplication involved. However, there is a general indication that rhyolitic glasses are higher in soda and lower in potash than the corresponding crystalline rocks.

Comparison of the analyses of the Magdalena perlite (in Socorro County, New Mexico), and the associated rhyolite and devitrified perlite, strengthens the suggestion that the soda-potash ratio (weight percent) in rhyolitic glasses is higher than that of the corresponding crystalline rocks (data from Dr. R. H. Weber, personal communication).

There should be soda rhyolites, of course, which are higher in soda content than their corresponding glasses. Unfortunately this cannot be checked by a review of tables of analyses, unless geologic conditions are known. In other words, high-soda glasses and rhyolites are well within the compositional limits of igneous rocks, and, therefore, variation of the soda-potash ratio during devitrification could not be studied by a review of analyses, but would require special sampling with this purpose in mind.

Fenner (1936, 1934) has shown that the hot-spring waters of Yellowstone Park have replaced soda and lime by potash and silica. This process has occurred in the crystalline lavas and with the devitrification of some glasses. On the other hand, Barth (1950) has demonstrated that replacement by the acid hot-spring waters of Iceland produces only an enrichment in Si and H, whereas leaching by the acid hot-spring waters produces an enrichment in Al, Fe, and K.

The first problem to be considered in detail is the origin of the crystalline rims. It is known that rapid cooling, suggested by the presence of the vitrophyre, is not conducive to crystallization. Are the rims the result of a primary crystallization, or of some secondary process similar to alteration? In this connection the following hypotheses are to be considered:

I. The rims originated during a crystallization which predates the present occurrence of the xenoliths and vitrophyres.

2. The xenolith acted as a seed crystal.

3. Leaching, hydrothermal replacement, or alteration of the vitrophyre produced the rims.

4. Volatiles lost by the xenolith caused crystallization of the rim.

5. The xenoliths reacted with the more acidic melt according to the reaction principle (Bowen, 1928).

The first two hypotheses may be discarded summarily. The con-centric and conformable rims around the xenoliths eliminate a previous

crystallization. Abundant phenocrysts in both the rim and vitrophyre prove that seed crystals did not determine crystallization.

Fresh primary minerals of the rim, which may be observed in hand specimen and thinsection, and identified by x-ray study, are not compatible with an origin by leaching, hydrothermal replacement, or alteration. It seems likely that such secondary processes in a near-surface volcanic rock of this nature would produce an abundance of the common alteration minerals. There are some fractures in the vitrophyric masses along which devitrification has proceeded, probably by leaching. These devitrified rocks, insofar as they have been examined, are very friable. In addition, all alteration seen in thinsections of the rocks of this region has resulted in an enrichment in calcite. Loss of calcium in the rim, relative to the rim surroundings, is clearly demonstrated in Tables 8 and 9. Finally, the demonstrated relationship between the sizes of the xenoliths and the crystalline rims precludes a postquenching generating process.

All rocks have a certain pore space which may be filled with meteoric water. If a rock containing interstitial water were to become incorporated in an igneous melt, the heat of the melt would cause the water to expand, so that a part of the connate water might be driven out into the surrounding liquid. This escaped water and other volatiles would act as a flux and reduce the viscosity of the surrounding melt, thus promoting its crystallization. Several geologists have offered this hypothesis as one explanation of the coarser-grained rims surrounding some igneous inclusions. In the xenoliths here described, such an expansion of volatiles would have had a cooling effect, but it is evident by the presence of the glass that cooling was already exceedingly rapid. Also, if devitrification is a simple process involving a thin zone of reduced viscosity surrounding a xenolith, then there is no reason why the rocks should differ chemically (table 8). However, this hypothesis can-not be completely eliminated.

According to Bowen (1928, pp 185-191) an acidic melt should react with a more basic inclusion, precipitating material which is, in equilibrium with the melt. Furthermore, this reaction is exothermic and, therefore, would tend to occur during a period of cooling. Because natural silicate melts in general crystallize incongruently, there should also be a difference in the composition of the melt and the crystals, or between the vitrophyre and the rim. The changes in the xenolith as a result of the reaction should be parallel to the differences between the melt and the crystalline material. If the "normal" quartz lathe can be compared with any validity, this is found to be so. Plotting these rocks in the ternary diagram, quartz-soda feldspar-potash feldspar (Schairer, 1950) shows that the liquid phase of a silicate melt of this composition should be precipitating silica, which would produce a rim enriched in quartz. Examination of the binary system $NaAlSi_3O_8$-$KA1Si_3O_8$ (Bowen and Tuttle, 1950) shows that a liquid of the vitrophyre's composition should precipitate feldspar of a higher potash content. In both cases, the rocks exhibit the expected phenomena, if one assumes a crystallization sequence.

It is concluded; therefore, that the rim is the crystallized equivalent

of the glass, and that it crystallized from the natural silicate melt now represented by the glass. This, was caused by the operation of the reaction principle, with some possible assistance from volatiles escaping from the xenolith.

In view of the lack of tridymite in the crystalline rim, it would appear that the temperature of formation was low. The fact that after a short heat treatment the soda-potash feldspars in the rim have not become homogeneous suggests that they are not cryptoperthitically intergrown. This in turn points toward a low temperature of formation, since soda-potash feldspars form a complete solid solution at high temperatures (Bowen and Tuttle, 1950).

Excluding gaseous transfer, because there is no evidence of vesiculation in the glass, diffusion and movement by liquid flow are the two most probable mechanisms by means of which material in the melt could have moved to its place of crystallization. Since the rims are con-centric and do not have any thicker sides, liquid flow in the melt could not have been very large. The viscosity of obsidian, approximately 10^{12} poises at 800°C (Birch, et al., 1942), is so great that neither diffusion nor flow could have been very rapid. Contemplated refractive index determinations on the glass may decide which of these two processes was more operative.

Tables 8 and 9 show that silicon, and potassium in the rim represent a geochemical culmination (defined by Reynolds, 1946, pp 391-392) with respect to the surrounding materials. Similarly, the remaining constituents indicate a geochemical depression (also defined by Reynolds). Those materials which show a geochemical depression must have moved away from the place of crystallization; consequently, adjacent areas may show geochemical culmination in these constituents. These rocks indicate that such geochemical phenomena can be produced by a lack of equilibrium in an igneous process. Recently Corn-wall (1951), Kahma (1951, pp 44-45), and others have shown that such culminations or depressions are common in igneous rocks.

If we assume that the time of quenching was the same for all constituents, then Table 9 shows that potassium has a greater proportional enrichment in the rim than silicon. From this it would appear that the movement of potassium toward the locus of crystallization was faster than that of the silicon. This phenomenon is not unexpected, if diffusion has played a significant role in the movement of material, since a large part of the silicon might be relatively fixed in highly polymerized silica tetrahedra.

The rate of movement of material away from the crystallizing rim must have been approximately the same as the movement toward the place of crystallization, since there is very little change in density during crystallization (see table 6). Assuming that the time of quenching was the same for all constituents, then a comparison of the crystalline rim with its surroundings (see table 9) shows that magnesium has been lost at a faster rate than iron, and that calcium has decreased more rapidly than sodium, which has increased in one case.

Because of the presence of the glass, the assumption of the previous paragraphs appears to be justifiable. It should be emphasized that the

order and arrangement of the data in Table 9 has value only as a relative qualitative estimate of the rates of movement, and then only for rocks of similar PTX conditions. It is interesting to note that Kahma (1951, p 70), with considerably more data on the compositional variation across a diabase-granite contact (where the basalt is intrusive into the granite) states, ". . . the fact that for example the migration ability of K_2O in. the upper and lower rock systems is considerably greater than that of SiO_2 seems to be real and not fortuitous." He also concludes that magnesia may migrate a little faster than total iron (calculated as FeO). Unfortunately, Kahma submits no migration data for sodium and calcium. Considering the fact that Kahma has sampled a diabase-granite contact, the agreement with the author's order (table 9) is striking.

The composition of those mineral phases which may crystallize from the melt, and which, therefore, are most stable, is probably the primary factor influencing the relative migration rates. The evidence for this is that like atoms (i.e., Ca, Na, K, etc.) do not behave in a like manner. Elements of the same order of magnitude of gain or loss cannot be divided into three groups (e.g., Ca-Na-K, Fe-Mg, Al-Si) on the basis of similar chemical behavior.

From this one might deduce that numerically accurate values of the migration rates cannot be calculated unless one knows to what extent crystallization has resulted in an effective separation of the crystal-line phase from the transporting medium of the surroundings. That such a separation exists is proven by geochemical culminations (Cornwall, 1951; Kahma, 1951; also see their bibliographies). If this were not so, material would have to diffuse toward an area of greater concentration, contrary to Fick's law (see Barrer, 1941), in a process analogous to the diffusion of heat from a cold source to a hotter zone. Barth (1952, pp 318-321) discusses the idea that crystallization may effectively separate a constituent from the transporting phase. It should be noted, however, that Table 9 shows no major changes in rock composition as a result of this crystallization process.

R.ABB CANYON PEGMATITE AREA

Kelley and Branson (1947) have described this shallow-depth, high-temperature pegmatite area which lies about 3 miles north of the mouth of Rabb Canyon (see pl 1), beyond the present map limits. The following summary utilizes Kelley and Branson's (1947) paper, data gathered by the author on a 1-day trip to the area with N. L. Bowen, Eugene Callaghan, V. C. Kelley, and C. Vitaliano, and subsequent laboratory study of the samples collected by Dr. Callaghan and the author. The unique feature of this pegmatite is the presence of large moonstone sanidine crystals. Many recent articles on high-temperature feldspars list one sample as "moonstone or sanidine, Grant County, New Mexico." All such samples were obtained from this pegmatite area through Ward's Natural Science Establishment or other collectors.

According to Kelley and Branson (1947):

> The pegmatites are small bodies within a rhyolite porphyry plug that has been injected into rhyolitic tuffs of Tertiary age. The pegmatites consist

dominantly of quartz and sanidine with accessory quantities of cleavelandite, biotite, sphene, magnetite, and ilmenite. The sanidine, which occurs in crystals up to one or two feet on a side, is the moonstone variety and displays limpid blue and white play of colors. Microcline is absent, and on the basis of the sanidine the pegmatites are believed to have crystallized at temperatures higher than those of the normal plutonic pegmatites. Textural and structural evidence indicates that the pegmatites crystallized prior to the enclosing rhyolite porphyry.

An analysis, norm, and mode (389-B-Cl) of the granitoid phase of the associated rhyolite porphyry are given in Table 6 and might well be compared with the average mode of the rhyolite porphyry given in Table 5. The texture and composition of the Rabb Canyon granitoid (term from Kelley and Branson, 1947, p 702) rhyolite porphyry appears to be almost identical with that of the rhyolite porphyry discussed in a previous section of this report. The Rabb Canyon rhyolite porphyry has a matrix which is whiter, more altered, and more friable than the rhyolite porphyry shown on Plate 1, except for the small mass of porphyry just south of the highway and northeast of the words "Gallinas Canyon" (on pl 1). Sanidine phenocrysts of the Rabb Canyon rhyolite porphyry, all of which are clear and unaltered, have the optic plane normal to (010) and a 2V of 20 degrees. Unheated sanidine phenocrysts consist of two phases with the compositions $Or_{81}Ab_{19}$ and nearly pure albite, whereas heated sanidine phenocrysts have a composition of $Or_{67}Ab_{33}$ (± 5 mole percent), on the basis of the 201 lines (Bowen and Tuttle, 1950) determined by means of a Phillips X-ray spectrometer according to techniques well described in geologic literature. Rounded and corroded plagioclase phenocrysts, averaging about 1 mm long, are An_{26} on the basis of U-stage extinction-angle Measurements. Cavities within the Rabb Canyon rhyolite porphyry are partly or completely filled with several zeolites, tentatively identified as stilbite, heulandite, and chabazite.

Kelley and Branson (1947) have concluded that the pegmatites crystallized prior to the enclosing rhyolite porphyry, because thin stringers of porphyry truncate the pegmatites and pegmatitic minerals. An exactly opposite conclusion would be reached on the basis of the

TABLE 12. FELDSPARS OF THE RABB CANYON PEGMATITE AREA

ROCK PHASE	FELDSPAR	SOURCE
Pegmatite	Sanidine, $Or_{58}Ab_{42}$	Laves (1952, p 565)
	Sanidine, $Or_{57.6}Ab_{42.1}An_{0.3}$	Kracek and Neuvonen (1952, p 300)
	Plagioclase, An_{16}	Kelley and Branson (1947, p 706)
Granitoid Rhyolite Porphyry	Sanidine, $Or_{67}Ab_{33}$	This report
	Plagioclase, An_{26}	This report

feldspar compositions (see table 12), inasmuch as the most calcic plagioclase and the most potassic sanidine occur in the granitoid rhyolite porphyry. However, temperature fluctuation might be able to explain the anomaly that feldspars of slightly higher crystallization temperatures occur in those rocks which have presumably crystallized last. Actually, there may be no anomaly whatsoever; in the author's opinion one part of the rhyolite porphyry could have crystallized before the pegmatite, and another afterward. A proper conclusion is that the rhyolite porphyry and pegmatite are consanguineous and nearly contemporaneous. Furthermore, there are no fundamental differences other than grain size between the rhyolite porphyry, the pegmatite, and the tuffaceous rhyolite. Pegmatite minerals (Kelley and Branson, 1947, fig 5) are almost, as rounded, corroded, and fractured as those in the tuffaceous rhyolite.

SUMMARY OF THE RHYOLITIC IGNEOUS ROCKS

The xenolith zones, pegmatite area, and large areas of intrusive rhyolite porphyry, all of which are very similar in texture and composition to the extrusive rhyolitic rocks, suggest proximity to a major eruptive center which existed before early Miocene-early Pliocene time. The fractured and broken phenocrysts, frequently regarded as indicating a pyroclastic origin, are equally common in both the intrusive and extrusive rocks, although somewhat less pronounced in the Rabb Canyon pegmatite. Consequently, both intrusive and extrusive rhyolitic rocks may have been emplaced, or extruded as crystalline, and glassy, granular masses. Features such as pegmatites, xenomorphic-granular phases (of the rhyolite porphyry), perthitic phenocrysts (in sills), and primary granophyric phenocrysts (in glass dikes), all commonly regarded as plutonic rock features, are here shown to occur in a volcanic igneous environment. Geochemical culminations in silicon and potassium have been produced by a lack of equilibrium during the formation of rhyolitic reaction rims about accidental xenoliths. All the evidence herein presented tends to invalidate the argument that igneous and plutonic processes are fundamentally different.

The rhyolitic extrusive rocks form extensive blanket deposits, which are little altered and less broken up by faulting than the under-lying rocks, so that many potential mining areas may be covered as a result.

SANDSTONE, CONGLOMERATE, AND TUFF

The exposures of this rock unit form discontinuous lenticular masses in the extreme western part of the area (see pl 1). These sediments and pyroclastics overlie the tuffaceous rhyolite and underlie the late andesite. With the exception of slight variations in dip, their structure is conformable to that of the containing volcanic rocks. On the basis of its stratigraphic position, this rock unit is correlated with the lake beds east of the mapped area, which are between early Miocene and early Pliocene in age.

The thickness of this unit ranges from a feather edge to 300 feet. At the base, in most localities, is a cobble conglomerate with well-rounded cobbles and boulders of the tuffaceous rhyolite in a coarse-grained, poorly-sorted, friable, arkosic matrix. Above are white, medium-grained, friable, tuffaceous siltstones or white rhyolitic tuffs of varying thicknesses. The top units are friable, red, sandy to silty arkoses in massive to thin-bedded units.

The rock fragments in these sediments, on the basis of the author's field examinations, consist exclusively of the tuffaceous rhyolite. This is the most valuable criterion for differentiating this rock unit from later Tertiary sediments. In view of the approximate structural con-formability of this deposit, the singularity of its rock fragments, and the presence of rhyolitic tuffs, it would appear that this sediment was formed shortly after the tuffaceous rhyolite.

LATE ANDESITE

These flows and agglomerates, comprising the youngest volcanic rocks, are found only in a narrow northwest-southeast zone in the extreme western part of the mapped area (see pl 1), where they overlie the above-described unit with approximate conformity. In some areas, the late andesite is missing; in others, it ranges in thickness up to a possible maximum of 800 feet. Southeast of Rabb Canyon, immediately adjacent to State Highway 180 near a low saddle, there are abundant rounded cobbles and boulders of the late andesite strewn about on the surface, but actual ledges are lacking. These boulders suggest that the late andesite extended to the east beyond the present outcrop area. This is the only locality in which the late andesite fragments were found east of its mapped exposures. Outcrops 3 miles south of San Lorenzo were not studied in any detail; it is thus possible that this rock is part of a different unit not recognized elsewhere in the area.

The major part of the late andesite weathers to a dark brown. Megascopically, the rock is a black aphanitic porphyry with sparse, glassy, white, or green phenocrysts, 2 mm and less in size. Many elongated gas cavities are present. It varies from a massive rock to one with abundant conchoidal joints.

Within the late andesite the following cyclical sequence of units may be differentiated easily:

1. At the top: massive andesite, scoriaceous near the top, but less so down the section.
2. Massive andesite with very abundant conchoidal joints. This is gradational with (1) above.
3. At the bottom: agglomerates and tuffs, which consist of blocks and smaller fragments of a pumiceous andesite in a sandy matrix. This bottom unit is 2-15 feet thick and red, black, or light yellow in color.

The thickness of one sequence varies from 20 to 50 feet, and similar sequences are repeated as one moves stratigraphically upward. Microscopically, the rock is porphyritic (phenocrysts 2 mm and

less in size), intersertal, and has a trachytic structure. The modal compositions are listed in Table 13. The plagioclase phenocrysts are zoned, partly resorbed, and embayed. Clear secondary overgrowths and myrmekitelike alteration of plagioclase are common. Pigeonite and augite form larger phenocrysts (2 mm and less) that are subhedral, rounded, fractured, and slightly altered. Hypersthene forms' smaller stubby prisms (0.2 mm and less), chiefly in the groundmass of the hypersthene andesite (see table 13). Sparse olivine remnants have been almost completely replaced by a deep red-brown material, probably iddingsite. Biotite has been oxidized peripherally to an opaque hematitic material. In the andesite (table 13) there are sparse, large, well-rounded, and corroded quartz phenocrysts. They have a yellow-brown stain along the peripheral corrosion surfaces and are transected along conchoidal fractures by a yellow-brown colored zone. Many of the quartz phenocrysts are surrounded by thin rims of closely intergrown, fine-grained, acicular pyroxene, or by thicker zones of pyroxene grains.

In addition to the modes given in Table 13, an analysis, norm, and mode of a specimen (389-C-87) of the late andesite is presented in Table 6. The appearance of labradorite in one mode (table 13), contrasted with its absence in the norm and other modes, along with the incipient reaction between the quartz and matrix to produce pyroxene, demonstrate again that many volcanic rocks have not attained chemical equilibrium (see Faust and Callaghan, 1948, pp 29-33).

TABLE 13. MODES OF THE LATE ANDESITE VOLCANIC UNIT

HYPERSTHENE ANDESITE		ANDESITE	
MINERAL	ABUNDANCE (PERCENT)	MINERAL	ABUNDANCE (PERCENT)
Plagioclase (An_{61})	41.	Plagioclase (An.)	14.
Hypersthene	22.	Pigeonite	6.
Augite	1.	Quartz	4.
Sphene	x	Biotite	2.
Magnetite	2.	Magnetite	3.
Olivine	x	Basaltic hornblende	x
Iddingsite	x	Uralite	2.
Calcite	1.	Hematite	4.
Sericite	1.	Matrix	65.
Matrix	32.		

x Indicates present.

LOCATION OF SPECIMENS

Andesite: 3 miles south of San Lorenzo, on the east bank of the Mimbres River, in the SW¼ sec. 5, R. 10 W., T. 18 S.
Hypersthene Andesite: N. line, NE¼ sec. 17, R. 10 W., T. 17 S.

EARLY GRAVEL DEPOSITS

These gravel deposits crop out over limited areas, primarily west of the western boundary of the late andesite volcanics (see pl 1). The maximum thickness in a single outcrop in the area studied is 211 feet. This was measured near its eastern extremity, and the thickness is probably much greater toward the center of the Mimbres Valley basin. The formation dips 8-25 degrees to the west or southwest.

Cobble and pebble conglomerates, sands, and sparse clays comprise this formation. These deposits are light brown, slightly lithified, and show slight sorting and stratification. Well-rounded fragments of the tuffaceous rhyolite, and fragments of both andesitic volcanic sequences are common. Locally, small yellow-brown clayey lenses with abundant small (4 mm and less) angular fragments, possibly representing volcanic ash deposits, are found within the gravel.

This unit is easily differentiated from the older arkosic sandstone, conglomerate, and tuff, previously described, by the presence of cobbles and smaller easily recognizable fragments of the late andesite. Combinations of the following criteria were used to differentiate the early gravels from the overlying late gravel (see fig 27):

1. Better sorting and stratification.
2. Locally, a greater lithification.
3. Lighter color.

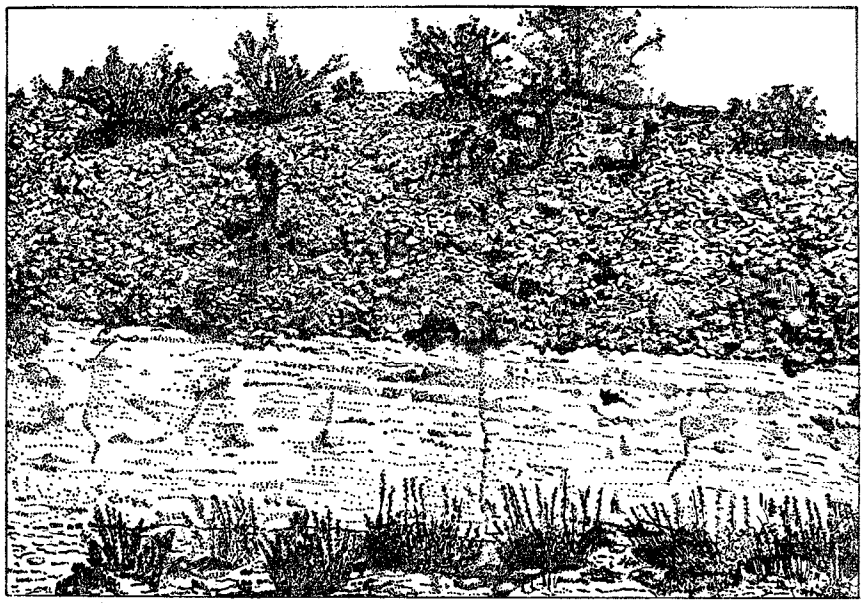

Figure 27
LATE TERRACE GRAVELS OVERLYING THE EARLY GRAVELS AND SAND IN GALLINAS CANYON. HEIGHT OF OUTCROP IS ABOUT 25 FEET.

4. Stratification truncated by the late gravels, or dips slightly steeper than those of the late gravels.

5. Almost no boulders found.

6. Late andesite fragments are less common than in the late gravels.

7. Where the two gravels are in contact, the overlying late gravels are much coarser-grained and show poorer sorting (see fig 27). How-ever, toward the center of the Mimbres Valley, both gravels become finer-grained and are difficult to separate.

Despite the criteria listed, the early and late gravels may be different facies of the same rock unit. If they are, the apparent unconformity may represent a truncated crossbedding. No soil zones were observed between these two gravels, but the matter was not investigated in detail.

The early gravels contain fragments of the late andesite, and yet, 2½ miles north of San Lorenzo, the basal red pumiceous agglomerate of this andesite overlies the early gravels. The early gravels, therefore, must be contemporaneous with at least a part of the late andesite volcanics, whereas for the most part the late gravels overlie the late andesite. In terms of geologic age, the early gravels have been tentatively correlated with the Gila conglomerate of Pliocene age (described by Knechtel, 1936) along the Gila and San Simon Valleys in southeastern Arizona, on the basis of their stratigraphic position and their similar position in the regional geologic history. There is no certainty, however, that such a correlation should not be made with the late gravels also. W. Elston (forthcoming publication of the New Mexico Bureau of Mines and Mineral Resources) has correlated sediments equivalent to both the early and late gravels with the Santa Fe formation of the Rio Grande trough, inasmuch as these alluvial sediments can be traced laterally into the Rio Grande alluvial sediments. However, northwest-ward from the present map area, reconnaissance studies suggest that the early and late gravels (and Santa Fe fanglomerates of Elston) can be traced almost continuously into the alluvial sediments of the Gila drainage.

Summary of Quaternary Deposits and Landforms

The late gravel deposits are found only in the extreme western part of the mapped area, where they overlie the early gravels with a small unconformity. It appears that the major divides within the out-crop area of the late gravels all lie approximately on a plane surface sloping gently to the southwest. The dark-brown alluvial gravels, sands, and conglomerates which comprise this formation are poorly sorted and stratified. They dip approximately 5 degrees or less to the south-west. Closer to the Mimbres River, the late gravels are finer-grained. The most predominant constituent of the late gravels, west of the late andesite outcrops, are the late andesite fragments. East of the late andesite outcrops, the late gravels are composed primarily of tuffaceous rhyolite fragments. The basis for classifying the gravels east of the late andesite with the late gravels, when one criterion for identification of the post-Paleozoic sediments is composition, is discussed below.

Two terraces which were mapped in the western part of the area are clearly visible on the aerial photographs. The high terrace, found only in the lower part of Noonday Canyon, is considerably dissected and lies at least 100 feet below the uppermost part of the late gravels.

The low terrace is approximately 50 feet below the high terrace, where both are present, and has been only slightly dissected. West of the late andesite, this low terrace lies approximately 30-50 feet above the present stream level and is formed by the late gravels. The late gravels east of the late andesite are only 6-20 feet above stream level. Also, east of the late andesite, the low terraces are formed on 10 feet or less of poorly sorted, unstratified, coarse boulder and gravel conglomerate (similar to fig 27), which overlies the volcanic bedrock. If mapped in detail, several smaller terraces could be separated which have been included here within the low terrace.

The low terrace truncates the late andesite and the tuffaceous rhyolite. It is concluded that the gravels capping the terraces east of the late andesite are contemporaneous with the late gravels in spite of their differing compositions, because of the continuity of the terrace levels.

The stream beds are entrenched 5 feet or less in the recent alluvium. Small, nearly horizontal, alluvium-filled areas are common in the higher parts of the range, where streams have spread laterally in weak rocks. Most of the slopes in the area are precipitous, and the regional relief is more than 3,000 feet. Highway road cuts show concentrations of colluvium along the steepest part of the range, on the sides of numerous moderately steep rock hills with thin mantle-rock cover. There is no obvious structural control of the landforms except in very limited areas.

Major Structural Features

Most of the structural features have been indicated in the discussions of the various rock units. Accordingly, this section should only integrate these features with the regional structural picture.

The Black Range is a part of the Mexican Highland portion of the Basin and Range province (Fenneman, 1931). According to Gordon (Lindgren, Graton, and Gordon, 1910, p 220), three genetic varieties of mountain structures are present, namely, (1) tilted crustal blocks, (2) upthrust granitic cores, and (3) accumulations of volcanic material. Gordon even states, "Of the second type are the Black and Mimbres (Black) Ranges, in which the uplifted strata slope away on both sides from a central mass of granite." However, in the Kingston area the almost continuous outcrops afforded by State Highway 180 (which Gordon did not have) show no central granite core, but rather many small Precambrian blocks and notable faulting and folding, as is illustrated by the map and section (pl 1).

The early andesite volcanic sequence and all older rocks were folded slightly into a series of open asymmetrical folds (pl 1). The fold axes range from N. 33° E. to N. 35° W., and plunge from 7 to 20 degrees northward.

Because of the small amount of folding and the absence of more than minor folds in adjacent areas of New Mexico, it seems most likely that both folding and faulting occurred during the same phase of tectonic activity. Normal faulting and folding are generally considered as evidences of regional tension and compression, respectively. How-ever, it is known that faulting or tilting of resistant rocks of the basement complex can modify the structural orientation of overlying sediments. Examples of gravitational adjustment to stable underlying rocks are voluminous (see Hills, 1943, pp 12-19).

North of the Lady Franklin mine a small volume of sediments has been synclinally folded between two large masses of Precambrian granite (see pl 1). Just to the east of the eastern granite mass, the sediments show no folding, but dip more steeply eastward close to the granite. Localized moderate folding suggests adjustment to basement-complex topography, or structural modification due to the igneous intrusion, rather than compression. The local variability in fold axes does not indicate a regional compression. In areas immediately to the east of the mapped area, up to and including the Animas Hills (near Hillsboro), and to the west in the Silver City region (Paige, 1916), there is no evidence of major compressional stresses. For these reasons, it is concluded that the folding in this area was produced by the adjustment of the weaker tabular rock bodies to the faulted and warped upper surfaces of the resistant basement rocks, with possible assistance from igneous intrusive forces.

The high-angle normal faulting is not restricted to those larger faults illustrated in Plate 1. Chert nodules in limestone in many outcrops show normal faulting, in which the apparent displacement is 4 inches and less, and where the surrounding limestone shows no evidence of

any fault. Small grabens and horsts with apparent displacements of from 2 to 10 feet are common, as are normal faults with apparent offset of 20 feet and less. Apparently the Percha shale was able to adjust itself plastically to much of the faulting, inasmuch as many of the small faults in the Fusselman and older rocks do not extend stratigraphically higher than the basal Percha shale. Faults are, therefore, more numerous in the lower Paleozoic than in the upper Paleozoic rocks. Wherever direction of movement can be ascertained on a fault zone, the motion appears to have been predominantly dip-slip in direction. Along the major north-south faults, the west block has been downdropped relative to the east block, as adjacent stratigraphic horizons indicate.

Before or during the quartz monzonite intrusion, the rocks of this area had undergone considerable high-angle faulting. Presumably because of the crustal weakness in faulted and fractured zones, these zones became favored loci for igneous emplacement. Such igneous bodies have nearly vertical contacts, and their distribution has no apparent relationship to the sedimentary rocks.

Distribution of the conformable parts of the quartz monzonite is probably related to the presence of shale horizons. Two possible causes of the lateral spreading of the quartz monzonite might be that the units with a large shale content were less competent and rigid with respect to the resistance offered the intrusive pressures, or that, at these upper horizons of the Paleozoic stratigraphy, the weight of the overlying rocks was insufficient to prevent the lateral spread of the igneous magma. At the time of intrusion, the sediments were covered by an estimated 400 feet (minimum) of the first volcanic sequence. If the lack of overburden were a dominant factor, all of the higher stratigraphic horizons should display an even greater irregularity in their position with respect to the quartz monzonite porphyry. The fact that the shale units were intruded, whereas the overlying or underlying massive limestone units were not, suggests that the weight of the over-burden was not the primary factor. In addition, the intrusion appears to have domed the enclosing sediments in a laccolithic manner. Lindgren, Graton, and Gordon (1910, pp 40-41) have mentioned many other laccolithic domes, sheets, and sills found in various sedimentary horizons in New Mexico.

The properties of the shale horizons which may have made them more conducive to igneous intrusion should be considered. Inasmuch as the bedding of all the Paleozoic sediments is approximately parallel, the shales would not be favored as intrusion loci as a result of their structure. However, a certain structural attitude of the sediments may have been important in determining whether crosscutting or conform-able igneous bodies would be formed. Thus, given a certain structure of the sediments, the shale horizons would be favored for the intrusion of conformable igneous masses because of differences in the intrinsic properties of the shales and the other sediments. In a geologic sense, the intrinsic properties of the shales, a function of composition, differ from the other sediments in their smaller rigidity, smaller shear strength, and in their greater anisotropy. The consequences of this are that in small-scale intrusions or in the peripheral regions of large

intrusions, differences in the mechanical properties of the country rocks may determine the loci of the igneous rocks.

The problem of how the quartz monzonite porphyry acquired the space which it now occupies cannot be solved, except in a manner which has not been considered adequate in previous geologic cases; namely, that the quartz monzonite magma made room by pushing the shales away. The shales are completely missing in most places, although not all of these shale units have been displaced by the quartz monzonite porphyry. Near a shale-quartz monzonite contact, the shale is considerably brecciated. In many localities the shale encloses thin anastomosing sills and dikes of the quartz monzonite porphyry. Microscopic examination of the quartz monzonite-shale contacts shows a slight flow structure parallel to the contacts, but no evidence of assimilation. Megascopically and microscopically, the shales show no contact effects, with the possible exception of a darker, more opaque shale matrix. In the light of the intimate penetration of the shale and the shale brecciation near the quartz monzonite contact, it is suggested that the magma squeezed out the shale by plastic flow. Such a room-making process in sills where flow structures are apparent has been illustrated by Tweto (1951, fig 13). To illustrate this hypothesis, the thickness of the shale horizons in several parts of the cross-section (see pl 1) has, been noticeably increased.

Ore Deposits

No careful study of the metal mines of the Kingston area was attempted in the course of the field work which forms the basis of this report. All the mines were idle, and only a small proportion of the original workings remains accessible. The main purpose of this study was to determine, insofar as was possible, the relation of former ore occurrences to the intrusive quartz monzonite and to the structure and stratigraphy that was worked out in the course of the mapping, with the hope that certain general guides to future exploration in this part of the Black Range might be established. The scale of the map (pl 1) is not sufficiently large to represent all the intricate structures and relationships that occur along the explored ore zones.

The general features of the mineral deposits, taken largely from the historic record (Lindgren, Graton, and Gordon, 1910; Harley, 1934), from individuals who have mined in . the area, notably Messrs. T. B. Everhart, K. A. Strand, James I. Moore, and G. Lotspeich, and from such observations as were made by the author, may be stated as follows:

The Kingston district had its greatest production, amounting to over $6,000,000, almost entirely in silver and minor gold, between the time of its discovery in 1880 and 1893, when the decline in the price of silver, together with other problems, led to the closing of the mines. They have been worked sporadically since, but only on a small scale.

The main productive area was in Paleozoic rocks a mile to the northwest and west of Kingston, where the Lady Franklin, the largest producer, the Black Colt, Comstock, the Iron King, and United States mines are located (see pl 1 and fig 28). Sulfides of copper, lead, zinc, iron, silver (minor), and manganese, and the corresponding oxidized minerals, were mined from high-grade discontinuous veins and pockets, primarily for their silver and gold content. Recent mining activity has produced manganese oxides from small open pits, where the oxides are weathering products from primary rhodonite, rhodochrosite, and minor alabandite (specimen from Mr. T. B. Everhart) in veins and replacement bodies in limestone and dolomite. Examination of old mine maps and current mining operations shows that ore deposits are found not only in the Silurian Fusselman dolomite and Upper Ordovician Montoya limestone, but also in the Lower Ordovician El Paso limestone.

The Gray Eagle mine (see pl 1 and fig 28), 3 miles southwest of Kingston in the deep canyon on South Percha Creek, has produced copper, lead, and zinc in the proportion of 1:3:4½ in terms of reconverted metal, and gold and silver in a ratio of 1:446 in shipments of 1,535 tons during 1943. Production has been from discontinuous veins (and possible replacement bodies) in the El Paso limestone.

The Grandview (see pl 1) and nearby mines, west of the crest of the Black Range and about 6 miles southwest of Kingston, shipped during the years 1924 and 1938-1944 a total of 22,079 tons of ore containing a copper-lead-zinc metal ratio of 1:19:37, and a gold to silver

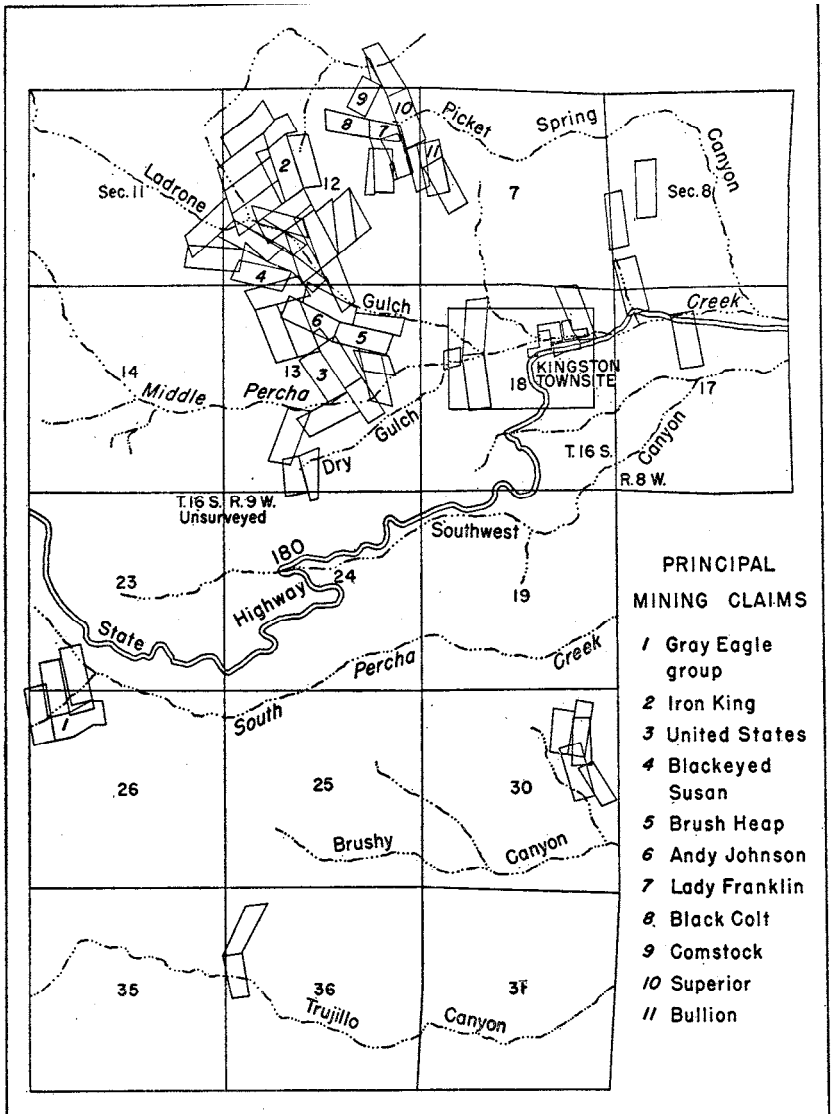

Figure 28. PATENTED CLAIMS OF THE BLACK RANGE (KINGSTON) MINING DISTRICT.

ratio of 1:1,000. Production was from veins and replacement bodies in the Fusselman and Montoya, just east of a major north-south fault.

Future possibilities may be summarized as follows: High-grade ore has been found in discontinuous pockets in veins (along faults or fissures) and replacement bodies in the Fusselman, Montoya, and El Paso limestones and dolomites, which would, barring erosion, underlie the Percha shale. Unless methods can be designed for mass treatment of low-grade ores disseminated throughout sedimentary rocks, it seems likely that small-scale operations will continue to be most successful.

Harley noted (1934, p 105) that most of the value of the ore was dependent on enrichment by weathering and other secondary processes. Certainly it is true today that manganese ores cease to be profitable when mining has proceeded to the rhodonite and rhodochrosite zones; therefore, secondary enrichment may limit future mine production.

Examination of Plate I shows that the carbonate rocks are domed or arched slightly near the Gray Eagle, United States, Iron King, and Lady Franklin mines, and in addition are faulted even more intricately than may be depicted on the map scale. Near these mines (northeast of the Gray Eagle, east and south of the United States mine, southeast and west of the Iron King mine, and almost all around the Lady Franklin mine) are large sills of the intrusive quartz monzonite porphyry. If no erosion had occurred, it is entirely possible that a part of the sill would overlie the mining areas. Future exploration for ore deposits not now exposed at the surface might well be directed toward areas of arched or domed Paleozoic rocks, or areas covered by sill-like intrusive bodies. Additional surface exploration might be undertaken in the area west of the crest of the range and between Silver Creek and State Highway 180, where the Magdalena limestone and older rocks are moderately folded.

References

Balk R. (1948) *Structural behavior of igneous rocks,* Ann Arbor, J. W. Edwards, Inc. (originally pub. Geol. Soc. Am. Mem. 5).

Barnes, V. E. (1930) *Changes in hornblende at about 800° C.,* Am. Mineralogist, v 15, 393-417.

Barrer, R. M. (1941) *Diffusion in and through solids,* Cambridge, England, Univ. Press.

Barth, T. F. W. (1931) *Proposed change in calculation of norms of rocks,* Min. pet. Mitt., v 42, 1-7.

---- (1948) *Oxygen in rocks: A basis for petrographic calculations,* lour. Geol., v 56, 50-60.

---- (1950) *Volcanic geology, hot springs, and geysers of Iceland,* Carnegie Inst. Wash. Pub. 587.

---- (1952) *Theoretical petrology,* New York, John Wiley and Sons.

Birch, F., Schairer, J. F., and Spicer, H. C. (1942) *Handbook of physical constants,* Geol. Soc. Am. Sp. Paper 36.

Bowen, N. L. (1928) *The evolution of the igneous rocks,* Princeton, Princeton Univ. Press.

----, and Tuttle, O. F. (1950) *The system $NaAlSi_3O_8$-$KAlSi3O_8$-H_2O,* Jour. Geol., v 58, 489-511.

Buddington, A. F., and Callaghan, E. (1936) *Dioritic intrusive rocks and contact metamorphism in the Cascade Range in Oregon,* Am. Jour. Sci., 5th ser, v 31, 421-449.

Callaghan, E. (1951) *Distribution of intermediate and basic igneous rocks in the Tertiary of Western United States,* Geol. Soc. Am. Bull., v 62, n 12, pt 2, 1428.

Cooper, G. A., et al. (1942) *Correlation of the Devonian sedimentary formations of North America,* Geol. Soc. Am. Bull., v 53, 1729-1794.

Cornwall, H. R. (1951) *Differentiation in magmas of the Keweenawan series,* Jour. Geol., v 59, 151-172.

Darton, N. H. (1917-a) *A comparison of Paleozoic sections in southern New Mexico,* U. S. Geol. Survey Prof. Paper 108-C.

---- (1917-b) *Deming, New Mexico folio,* U. S. Geol. Survey Folio 207.

---- (1926) *The Permian of Arizona and New Mexico,* Am. Assoc. Petrol. Geol. Bull., v 10, n 9, 819-852.

---- (1928-a) *"Red beds" and associated formations in New Mexico,* U. S. Geol. Survey Bull. 794.

---- (1928-b) *Geologic map of New Mexico,* U. S. Geol. Survey.

Drescher-Kaden, F. K. (1948) *Die Feldspat-Quarz-Reaktionsge fiige der Granite and Gneise,* Berlin, Springer.

Dunham, K. C. (1935) *The geology of the Organ Mountains,* N. Mex. School of Mines, State Bur. Mines and Min. Res., Bull. 11.

Ellison, S. P., Jr. (1946) *Conodonts as Paleozoic guide fossils,* Am. Assoc. Petrol. Geol. Bull., v 30, n 1, 93-110.

Emmons, R. C. (1943) *The universal stage,* Geol. Soc. Am. Mem. 8.

Fairbairn, H. W., and Podolsky, T. (1951) *Notes on precision and accuracy of optic angle determinations with the universal stage,* Am. Mineralogist, v 36, 823-832.

Faust, G. T., and Callaghan, E. (1948) *Mineralogy and petrology of the Currant Creek magnesite deposits and associated rocks of Nevada,* Geol. Soc. Am. Bull., v 59, 11-74.

Fenneman, N. M. (1931) *Physiography of western United States,* New York, McGraw-Hill.

Fenner, C. N. (1934) *Hydrothermal metamorphism in geyser basins of Yellow-stone National Park,* Am. Geophys. Union Trans., 15th Ann. Mtg., 241-243.

---- (1936) *Bore-hole investigations in Yellowstone Park,* Jour. Geol., v 44, 225-315.

---- (1937) *Tuffs and other volcanic deposits of Katmai and Yellowstone Park,* Am. Geophys. Union Trans., 18th Ann. Mtg., 236-239.

---- (1948) *Incandescent tuff flows in southern Peru,* Geol. Soc. Am. Bull., v 59, 879-893.

Flower, R. H. (1953) *Age of the Bliss sandstone, New Mexico,* Am. Assoc. Petrol. Geol. Bull., v 37, 2054-2055.

Fritz, M. A. (1944) *Upper Devonian bryozoa from New Mexico,* Jour. Paleont., v 18, 33-41.

George, W. O. (1924) *The relation of the physical properties of natural glasses to their chemical composition,* Jour. Geol., v 32, 353-372.

Gilbert, C. M. (1938) *Welded tuff in eastern California,* Geol. Soc. Am. Bull., v 49, 1829-1862.

Gordon, C. H. (1907-a) *Mississippian formations in the Rio Grande Valley, New Mexico,* Am. Jour. Sci., 4th ser, v 24, 58-64. See also Jour. Geol., v 15, 91-92.

---- (1907-b) *Notes on the Pennsylvanian formations in the Rio Grande Valley, New Mexico,* Jour. Geol., v 15, 805-816.

Harley, G. T. (1934) *The geology and ore deposits of Sierra County, New Mexico,* N. Mex. School of Mines, State Bur. Mines and Min. Res., Bull. 10.

Hills, E. S. (1943) *Outlines of structural geology,* London, Methuen & Co., Ltd.

Iddings, J. P. (1899) *Geology of Yellowstone National Park,* U. S. Geol. Survey Mon. 32, pt II.

Ingerson, E. (1940) *Fabric criteria for distinguishing pseudo ripple marks from ripple marks,* Geol. Soc. Am. Bull., v 51, 557-570.

Jaggar, T. A., Jr. (1917) *Volcanologic investigations at Kilauea,* Am. Jour. Sci., 4th ser, v 44, 161-220.

Johannsen, A. (1932) *A descriptive petrography of the igneous rocks, v II,* Chicago, Univ. of Chicago Press.

Kahma, A. (1951) *On contact phenomena of the Satakunta diabase, Comm. géol.* Finlande Bull. 152, 84.

Kelley, V. C., and Branson, O. T. (1947) *Shallow, high-temperature pegmatites, Grant County, New Mexico,* Econ. Geol., v 42, 699-712.

---- (1951) *Oolitic iron deposits of New Mexico,* Am. Assoc. Petrol. Geol. Bull., v 35, 2199-2228.

---- and Silver, C. (1952) *Geology of the Caballo Mountains,* Univ. of N. Mex. Pub. in Geol. 4.

Kennedy, G. C. (1947) *Charts for correlation of optical properties with chemical composition of some common rock-forming minerals, Am.* Mineralogist, v 32, 561-573.

King, P. B. (1940) *Older rocks of the Van Horn region, Texas, Am. Assoc.* Petrol. Geol. Bull., v 24, 143-156.

---- (1942) *Permian of west Texas and southeastern New Mexico, Am. Assoc.* Petrol. Geol. Bull., v 26, 535-763.

Kirk, E. (1934) *The lower Ordovician El Paso limestone of Texas and its correlatives,* Am. Jour. Sci., 5th ser, v 28, 443-463.

Knechtel, *M. M. (1936) Geologic relations of the Gila conglomerate in south-eastern Arizona,* Am. Jour. Sci., 5th ser, v 31, 81-92.

Kracek, F. C., and Neuvonen, K. J. (1952) *Thermochemistry of plagioclase and alkali feldspars,* Am. Jour. Sci., Bowen v, pt 1, 293-318.

Krynine, P. D. (1948) *The megascopic study and field classification of sedimentary rocks,* Jour. Geol., v 56, 130-165.

Lacroix, A. (1904) *La Montagne Pelee et ses eruptions, Paris.*

Langston, W., Jr. (1949) *Permian amphibians from the Abo formation of New Mexico,* Geol. Soc. Am. Bull., v 60, 1903.

Laudon, L. R., and Bowsher, A. L. (1949) *Mississippian formations of southwestern New Mexico,* Geol. Soc. Am. Bull., v 60, 1-88.

Laves, F. (1952) *Phase relations of the alkali feldspars. II. The stable and pseudo-stable phase relations in the alkali feldspar system,* Jour. Geol., v 60, 549-574.

Lindgren, W., Graton, L. C., and Gordon, C. H. (19'10) *The ore deposits of New Mexico,* U. S. Geol. Survey Prof. Paper 68.

Lloyd, E. R. (1949) *Pre-San Andres stratigraphy and oil-producing zones in southeastern New Mexico,* N. Mex. School of Mines, State Bur. Mines and Min. Res., Bull. 29.

MacDougall, F. H. (1947) *Physical chemistry,* New York, Macmillan Co.

Mansfield, G. R., and Ross, C. S. (1935) *Welded rhyolitic tuffs in southeastern Idaho,* Am. Geophys. Union Trans., 16th Ann. Mtg., 308-321.

Marshall, P. (1935) *Acid rocks of the Taupo-Rotorua volcanic district,* Royal Soc. New Zealand Trans., v 64, 1-44.

Melton, F. A. (1925) *The ancestral Rocky Mountains of Colorado and New Mexico,* Jour. Geol., v 33, 85-89.

Miller, A. K., and Parizek, E. J. (1948) *A lower Permian ammonoid fauna from New Mexico, Jour.* Paleont., v 22, 350-358.

Moore, B. N. (1934) *Deposits of possible nude ardente origin in the Crater Lake region, Oregon,* Jour. Geol., v 42, 358-375.

Needham, C. E. (19'37) *Some New Mexico fusulinidae,* N. Mex. School of Mines, State Bur. Mines and Min. Res., Bull. 14.

---- , and Bates, R. L. (1943) *Permian type sections in central New Mexico,* Geol. Soc. Am. Bull., v 54, 1653-1668.

Osten, J. F. (1951) *Identificatie van natuurlijke alkaliveldspaten met behulp van rontgen-poederdiagrammen,* Leiden, Eduard Ijdo N. V.

Paige, S. (1916) *Silver City, New Mexico folio,* U. S. Geol. Survey Folio 199.

Perret, F. A. (1935) *The eruption of Mt. Pelee 1929-1932,* Carnegie Inst. Wash. Pub. 458.

Pettijohn, F. J. (1949) *Sedimentary rocks,* New York, Harper & Bros.

Read, C. B., and Wood, G. H. (1947) *Distribution and correlation of Pennsylvanian rocks in late Paleozoic sedimentary basins of northern New Mexico,* Jour. Geol., v 55, 220-236.

Reynolds, D. L. (1946) *The sequence of geochemical changes leading to granitization,* Geol. Soc. London Quart. Jour., v 102, 389-464.

Richardson, G. B. (1909) *El Paso, Texas folio,* U. S. Geol. Survey Folio 166.

Rogers, A. F., and Kerr, P. F. (1942) *Optical mineralogy,* New York, McGraw-Hill.

Schairer, J. F. (1950) *The alkali feldspar join in the system $NaAlSiO_4$-$KAlSiO_4$-SiO_2,* Jour. Geol., v 58, 512-517.

Schuchert, C. (1930) *"Ancestral Rocky Mountains" and Siouis,* Am. Assoc. Petrol. Geol. Bull., v 14, 1224-1227.

Skinner, J. W. (1946) *Correlation of Permian of west Texas and southeast New Mexico,* Am. Assoc. Petrol. Geol. Bull., v 30, 1857-1874.

Spencer, A. C., and Paige, S. (1935) *Geology of the Santa Rita mining area, New Mexico,* U. S. Geol. Survey Bull. 859, 1-78.

Stainbrook, M. A. (1947) *Brachiopoda of the Percha shale of New Mexico and Arizona,* Jour. Paleont., v 21, 297-328.

Stevenson, F. V. (1945) *Devonian of New Mexico,* Jour. Geol., v 53, 217-245.

Stoyanow, A. (1948) *Some problems of Mississippian stratigraphy in southwestern United States,* Jour. Geol., v 56, 313-326.

Terzaghi, R. D. (1935) *The origin of the potash-rich rocks,* Am. Jour. Sci., 5th ser, v 29,, 369-380.

Thompson, M. A. (1942) *Pennsylvanian system in New Mexico,* N. Mex. School of Mines, State Bur. Mines and Min. Res., Bull. 17.

Tuttle, O. F., and Bowen, N. L. (1950) *High-temperature albite and contiguous feldspars,* Jour. Geol., v 58, 572-583.

Tweto, O. (1951) *Form and structure of sills near Pando, Colorado,* Geol. Soc. Am. Bull., v 62, 507-532.

Weller, J. M. (1947) *Invertebrates in Pennsylvanian correlations,* Jour. Geol., v 55, 254-276.

Wentworth, C. IL, and Williams, H. (1932) *The classification and terminology of the pyroclastic rocks,* Nat. Res. Council, Rept. Comm. Sed. 1930-1932, Bull. 89, 19-53.

Wheeler, R. R. (1942) *Cambro-Ordovician of the southwest,* Geol. Soc. Am. Bull., v 53, 1812-1813.

Wilmarth, M. G. (1938) *Lexicon of geologic names of the United States,* U. S. Geol. Survey Bull. 896.

Winchell, A. N. (1945) *Elements of optical mineralogy, Part II,* New York, John Wiley & Sons.

Index

Numbers in *italics* indicate figures and plates; boldface indicates main references.

GEOLOGIC SECTION OF BLACK RANGE AT KINGSTON, NEW MEXICO

EXPLANATION

- QUATERNARY
  - Qal — Alluvium
  - Qlg — Late gravels Low Terrace
  - Qlg — Late gravels High Terrace
  - Qlg — Late gravels
- TERTIARY
  - Teg — Early gravels
  - Tla — Late Andesite
  - Tst — Sandstone, conglomerate & tuff
  - Trp — Rhyolite porphyry
  - Tr — Tuffaceous rhyolite
  - Tr — Xenolith zone
  - Rhyolite dikes & sills
  - Quartz-monzonite dikes & sills
  - Tm — Quartz-monzonite porphyry
  - Ta — Andesite & latite, flows, tuffs & agglomerates
- PERMIAN
  - Pa — Abo formation
- PENNSYLVANIAN
  - Cm — Magdalena limestone
  - Clv — Lake Valley limestone
- MISSISSIPPIAN
  - Dp — Percha shale
- DEVONIAN
  - OSmf — Fusselman & Montoya formations
- SILURIAN
- ORDOVICIAN
  - Oep — El Paso limestone
- CAMBRIAN?
  - €b — Bliss sandstone
- PRE-CAMBRIAN
  - p€gw, p€g — Graywacke, meta-diabase Granite, meta-diabase

Contact — *dashed where within 80 feet, dotted where inferred*

Fault — U, upthrown; D, downthrown; *dashed where probable, dotted where inferred*

Dip and strike of bed

Planar flow structure

Lineation

Index map of New Mexico showing location of area.

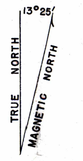

APPROXIMATE MEAN DECLINATION, 1951

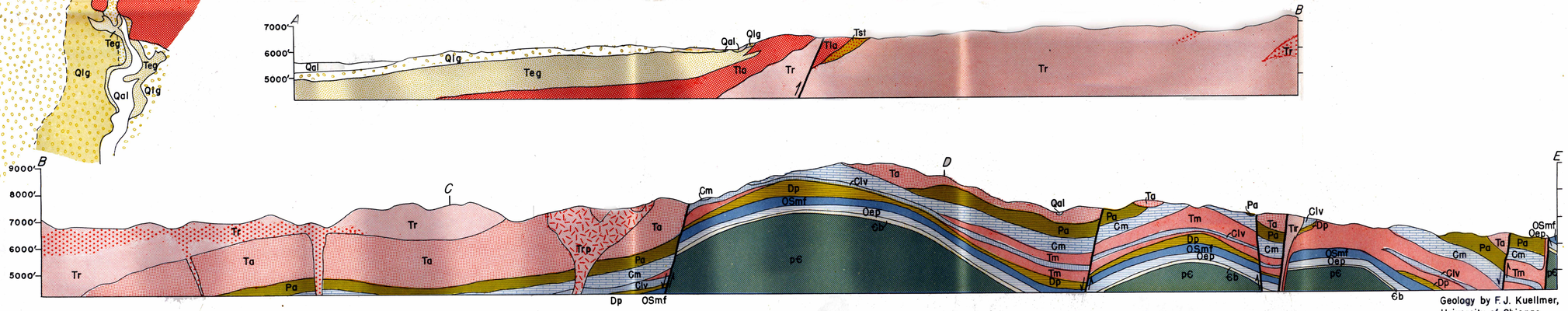

Base map from U.S. Geological Survey map of Hillsboro quadrangle, U.S. Forest Service map of Mimbres area and U.S. Soil Conservation Service sheet 389.

Geology by F. J. Kuellmer, University of Chicago. Surveyed 1950-51 as part of Field Assistance Fellowship program.

Scale 1/31680

0 1 2 3 MILES

Contour interval 200 feet